Muscle Loading Treatments for Achilles Tendinopathy

Dylan Cole Easley

Dissertation submitted to the faculty of the
Virginia Polytechnic Institute and State University
in partial fulfillment of the requirements for the degree of:

Doctor of Philosophy In

Translational Biology, Medicine, and Health

Vincent M. Wang, Chair
Per Gunnar Brolinson
Linda A. Dahlgren
Robert W. Grange
Liwu Li

August 5, 2024

Blacksburg, Virginia

Keywords: Achilles, Tendinopathy, Tendon Healing, Eccentric Muscle Loading, Biomechanics, Transcriptomics

Muscle Loading Treatments for Achilles Tendinopathy

Dylan Cole Easley

Abstract

Tendinopathies are common, painful, and debilitating injuries that can be challenging to treat. Current treatment methods are limited to surgery, nonsteroidal anti-inflammatory drugs, dry needling, and injectable therapeutics, platelet rich plasma and corticosteroids. Unfortunately, these existing treatments display poor long-term outcomes and have an increased risk of reinjury. Additionally, the healing mechanism for injured tendons forms scar tissue which is characterized by disrupted extracellular matrix rather than complete injury resolution. These structural changes impact the mechanical properties of tendon, reducing their capacity to transfer and store energy, making them inferior to uninjured tendons. The reduced mechanical properties increase the risk of rupture, exacerbating this debilitating disease and decreasing quality of life. Physical therapy (eccentric loading) decreases the symptoms of tendinopathy and restores Achilles tendon functionality. However, the mechanism by which these mechanical stimulations induce healing is poorly understood. There is a clinically relevant motivation to better understand the healing cascade in response to eccentric exercises. We aim to identify and characterize the effects of eccentric rehabilitative muscle loading on the Achilles tendon and gastrocnemius muscle complex using our preclinical TGF-ß1-induced murine model of Achilles tendinopathy. To accomplish our objective, we tested three muscle loading magnitudes (50%, 75%, and 100% body weight), over three treatment durations (1, 2, and 4 weeks) to determine their effects on tendon healing. Age-matched injured/untreated and naïve groups accompanied each loading magnitude and duration period. The functional biomechanical properties, morphological adaptations, transcriptomic response, and muscle strength of the Achilles tendon were assessed.

Injured/untreated tendons had a significantly increased cross-sectional area compared to naïve and all loading groups at 2 and 4 weeks. Maximum stress and elastic modulus of injured/untreated tendons were significantly lower compared to naïve and all loading groups after 4 weeks. Gastrocnemius muscle strength was maintained over time as loading magnitude increased. Force output was lower after 2 weeks at 100% body weight loading compared to the naïve group, then recovered to naïve levels after 4 weeks. Histological findings included increased cross-sectional

area, matrix disorganization, and increased cellular density of injured/untreated tendons. The transcriptomic evaluation revealed several patterns of expression among exercised groups. Biological processes associated with exercised groups revealed genes responsible for inflammation, extracellular matrix organization, and cell to cell signaling. Overall, eccentric muscle loading improved tendon geometry and material properties compared to naïve levels and improved muscle strength over time. Morphological evaluation also showed improvements in cross-sectional area, and collagen orientation, and cell appearance after 2 and 4 weeks of eccentric loading. Similarly, the transcriptomic changes showed an effect from exercise and upregulation of genes essential for extracellular matrix organization, inflammatory regulation, and cell to cell signaling.

Muscle Loading Treatments for Achilles Tendinopathy

Dylan Cole Easley

General Audience Abstract

Tendons are connective tissues that join muscle to bone to facilitate movement. Tendons are prone to injury because of their consistent use for daily activities. The Achilles tendon is particularly at risk for injury since it is responsible for walking, running, and jumping, making it susceptible to overuse. Current treatment methods such as surgery and pain relief medication can provide immediate symptomatic relief, but have limited long-term success. Physical therapy provides relief of symptoms of chronic Achilles tendinopathy and improves the tendon healing response. Eccentric-based exercises (lengthening of the muscle while it contracts) are known as 'heel drops' and have been the most successful physical therapy technique to improve Achilles tendon healing. However, the way these rehabilitative exercises facilitate healing is poorly understood. It is difficult to determine the exact methods of healing because the required frequency and amount of exercise varies between patients, and recovery times can take weeks or months. In this research, we aim to better characterize how different 'heel drop' routines improve tendon healing, providing a foundation for determining the intensity and duration of rehabilitative exercises that can be applied for better clinical outcomes.

To examine the effects of different eccentric-based loading profiles, we used a previously developed mouse model of chronic Achilles tendinopathy and customizable muscle stimulation device to simulate human physical therapy exercises at different intensity levels: full body weight (100%), assisted body weight (75%), and half body weight (50%). Prior to beginning treatments, we induced a tendon injury that mimics human injury and measured muscle strength before any exercise was performed. Mice were then introduced to muscle loading treatments that mimic clinical exercise routines: 3 sets of 10 heel drops, performed twice a week for 1-, 2- or 4-weeks. After the final day of exercise, muscle strength was measured again to see how the heel drop exercises impacted the muscle tissue. Tendons were collected and the mechanical properties, histologic changes, and transcriptomic adaptations were evaluated. Eccentric-based exercises improved the mechanical properties injured tendons and improved the architecture compared to

injured/untreated controls. Injured tendons without treatment had inferior tendon mechanical properties and inferior structural changes. We also saw improved tissue changes and upregulation of genes responsible for tendon healing after exercise compared to naïve or injured/untreated mice. Our research demonstrates that performing consistent eccentric-based exercises for 2 or more weeks positively impacts tendon healing.

Acknowledgements

This has been a whirlwind experience! As an undergraduate student, I would have never thought that after 11 years I would still be in school… but, I am so glad I stuck with it. I would not be here today without the countless people who have been so influential during my education. Firstly, I must acknowledge Dr. Wang, you have been a constant source of guidance, support, and confidence. I am truly at a loss on how to describe the tremendous impact you have had on my life. You have inspired me to be a better researcher, and role model for those around me and I am eternally grateful for your mentorship. I hope to emulate all that you have taught me as I move forward with my career. I also want to express my deepest gratitude to Dr. Dahlgren. You always push me to expand my knowledge, skills, and to go past my comfort zone. Throughout this process you were always a wealth of knowledge that I could count on to help me in the right direction. Your leadership allowed me to develop a diverse skillset and evaluate every step of the process no matter how new it was to me. I would not have been able to reach this stage if it wasn't for the two of you and for that I am beyond appreciative. Dr. Theus, your unyielding confidence in me has not gone unnoticed. While our research areas did not overlap, I knew I could always reach out to you if I had any question or needed advice. Your presence during this process has been so influential and I hope to be as compassionate and insightful moving forward. Dr. Grange- thank you for allowing me access to your lab spaces to complete my projects and facilitating this collaborative process. Dr. Brolinson and Dr. Li, thank you for the direction, your availability, and for pushing me when I needed. I greatly appreciate your diverse outlooks to make me critically think through all aspects of my projects.

My family has always been there to support me through this process, even if you did not fully understand what I was doing. You have always shown me that I can finish anything if I put my mind to it. Through all of my ventures, you have been there when I needed and cheering me on the whole way even if it meant freezing during my graduation ceremony or baking in the Texas heat while moving. I love you all to the moon and back!

Finally, to my friends and lab mates- thank you for putting up with me. I do not know if I would have been able to get through this without you. From the weekly or sometimes daily coffee sessions to the late nights spent trying to finish up just one more sample, I appreciate you being there to

listen to me vent or telling me to calm down. I know I can count on each of you to pull me up when I am down, and you rein me in when needed. There are too many to list individually, but you all have had a tremendous influence on my life, and you are all truly amazing people and I wish you nothing but the best wherever life takes you!

Table of Contents

List of Figures x
List of Tables xiv
Chapter 1 - Introduction 1
1.1 Background 1
1.2 Objectives and Hypotheses 1
1.3 Specific Aims 2
References 4
Chapter 2 - Literature Review 6
2.1 Tendons: Structure and Function 6
2.2 Tendon Biomechanics 10
2.3 Tendon Injuries, Animal Models, and Natural Repair Process 12
2.3.1 Acute and Chronic Tendon Injuries 12
2.3.2 Animal Models of Tendon Injuries 13
2.3.3 Natural Repair Process 14
2.4 Tendinopathy 15
2.4.1 Morphological and Cellular Changes of Tendinopathy 16
2.4.2 Clinical Management Practices 18
2.4.3 Muscle Loading Therapies 19
References: 22
Chapter 3 - Treatment Duration and Load Magnitude Differentially Affect Biomechanical Properties in a Preclinical Model of Achilles 49
3.1 Introduction 49
3.1.1 Achilles Tendinopathy and Treatments 49
3.1.2 Muscle Loading Therapies 49
3.1.3 Pre-clinical Exercise Models 50
3.2 Materials and Methods 51
3.2.1 Experimental Design 51
3.2.2 Animals 51
3.2.3 Tendinopathy Induction 52
3.2.3 Tissue Targeted Muscle Loading and *In Vivo* Muscle Strength Measures 54
3.2.4 Eccentric Loading Protocols 57
3.2.7 Biomechanical Testing 59

3.2.8 Histology 62
3.2.9 Statistical Analysis 63
3.3 Results 63
3.3.1 Muscle Strength Evaluations 63
3.3.1 Effects of Eccentric Loading Magnitude and Duration on Tendon Healing 66
3.3.2 Histological Evaluation of Tendon from Different Eccentric Loading Protocols 71
3.4 Discussion 76
3.5 Conclusions 79
3.6 Acknowledgements 80
References: 81
Chapter 4 - Transcriptional Adaptations to Muscle Loading in a Murine Model of Achilles Tendinopathy 90
4.1 Introduction 90
4.1.1 Achilles Tendinopathy and Current Treatments 90
4.1.2 Rehabilitative Exercises 90
4.1.3 Tendon Cellular Response to Mechanical Loading 91
4.2 Materials and Methods 92
4.2.1 Animals 92
4.2.2 Experimental Design 92
4.2.3 Tendinopathy Induction 93
4.2.4 Tissue Targeted Muscle Loading 95
4.2.5 Eccentric Loading Protocol 95
4.2.6 RNA sequencing in Isolated Achilles Tendons 96
4.2.7 RNA Sequencing Pipeline and Statistical Analysis 97
4.3 Results 98
Differential Gene Expression 98
Co-Expression Network Analysis from Tendon in Response to Exercise 102
4.4 Discussion 109
4.5 Conclusions 111
4.6 Acknowledgements 111
References: 112
Chapter 5- Conclusions and Future Directions 119
Appendix A 121

Appendix B 148
Appendix C 159

List of Figures

Figure 2.1*:* Schematic of the tendon hierarchical structure [7]. 7

Figure 2.2: Schematic of the stress-strain relationship curve of tendon tissue and its components. 11

Figure 2.3: Schematic of the morphological differences between naïve and tendinopathic tissue [169]. 16

Figure 3.1: Human heel drop loading exercises. Range of motion dorsiflexion (left), plantarflexion (middle), and return to dorsiflexion (right). 50

Figure 3.2: Locations of the TGF-β1 injections in the Achilles tendon (midportion and distal) [51]. 53

Figure 3.3: Tendinopathy induction and treatment timeline. Mice in treatment groups received treatment twice weekly for either 1-, 2-, or 4-weeks. Upon the conclusion of the treatment duration, mice were euthanized, and tendons harvested for biomechanical testing (50%, 75% and 100% BW) and histology (50% and 100% BW). 54

Figure 3.4: In vivo murine muscle loading set up. Insert to the right shows the (a) footplate to rotate the ankle through its range of motion and (b) electrodes to stimulate the tibial nerve to produce muscle contraction. 55

Figure 3.5: Overview of electrode stimulation pattern and footplate movement through one repetition of the exercise routine. Electrodes were stimulated in conjunction with the footplate movement to mimic physical therapy exercises. Length corresponds to the movement of the footplate, with a negative values denoting dorsiflexion and positive values denoting plantarflexion. 56

Figure 3.6: Dissected Achilles tendon-calcaneus unit set into MTS Insight 10 for biomechanical testing. Inset at right shows potted foot and attached Achilles tendon under preload. 60

Figure 3.7: Initial in vivo muscle strength collected prior to experimental muscle stimulation. 100 Hz outlined in the orange rectangle. * denotes a significant difference from the naïve group. Mean ± SD. 64

Figure 3.8: In vivo muscle strength after 1 (A), 2 (B), and 4 (C) weeks of treatment and over time within treatments (at 100 Hz). Muscle strength decreased significantly when measured at 100 Hz for all 3 treatment durations compared to the naïve group as indicated by * (highlighted by orange box). Significant differences over time within a single treatment group (D) indicated by colored lines. A) The 50% BW, 100% BW, and IU groups muscle strength was significantly lower than the naïve group at 1 week. B) The 75% BW and 100% BW was significantly lower than the naïve group at 2 weeks. C) The 50% and 75% BW groups were significantly lower than the naive group at 4 weeks. Mean ± SD. 66

Figure 3.9: Biomechanical properties of healing Achilles tendons following 1 week of muscle loading. Horizontal lines denote significant differences between two groups ($p<0.05$). 67

Figure 3.10: Biomechanical properties of healing Achilles tendons following 2 weeks of muscle loading. Symbols above groups denote differences from the naïve group ($p<0.05$). Horizontal lines denote significant differences between two groups ($p<0.05$). 68

Figure 3.11: Biomechanical properties of healing Achilles tendons following 4 weeks of muscle loading. Horizontal lines denote significant differences between two groups ($p<0.05$). 69

Figure 3.12: Biomechanical properties of healing Achilles tendons over time. * Indicates significant differences between groups at that time point ($p<0.05$). Mean ± SD. 70

Figure 3.13: Representative low magnification images of Toluidine Blue- (Top) and Safranin-O/Fast Green-stained (Bottom) naïve Achilles tendon showing cellularity in muscle and tendon and collagen orientation. M: Muscle, T: Tendon. Left of images is proximal. 72

Figure 3.14: Representative Toluidine Blue- (A, C, E) and Safranin-O/Fast Green-stained (B, D, F) Achilles tendons after 1 week of exercise showing increased cellularity, collagen orientation, and Safranin-O staining intensity between the 50% BW, 100% BW and Injured/Untreated groups.

Top left: 50% BW, Top right: 100% BW, Bottom Injured/Untreated. M: Muscle, T: Tendon. Left side of each image is proximal..... 73

Figure 3.15: Representative Toluidine Blue (A., C., & E.) and Safranin-O/Fast Green (B., D., & F.) stained tissues at 2 weeks of exercise showing increased cellularity, collagen orientation, and Safranin-O staining intensity between the 50% BW, 100% BW and Injured/Untreated groups. Top left: 50% BW, Top right: 100% BW, Bottom Injured/Untreated. M: Muscle, T: Tendon. Left of side of images is proximal..... 74

Figure 3.16: Representative Toluidine Blue (A. & C.) and Safranin-O/Fast Green (B. & D.) stained tissues at 4 weeks of exercise showing increased cellularity, collagen orientation, and Safranin-O staining intensity between the 50% BW and 100% BW groups. Top left: 50% BW, Top right: 100% BW, Bottom Injured/untreated. Left of images is proximal. 75

Figure 3.17: Representative Toluidine Blue (A. & C.) and Safranin-O/Fast Green (B. & D.) of the injured untreated tendons at 4 weeks. Left: Midportion of Achilles tendon. Right: Insert showing intense Safranin-O staining highlighting sulfated GAG concentration. Left of images is proximal. 76

Figure 4.1: Principal component analysis from the entire transcriptome (49,437 genes) showing the different patterns of gene expression in response to TGF-β1 model induction and muscle loading over 4 weeks in response to no exercise (IU) and 50% and 100% body weight loading. Naïve tendons served as baseline gene expression controls. Each dot represents an individual sample. 99

Figure 4.2: Numbers of differentially expressed genes between treatment groups over time and between treatment groups at each time point. Naïve controls served as normal tendon and a basis for comparison following induction of the injury model and exercise at 50% or 100% BW loading or IU controls. Numbers of upregulated genes are in shown in red and numbers of downregulated genes in blue..... 100

Figure 4.3: Heatmap of weighted gene co-expression network analysis (WGCNA) module-trait relationships. Top number is R^2 with the associated p value below for each module-trait relationship. The brown (50% BW), and red and yellow (100% BW) modules were significantly positively associated with loading at 2 weeks and the grey module was significantly negatively associated with the injured/untreated group at 2 weeks. 103

Figure 4.4: Mean expression profile (mean GeTMM values for all genes) for each significant eigengene module positively associated with exercise plotted over time for both exercise groups (50% and 100% BW). Expression in the yellow module was highest, increased from 1 to 2 weeks then decreased by 4 weeks. Expression of the red module was intermediate and showed a similar pattern with a lower magnitude of differential expression. Expression in the brown module was much lower and more static over time. 104

Figure 4.5: Mean expression profile (mean GeTMM values for all genes) of significant eigengene module negatively associated with the injured/untreated group showing relatively low expression and a steady increase in expression over time. 105

List of Tables

Table 2.1: Percentages of collagen and non-collagen components of tendon tissues [13-16]..... 8

Table 3.1: Experimental design outlining treatment groups, treatment duration, and outcome measures with the associated number of mice included per group..... 58

Table 3.2: List of biomechanical properties and respective units..... 61

Table 3.3: Histology grading scale used to identify morphological and cellular changes in response to TGF-β1 injury induction and muscle loading treatments..... 62

Table 4. 1 Treatment groups, treatment durations, and animal usage for each group. 94

Table 4.2 Number of differentially expresses genes (upregulated and downregulated) for each comparison of interest. 101

Table 4.3: Significantly expressed modules and associated treatment group. 104

Table 4. 5: Overrepresented biological processes in yellow module and their corresponding fold enrichment and p-value. 106

Table 4. 4: Overrepresented biological processes in the red module and their corresponding fold enrichment and p-value. 106

Table 4. 6: Overrepresented biological processes in brown module and their corresponding fold enrichment and p-value. 108

Table 4. 7: Overrepresented biological processes in grey module and their corresponding fold enrichment and p-value. 108

Chapter 1 - Introduction

1.1 Background

Tendons function to transfer forces between muscle and bone to facilitate movement. Consequently, they must withstand periods of intense forces and accumulate damage from daily activities, making them susceptible to both acute and chronic injuries. Approximately 46 million Americans suffer from tendon injuries each year, with 67% experiencing tendon reinjury [1]. Tendinopathies are chronic injuries caused by an accumulation of damage from daily activities and can be debilitating. If left untreated, tendinopathy can result in persistent pain, reduced mobility, loss of function, and can even lead to rupture of the tendon [2-4]**.** Current treatment strategies are fairly limited to surgical techniques, pain management, and conservative therapies (e.g. anti-inflammatory drugs, biologic injectables, therapeutic ultrasound, and debridement), all of which result in poor long-term outcomes and increased risk of reinjury [5, 6]. Although, Achilles tendinopathy (AT) remain challenging to treat, they respond positively to physical therapy treatments (eccentric-based muscle loading) have been shown to provide symptomatic relief [7].

Eccentric loading exercises (lengthening of the muscle while it contracts) can be used to stimulate the Achilles-muscle unit. “Heel Drop” exercises are commonly prescribed for Achilles tendinopathy (AT) patients to provide pain relief, reduce swelling, and improve functional mobility. However, there is a lack of standardization of prescribed loading interventions and the mechanism of tendon healing is poorly understood [8-10]. Loading protocols vary widely (ranging from weeks to months) and it remains unclear if high, intermediate, or low loading magnitudes are more beneficial to the healing of Achilles tendon-muscle complex.

1.2 Objectives and Hypotheses

Recent studies have shown that eccentric loading protocols enhance the healing of AT [11-13]; however, they do not characterize the effects of different loading magnitudes and treatment durations. Furthermore, they do not expand on muscle function, transcriptomic changes, or morphological adaptations in response to rehabilitative loading. To investigate the effects of

eccentric loading on tendon healing, we used a modified version of a previously established preclinical model of Achilles tendinopathy and eccentric hind limb muscle loading [11, 14, 15]. **The central objective of this project was to provide a comprehensive analysis of the musculotendinous unit adaptations in response to different loading protocols while characterizing the mechanisms by which eccentric muscle loading improves tendon healing**. We hypothesized that as eccentric muscle loading magnitude and treatment duration increased there would be significant improvements in the biomechanical properties of injured Achilles tendons, morphological improvements, and upregulation of signaling and metabolic networks associated with extracellular matrix production and organization, focal adhesions, and oxidative stress.

1.3 Specific Aims

Current literature supports the efficacy of eccentric loading exercises for the treatment of AT [8, 10, 11]. However, tendon healing is complex and often varies between patients due to intrinsic and extrinsic factors. Loading regimes can be prescribed over the course of several weeks or months with variation in the amount of healing achieved. Furthermore, the degree of healing is classified based on the functional resolution of symptoms and not an evaluation of tendon mechanical properties and there is a lack of characterization of specific tissue modifications. *We hypothesized that more intense loading magnitudes and longer treatment durations would improve the healing response of injured Achilles tendons.* Additionally, we hypothesized that loading protocols would upregulate genes required for extracellular matrix remodeling, inflammatory regulation, and cellular signaling.

Aim 1: <u>Compare the healing response among three muscle loading magnitudes and three treatment durations for improved tendon healing</u>.

Evaluate the biomechanical properties, muscle strength, and morphological adaptations of injured Achilles tendons using an established preclinical murine model. Two days following the induction of Achilles tendinopathy, the plantar-flexion muscle tendon complex received an eccentric loading therapy simulating 50%, 75%, or 100% of body weight loading for 1, 2, or 4 weeks of treatment.

Loading was performed twice a week for each of the 3 treatment durations and consisted of 3 sets of 10 repetitions.

We hypothesized that increasing loading magnitude and treatment duration would result in tendon healing that exhibited superior Achilles tendon biomechanical properties to injured untreated groups at matched timepoints.

Aim 2: Identify differentially regulated signaling and metabolic pathways involved in the adaptive response to tendon healing following eccentric muscle loading.

Performed in parallel with Aim 1, using the 50% BW and 100% BW groups (loading magnitude and treatment duration) we catalogued the transcriptomic response to the different rehabilitative loading protocols.

We hypothesized that metabolic and signaling pathways associated with extracellular matrix remodeling regulation, focal adhesions, and oxidative stress would be upregulated in groups that received eccentric loading treatments.

Successful completion of these studies will elucidate mechanisms by which rehabilitative loading protocols stimulate tendon healing in chronically damaged tendons. Additionally, it will characterize the adaptations of the tendon-muscle unit and the alterations to tendon mechanics and muscle strength. By understanding the musculotendinous modifications and underlying healing mechanisms, we hope to provide a foundation for clinical applications of eccentric loading therapies for robust tendon healing. Exploration of these healing mechanisms can then be used as targets of future therapeutic approaches, ultimately translating to advancements in tendon healing and furthering the understanding behind the effectiveness of eccentric-based muscle loading.

References:

1. Rajpar I, Barrett JG. Multi-differentiation potential is necessary for optimal tenogenesis of tendon stem cells. *Stem Cell Res Ther*. 2020;11(1):152. Published 2020 Apr 9. doi:10.1186/s13287-020-01640-8
2. Yasui Y, Tonogai I, Rosenbaum AJ, Shimozono Y, Kawano H, Kennedy JG. The Risk of Achilles Tendon Rupture in the Patients with Achilles Tendinopathy: Healthcare Database Analysis in the United States. *Biomed Res Int*. 2017;2017:7021862. doi:10.1155/2017/7021862
3. Longo UG, Ronga M, Maffulli N. Achilles tendinopathy. *Sports Med Arthrosc Rev*. 2009;17(2):112-126. doi:10.1097/JSA.0b013e3181a3d625
4. Nourissat G, Berenbaum F, Duprez D. Tendon injury: from biology to tendon repair. *Nat Rev Rheumatol*. 2015;11(4):223-233. doi:10.1038/nrrheum.2015.26
5. Cardoso TB, Pizzari T, Kinsella R, Hope D, Cook JL. Current trends in tendinopathy management. *Best Pract Res Clin Rheumatol*. 2019;33(1):122-140. doi:10.1016/j.berh.2019.02.001
6. Maffulli N, Longo UG, Denaro V. Novel approaches for the management of tendinopathy. *J Bone Joint Surg Am*. 2010;92(15):2604-2613. doi:10.2106/JBJS.I.01744
7. Kujala UM, Sarna S, Kaprio J. Cumulative incidence of achilles tendon rupture and tendinopathy in male former elite athletes. *Clin J Sport Med*. 2005;15(3):133-135. doi:10.1097/01.jsm.0000165347.55638.23
8. Rees JD, Lichtwark GA, Wolman RL, Wilson AM. The mechanism for efficacy of eccentric loading in Achilles tendon injury; an in vivo study in humans. *Rheumatology (Oxford)*. 2008;47(10):1493-1497. doi:10.1093/rheumatology/ken262
9. Silbernagel KG, Brorsson A, Lundberg M. The majority of patients with Achilles tendinopathy recover fully when treated with exercise alone: a 5-year follow-up. *Am J Sports Med*. 2011;39(3):607-613. doi:10.1177/0363546510384789
10. Yu J, Park D, Lee G. Effect of eccentric strengthening on pain, muscle strength, endurance, and functional fitness factors in male patients with achilles tendinopathy. *Am J Phys Med Rehabil*. 2013;92(1):68-76. doi:10.1097/PHM.0b013e31826eda63

11. Rezvani SN, Nichols AEC, Grange RW, Dahlgren LA, Brolinson PG, Wang VM. A novel murine muscle loading model to investigate Achilles musculotendinous adaptation. *J Appl Physiol (1985)*. 2021;130(4):1043-1051. doi:10.1152/japplphysiol.00638.2020
12. O'Neill S, Watson PJ, Barry S. WHY ARE ECCENTRIC EXERCISES EFFECTIVE FOR ACHILLES TENDINOPATHY?. *Int J Sports Phys Ther*. 2015;10(4):552-562.
13. Silbernagel KG. Does one size fit all when it comes to exercise treatment for Achilles tendinopathy?. *J Orthop Sports Phys Ther*. 2014;44(2):42-44. doi:10.2519/jospt.2014.0103
14. Bell R, Li J, Gorski DJ, et al. Controlled treadmill exercise eliminates chondroid deposits and restores tensile properties in a new murine tendinopathy model. *J Biomech*. 2013;46(3):498-505. doi:10.1016/j.jbiomech.2012.10.020
15. Bell R, Li J, Shewman EF, et al. ADAMTS5 is required for biomechanically-stimulated healing of murine tendinopathy. *J Orthop Res*. 2013;31(10):1540-1548. doi:10.1002/jor.22398

Chapter 2 - Literature Review

2.1 Tendons: Structure and Function

Tendons are dense fibrous tissues that transfer forces between muscle and bone to facilitate movement. Under normal conditions, tendons are predominantly subjected to tensile forces, but they can also endure compressive and shear forces where they interface with bone or muscle. Tendons have a specific hierarchical organizational structure that allows them to withstand intense forces over a relatively short length (Figure 2.1) [1-3]. The mechanical properties of tendons are dependent upon their unique extracellular matrix (ECM) composition. The principal components of the ECM are collagen fibrils, proteoglycans, glycosaminoglycans, glycoproteins, and elastin. Collagen type I is the primary collagen type, making up 95% of all collagen content and 60%-85% of the total dry mass [4], while elastin comprises 1-2% of the total dry mass. Collagen types III, V, XI, XII, and XIV are present, but in drastically lower quantities [2, 5, 6].

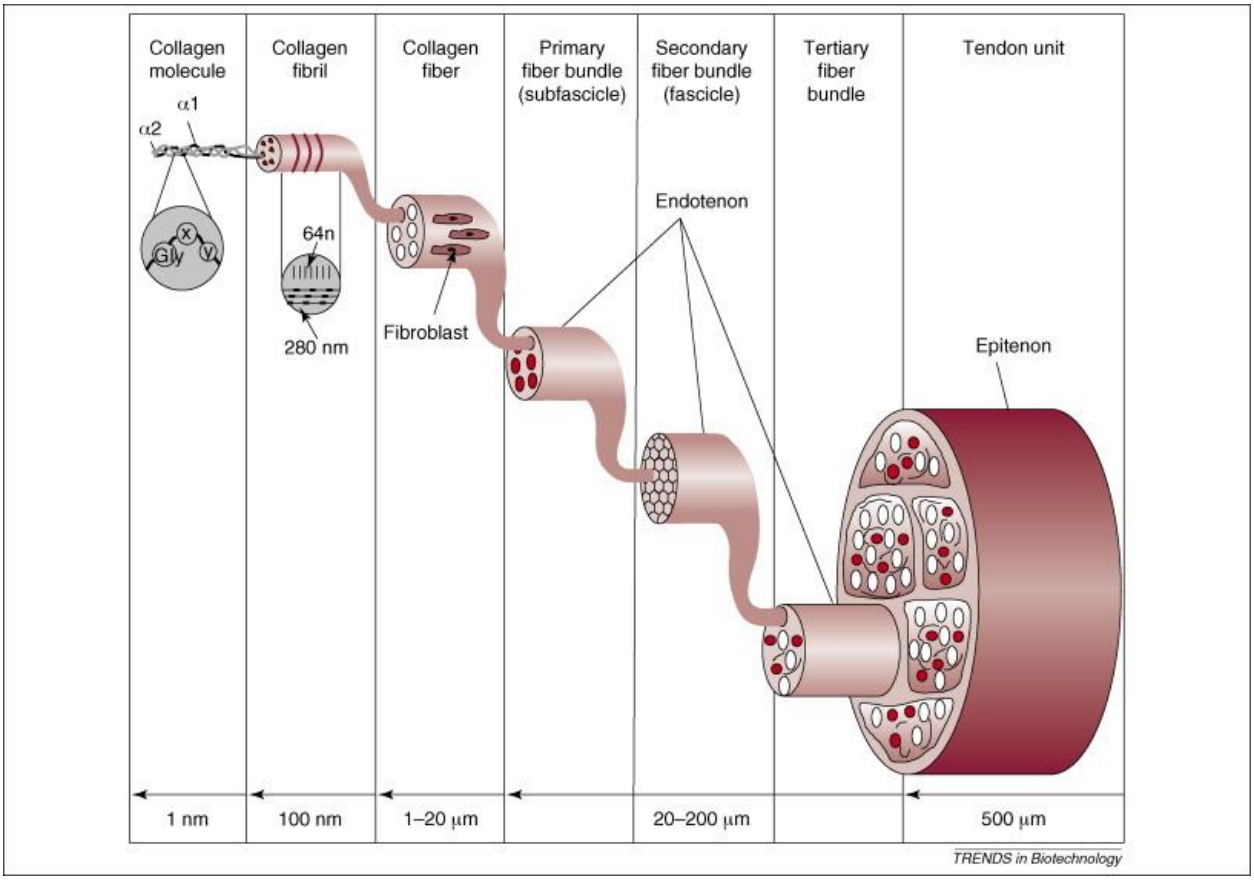

Figure 2.1*:* Schematic of the tendon hierarchical structure [7].

The foundation of the tendon unit is the collagen type I macromolecule made up of three collagen molecules in a triple helix arrangement [8]. These molecules adhere together during fibrillogenesis to form small (<100 nm diameter) collagen fibrils. Collagen fibrils align together in a parallel organization in the direction of their primary forces and are stabilized by covalent bonds. Multiple fibrils aggregate with proteoglycans and other collagen fibrils (types III and V) to form fibril bundles ranging in size from 10-20 μm in diameter [4, 9]. Fibril bundles then combine to form fascicles that are bound by the endotenon. Endotenon is a loose sheath that envelops the fiber bundles to aid with movement between the other fiber bundles. The epitenon encapsulates multiple endotenon bundles. Some tendons, including the Achilles tendon, are unique and have an additional outer layer to the sheath called the paratenon, which is composed of loose tissue. The vasculature, nerve, and lymphatic networks that service the tendon are predominantly in the endotenon, epitenon and paratenon [10]. Together the epitenon and paratenon are labeled as

peritenon, and its composition is similar to that of tendons, being predominantly collagen type I, while types III, IV, and V are present in lesser amounts (Table 2.1) [5, 11, 12].

Table 2.1: Percentages of collagen and non-collagen components of tendon tissues [13-16].

Components of Tendon Extracellular Matrix			
Collagen Components		**Non-collagen Components**	
Collagen 1	60-80%	Cartilage oligomeric matrix protein	~3%
Collagen 3	0-10%	Elastin	~2%
Collagen 4	2%	Proteoglycans	~2%
Collagen Types 5 & 6	<1%	Inorganic compounds	<1%

While collagen makes up the majority of tendon ECM, other components are just as vital to tendon function. Proteoglycans (PG), glycosaminoglycans (GAG), elastin, and glycoproteins [5] all play critical roles in the ECM of tendons. PG are comprised of a core protein and one or more negatively charged sulfated glycosaminoglycan chains and make up less than 0.2% of the overall dry weight of tendons. The negatively charged sulfate group gives them substantial hydrophilic properties. They can retain up to 50 times their weight in water, allowing them to rapidly diffuse water-soluble molecules and aid with cell migration [17]. This ability to retain water is one of contributing factors that allows collagen fibrils to withstand high tensile forces. Furthermore, PGs regulate the main structural component, collagen Type 1 [2, 18, 19]. Different types of forces exerted on tendon tissue result in the production of different PGs. Compressive forces initiate the production of aggrecan, a large (220 kDa) PG. Inversely, tensile forces result in the production of decorin, a small (36 kDa) leucine-rich PG (SLRP) [20-22]. There are several classes of SLRPs based on their N-terminus residue: Class I (cystine residue), which includes decorin (36kDa) and biglycan (38kDa)[20, 21], and Class II (tyrosine residue), which contains fibromodulin (42kDa) and lumican (38kDa)[2, 19]. These are the most well-defined classes of SLRPs that aid with the regulation of collagen fibrillogenisis and tendon health [19, 20, 23-25]. Additionally, they assist in the modulation of tendon/progenitor stem cell growth and development [26, 27]. Previous research has highlighted the role of decorin and biglycan in the regulation of tendon composition and function, each affecting different phases of development. Decorin levels peak during tendon development, whereas biglycan is noticeably higher during post-natal growth [28]. Fibromodulin and lumican are important regulators of collagen fibril shape, size, and orientation [29].

Glycosaminoglycans are linear polysaccharide compounds with repeating disaccharide units that are embedded in the ECM of tendons [30]. They play a key role in cellular signaling, cell hydration and structure, and modulation of biological processes, including those responsible for wound healing [31]. The disaccharide units can be altered based on sulfation, which gives them unique capabilities [32]. There are four sulfated GAGs: dermatan sulphate (DS), keratan sulphate (KS), chondroitin sulphate (CS), heparin sulphate (HS), and one non-sulphated GAG: hyaluronic acid (HA). Under normal homeostatic conditions, the negatively charged GAGs become enveloped in water, which is dispersed when the tendon is mechanically loaded, allowing them to withstand the loading. Water returns when the load dissipating [33-38]. DS and CS are the most prevalent GAGs in mature tendon tissue; DS controls collagen fibril assembly and size, while CS is important for aggregation of PG and matrix organization [34, 39, 40]. These two GAGs are vital for maintaining tendon elasticity, lubrication, and proper function.

Glycoproteins are composed of oligosaccharide chains that form covalent bonds with amino acid side chains. Fibronectin is a specific glycoprotein that has been shown to help regulate tendon remodeling and regeneration. Tenascin-C is an elastin protein that is expressed in the ECM and contributes to collagen fiber alignment and orientation, both of which are important to maintain tendon strength. Tenascin-C expression is regulated by mechanical strain and expression is upregulated during tendon injuries. Elastin constitutes approximately 2% of the total tendon mass, but can vary between tendons with specialized functions [41]. Tendons that regularly transfer mechanical forces (e.g., Achilles tendon) have higher concentrations of elastin compared to support tendons (e.g., anterior tibial tendon) [42]. Elastin content is responsible for the unique tensile characteristics of tendons [5, 11, 12].

A wide range of components contribute to the ECM structure and homeostasis of tendon tissue [43, 44]. Tendons are relatively hypocellular, and primarily (90-95%) composed of tenocytes and tenoblasts, which are responsible for ECM turnover, and collagen production and structuring [45-47]. Cells assemble in longitudinal rows between collagen fiber bundles [6]. Tendon cells are regenerated by the differentiation of tendon/progenitor stem cells [48, 49]. The remaining cell populations include endothelial and synovial cells in the tendon sheath, as well as chondrocyte-like cells at tendon-bone interfaces, respectively [4, 50, 51]. When tendons experience mechanical stress, resident tenocytes sense the force and stretch along with the collagen fibrils. This stretching

triggers cytoskeleton and chemical changes, which translate to signaling changes within the cells to produce more collagen. By adjusting their alignment and cell-cell and cell-ECM communication due to the mechanical environment, tenocytes ultimately remodel the composition and structure of the surrounding ECM [52-54].

2.2 Tendon Biomechanics

The mechanical properties of tendons are highly dependent upon their hierarchical structure, collagen organization, and non-collagenous components. Tendons are exposed to a variety of forces, including tensile, shear, rotational, and compressive forces. Tendons are physiologically designed to distribute tensile forces generated from muscle tissue to bone [9]. The complex structure of tendons allows them to exhibit flexibility, viscoelastic properties, and resistance to high mechanical loads. The forces tendons are subjected to are dependent upon the anatomical location, size, shape, and frequency/intensity of use [55]. Tendons are considered viscoelastic, meaning they exhibit both viscous and elastic properties to resist damage from loading. When under constant strain, the stress in the tissue decreases (stress-relaxation), but when under constant stress, the strain in the tendon increases (creep) [56]. The viscoelastic capacity of tendons is predominantly from collagen and the molecular interactions between PGs and the surrounding fibrils, with their hydrophilic capacity aiding with lubrication [17].

The stress-strain curve, a function of tissue displacement in response to increasing mechanical load, demonstrates a specific shape for tendon (Figure 2.2 [57]). This unique relationship between tendon tissue and the forces exerted on it is characterized by 4 distinct regions: a toe region, a linear region, a yield point, and a failure region. Tendon tissue behaves differently in each phase. When tendon fibers are in a relaxed state, they display a crimped orientation [58, 59], which helps withstand lower strain levels. The collagen fibrils begin to uncrimp as load increases, dissipating the energy that the load is generating without causing damage. This uncrimping occurs in the minimal loading of the toe region [60, 61]. Within the linear region, the load increases and the fibrils become uncrimped and glide against one another in the same direction in which the load is being applied, increasing the stiffness of the tendon [61-63]. In people, most of normal physiological loading occurs within the toe and linear regions. These two regions are referred to as the elastic region, which can reach strain levels of approximately 4% without altering tendon

structure [63-66]. Conversely, once the yield point has been reached (between 4-10% strain) [67], the tendon begins to deform plastically, resulting in significant damage to the tissue. Once it has reached the yield point, tendon can no longer return to its naïve physiological properties once the load is removed. Beyond the plastic region, the tissue reaches the failure point and is completely deformed (approximately 16% strain) [68].

The viscoelastic properties of tendon are dependent upon the rate at which the force is applied to the tendon and are defined by three main characteristics: creep, stress-relaxation, and hysteresis [69, 70]. Creep is the increase in deformation under constant loading, stress-relaxation describes the stress under constant deformative loading, and hysteresis is the energy lost during repetitive loading cycles. Damage accumulation in tendons occurs when the strain within the tissue exceeds the viscoelastic capacity of the constituents of the tendon tissue [71, 72].

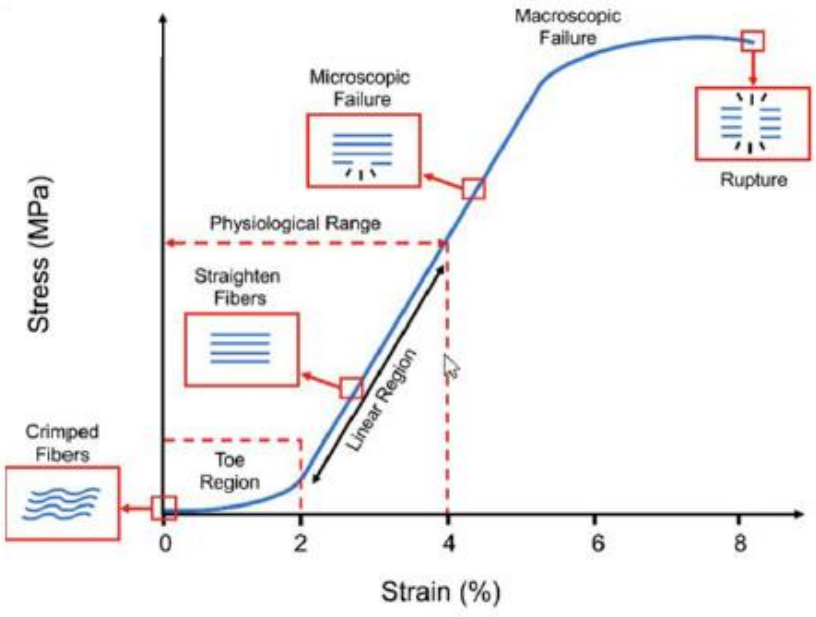

Figure 2.2: Schematic of the stress-strain relationship curve of tendon tissue and its components.

Physiologically tolerable mechanical loading is advantageous for tendon health [73, 74]. It is well documented that mechanical stimulation is crucial for maintaining a homeostatic environment and the interactions between the molecular components of tendon tissue [52, 55, 75, 76]. Mechanical loading upregulates growth factors responsible for collagen synthesis and cellular signaling [22, 77, 78]. Mechanical stimulation that is greater or less than ideal can have damaging effects. Overstimulating forces can lead to minor tears or acute injuries, while understimulation can lead to tissue degradation, impairing mechanical function [79-81].

2.3 Tendon Injuries, Animal Models, and Natural Repair Process

2.3.1 Acute and Chronic Tendon Injuries

Tendon injuries have two distinct etiologies: acute or chronic. Acute injuries occur suddenly, usually due to a fall or dramatically overloading the tissue, and result in a partial tear or complete rupture of the tendon. Following acute injury there is an increase in localized inflammation followed by new ECM formation and matrix remodeling. Chronic injuries or tendinopathies are characterized by pain, swelling and impaired mobility. To date, the exact pathogenesis is not fully defined, but it is believed to stem from overaccumulation of microdamage from habitual overuse without adequate recovery time [82, 83]. Microdamage leads to ECM disruption and structural deformity, reducing the mechanical function of tendon and making it susceptible to further damage or catastrophic failure [83-87]**.**

Tendon injuries are more common in aging and athletic populations [71, 88, 89]. They are becoming increasingly more common throughout all populations due to increases in working age, life expectancies, and the popularity of physically strenuous recreational activities [89]. Approximately 50% of all soft tissue injuries involve tendons, and tendinopathies are the leading diagnosis, accounting for approximately 30% of all reported injuries diagnosed [90, 91]. The development of tendinopathy is multifactorial and includes age, sex, athletic capacity, and genetic factors [74]. Furthermore, tendons have a poor natural healing response, leading to prolonged recovery periods and incomplete return of tissue strength. Further compounding issues, healing is determined by tendon type, location, and functionality. The Achilles tendon and other

extrasynovial tendons often respond to injury by forming fibrous tissue deposits that develop into scar tissue with the injured tendon never returning to its prior material properties [53, 83, 92]. Intrasynovial tendons (e.g., digital flexor tendons) exhibit an inferior intrinsic healing response [92-94].

2.3.2 Animal Models of Tendon Injuries

Human tendon injuries are particularly challenging to study for a variety of reasons, including insidious disease onset, tissue procurement, injury causation, and an incomplete understanding of the healing mechanism. These factors make animal models an attractive alternative to study tendon injuries. Models can be divided into categories based on whether the injury is acute or chronic. Tendon healing has been predominantly investigated using acute models (transections) or induced tendon insults that lead to chronic injury [11, 46, 95-99].

To address the limitations of studying human tendinopathies, several preclinical overuse models have been developed [74, 100-104]. Treadmill running can be adapted to rodent models to induce tendinopathies similar to those observed in athletic human populations [105-110]. Mice or rats are subjected to intense sessions of treadmill running to overstimulate the tendon. The orientation angle (incline or decline) of the treadmill can be adjusted to induce overuse in the hind or forelimb, respectively [111-113]. Another rodent model used to mimic tendinopathy is *in vivo* tendon fatigue, where the tissue is repeatedly loaded to increasing levels of force and time until it is unable to effectively respond [106, 114, 115]. However, these methods all have their shortcomings, particularly the time and effort required to induce the injury and the variability with which the injury can be reproduced [116]. Alternatively, biochemical methods, such as injection of collagenase, cytokines, or transforming growth factor (TGF)-β1 have been used to target and corrupt the ECM of tendons in a variety of species [117-123].

The majority of the progress to better understand the healing cascade has been made through the use of surgical repair following tendon transection. Researchers have discovered several underlying genes responsible for modulating the tendon's healing response in partial tears and full detachment of the supraspinatus tendon [124, 125]. The effects of mechanical stimulation (cyclical

or fatigue) have been well documented using repetitive loading to induce a healing response [71, 114]. *In vitro* cell culture and *ex vivo* tendon explant models show improvements with cellular proliferation and tissue properties post-stimulation [126-128]. Recently, an innovative and reproducible model was developed using TGF-β1 injection to induce Achilles tendinopathy in adult mice [112, 113, 121, 129-131]. In this murine model, intratendinous injection of active human recombinant TGF-β1 injections resulted in increased interfibrillar GAG deposits, increased chondrocyte-like cells, and a loss of collagen fiber alignment surrounding the areas of increased GAG 2 and 4 weeks post injection [121]. These finding are consistent with the manifestation seen in human tendinopathy [121]. Furthermore, this model is adaptable to multiple therapeutic models., such as muscle loading and therapeutic ultrasound [132].

2.3.3 Natural Repair Process

The healing mechanism of tendon injuries are based on their etiologies: acute or chronic manifestations [27, 85]. The healing response occurs in overlapping but distinct phases: inflammation, cellular proliferation, and ECM remodeling [46, 83]. Notably, the healing process in tendon often does not completely restore the tissue to its normal hierarchical organization and the results is scar tissue formation rather than native tendon [83]. This newly formed scar tissue is has an increased percentage of collagen type III and fails to completely remodeling to a highly organized matrix that is seen in naïve tendon [133]. The inflammatory phase begins directly after injury onset and lasts 3-7 days [134]. Initially, it manifests as a marked increase in platelet activation, initiating cytokine-mediated inflammatory response and recruitment of immune cells, such as monocytes, neutrophils, and lymphocytes [134]. Interleukin (IL)-1β, IL-12, tumor necrosis factor (TNF)-α, and other cytokines control the inflammatory response by signaling proinflammatory macrophages. Proinflammatory macrophages initiate fibroblast recruitment andproliferation, and scar-tissue formation and inflammation [135]. Proresolving macrophages are recruited to the injury site later in the healing cascade to regulate inflammation, phagocytosis, matrix remodeling and reabsorption [136-138]. Macrophages vary their phenotype in response to the environment and work in what may seem like contradictory ways to modulate the healing response over time. A balance between inflammation and resolution of inflammation once healing has occurred results in tissue homeostasis. An imbalance in the process can lead to chronic inflammation and ongoing disease. The inflammatory phase is critical for an effective healing

cascade as the influx of immune cells increases fibroblast recruitment to the injury area [136, 139]. Equally important is a finite end to the inflammatory phase to prevent impaired healing [140].

The proliferation stage is defined by fibroblast recruitment and proliferation, resulting in increased collagen synthesis. The temporary collagen type III serves as a scaffold to guide repair the ECM. Fibroblast proliferation is stimulated by several growth factors (i.e., basic fibroblast growth factor, TGF-β1, and vascular endothelial growth factor) that initiate migration from the surrounding epitenon and endotenon. TGF-β is a key regulator during tendon development and promoter of matrix remodeling, with the TGF-β1 and TGF-β2 isoforms acting as the dominant growth factors responsible for scar-mediated wound healing [141, 142]. The majority of fiber and tenocyte alignment and component assembly are completed between the proliferation and remodeling phases. There is a transition from collagen III scar tissue to collagen type I and a reduction of GAG concentration that begins months post injury [143]. However, during the proliferation phase, prior to remodeling, the scar tissue displays inferior mechanical and biomechanical properties due to disorganization of collagen fibers and reduced size of collagen fibrils [3, 5, 134, 144]. Tendinopathy is likely the result of an accumulation of microdamage and a failure of the normal healing process.

2.4 Tendinopathy

Tendinopathy is broadly classified as an incomplete or flawed healing response that causes pain, loss of function, and risk of complete rupture if left unmanaged [145, 146]. Tendinopathy does not result due to a single failure event and can be exacerbated by several metabolic or environmental conditions [147-149]. Forms of metabolic dysregulation such as obesity, diabetes, and rheumatoid arthritis increase the likelihood of developing tendinopathy. Furthermore, age, exercise intensity, and treatment with some pharmacological agents (e.g., the antibiotics fluoroquinolone and ciprofloxacin) are key factors predisposing to tendinopathy [150-157]. Repetitive and excessive loading are thought to be the primary causative agent behind the development of tendinopathy [158, 159]. Daily activities accumulate microdamage, compromising tissue integrity, rather than a singular failure event [160]. Clinical presentations of tendinopathy include pain and swelling, and reduced mobility, which are caused by the dysregulated inflammatory response and resulting

negative alterations to the tissue structure [161]. Structural and cellular alterations to the tendon can further compromise tendon integrity [162, 163]. The end result is a significant negative impact on quality of life for those suffering from tendinopathy.

2.4.1 Morphological and Cellular Changes of Tendinopathy

Some of the most distinguishing histopathological changes of tendinopathic tissues include a loss of hierarchical organization of collagen, increased with rounded cell and misaligned collagen type I fibers with increased quantities of type III collagen fibers and neovascularization dispersed through the matrix [164-166]. Cellular alterations include tenocytes transitioning to a more chondrocyte-like phenotype and increase PG and GAG concentration within the ECM [90, 160, 167, 168]. These pathological changes further intensify the reduction of tendon strength compared to naïve tendon properties.

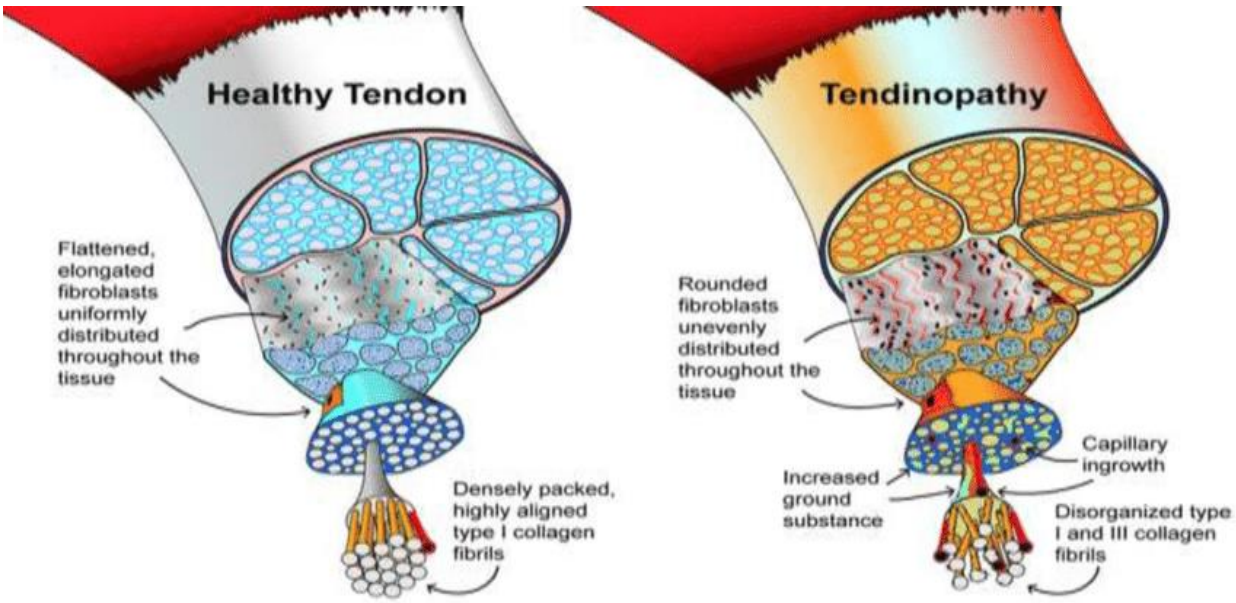

Figure 2.3: Schematic of the morphological differences between naïve and tendinopathic tissue [169].

Collagen fibers are highly organized into a compact parallel orientation, with non-collagen constituents situated in between the endotenon (Figure 2.3)[90]. Collagen fibers form interfibrillar and intrafibrillar cross-linking which facilitate a tendon's tensile strength [170, 171]. However, tendinopathic tendons are characterized by lack of collagen fiber alignment and a relative abundance of type III collagen fibers compared to normal tendon [169, 172, 173]. Rapid collagen type III deposition occurs during the proliferation phase of healing and initial collagen alignment is lacking, creating a "crosshatch" orientation. As collagen type III is gradually replaced with type I collagen, collagen linearity is restored. Human studies have shown that type I collagen synthesis is increased after strenuous exercise [174, 175]. Furthermore, TGF-β1, a stimulator of type I collagen production, is locally increased in human Achilles tendons after treadmill running [176]. During chronic disease development, collagen damage outpaces collagen synthesis, in part due to reduced expression of key transcription factors [90]. Matrix metalloproteinases (MMP), key regulators of ECM remodeling and turnover, are upregulated during tendinopathy, adversely altering the microstructure and composition of the tendon [177]. Non-collagen components (i.e., elastin, PG, GAG, and lubricin) aid with ECM assembly and function and regulate tenocyte growth and differentiation [2]. Alteration or absence of these non-collagen components can negatively impact the tendon's viscoelastic capacity, decreasing the mechanical properties of diseased tendons [85, 178]. Neovascularization is frequently observed in tendinopathy and it thought to spread fibrin-rich deposits into the tendon, causing fibroid disruption, degeneration and altering the tendon [179].

Various immune cells play a key role with the initiation and progression of tendinopathy [180-184]. Immune cells and tenocytes produce proinflammatory cytokines and chemokines that, when dysregulated, adversely affect tendon composition and function [185-187]. Tissue macrophages cells and the cytokines they produce are prime regulators of ECM remodeling [185]. Injury stimulates tenocytes and immune cells to produce growth factors (TGF-β and platelet-derived growth factor) and pro-inflammatory cytokines (TNF, interferon-γ, interleukins (i.e., IL-1β and IL-6) [188-190].

Prolonged running is one of the most common activities that leads to the development of tendinopathy and has shown to drastically increase local concentration of IL-6 [191]. IL-6 can have both pro- and anti-inflammatory actions, and closely regulates the production of collagen

synthesis [192]. An *in vitro* study using human-derived tendon cells demonstrated an inhibitory effect of TNF-α on collagen type I deposition with simultaneous upregulation of deleterious cytokine production [193]. Human tendon cells have been shown to produce several proinflammatory cytokines such as IL-1β, IL-6, IL-18, IL-33, C-C motif ligand 2. Production of IL-6, C-C motif ligand 2, and IL-18 was increased in human tendon explants increase following exposure to mechanical overloading of 9% strain [180]. In *in vitro* human tenocyte cultures and an *in vivo* murine model of tendinopathy, IL-33 is upregulated in the early stages of tendinopathy, implying a key role in the transition of collagen type I to type III [181, 194]. Damage-associated molecular patterns, such as alarmins, activate innate immune cells to begin the tissue repair process and, by association, maintain tendon homeostasis [190, 195, 196].

2.4.2 Clinical Management Practices

Current clinical management practices for chronic tendinopathy include surgical and conservative approaches. Nonsteroidal anti-inflammatory drugs (NSAIDs), injectable orthobiologic therapies (e.g., platelet-rich plasma), noninvasive stimulating therapies (e.g., shockwave and therapeutic ultrasound), and surgery to remove degraded tissue [197-201] are common treatments; however, they often result in poor long-term success and reinjury is common [202, 203]. NSAIDs provide temporary relief from inflammation and pain, but studies have shown that they interfere with the natural healing response by blocking the inflammatory phase of healing [204]. Injections of corticosteroids, local anesthetics, and saline have been utilized, but their efficacy is questionable, yielding inconclusive results [205, 206]. Platelet-rich plasma is an autologous blood-derived product containing enhanced concentrations of growth factors and proteins hypothesized to stimulate the healing response. Clinical trials have demonstrated that platelet-rich plasma performs similarly to saline injections to treat tendon injuries [207, 208]. Shockwave therapy has been effective at treating insertional tendinopathy, but is more advantageous when used in conjunction with eccentric loading protocols [209, 210].

Therapeutic ultrasound is used to treat injured tendon tissues and is an attractive noninvasive option to reduce pain and stimulate tendon healing [211-213]. It can be widely implemented and does not require physical loading and exercise routines, making it ideal for patients that are limited

by pain and lack of mobility. Though it has been sparsely studied in clinical trials with limited data regarding its efficacy (in both acute and chronic injuries), *in vitro* and *in vivo* studies have shown it increases cell proliferation and differentiation, reducing inflammation and tissue deposition [214-217]. However, the mechanisms by which therapeutic ultrasound may initiate tissue healing are still under investigation [214-217]. Dry needling and ultrasound-guided techniques such as percutaneous soft tissue release have also been used to treat tendinopathy [218-221]. Dry needling consists of repetitive ultrasound-guided needle insertions into the tendon to slow the progression of chondroid degeneration while promoting localized bleeding and fibroblast proliferation. However, inconsistencies in technique between practitioners with needling techniques and applications of the therapy have been reported [222]. Trials showed a reduction in pain in human patients after 4 months of treatment, but no reductions in tissue thickening [223-226]. Percutaneous soft tissue release aims to remove adhesions around the thickened peritenon and was effective in reducing inflammatory cell infiltration in preclinical murine models and reducing pain in people [219-221, 223]. Surgical treatment options (e.g., debridement or reattachment using sutures/anchors) are typically explored when conservative treatments are unsuccessful, but the likelihood of additional operations increases [227-229]. Human surgical procedures involve excision of the damaged and disorganized tissue followed by limb immobilization for the initial post-operative period until rehabilitative therapies are implemented [230, 231].

2.4.3 Muscle Loading Therapies

Physical therapy is a common treatment strategy to address chronic symptoms from Achilles tendinopathy and improve patient outcomes. Tendons are dynamic tissues that respond positively to mechanical stimulation to promote a more robust healing response. A variety of muscle loading approaches (i.e., heavy slow resistance training and eccentric-based therapies) have been prescribed to stimulate lower limb tendon healing [232-234]. Depending on anatomical location, severity, and injury type (acute or chronic), different loading protocols have shown varying success [235-237].

In the clinical management of Achilles tendinopathy in athletes, the rehabilitation process is divided into 4 phases: symptom management and load retention, recovery, rebuilding, and return

to activity [232]. The overarching goals are to manage symptoms in the early phases, then return the athlete to their prior activity level. The symptom management phase aims to reduce pain and halt continuous overloading, which results in injury progression. Complete immobilization results in underloading the tendon and is deleterious to tendon health, delaying recovery time [238-241]. The recovery phase emphasizes the return of muscle strength and improvements to the tendon's capacity to withstand loading [232]. Exercise routines increase in frequency and number of repetitions performed throughout the recovery phase [232]. The rebuilding phase is a transition period that focuses on increasing load and resistance capacities using distinct protocols to train the muscles and tendons to return to activity and further improve tendon healing. The final phase is adapted for each patient to return to prior sport-specific activity levels, while strengthening the musculotendinous unit function [242]. The overarching themes from each phase focus not only on improving tendon properties, but also patient education. Patient education results in improved performance of the exercises and consistent reporting of progress to better document patient outcomes, providing clinicians valuable insight of healing progression [232].

Heavy slow resistance training protocols apply heavy loads while performing rehabilitative loading, and have shown positive outcomes when used for patellar and Achilles tendinopathy [243, 244]. However, these studies have not investigated changes in tendon architecture (e.g., fiber alignment and microstructure adaptations) caused by tendinopathy [243, 245]. Eccentric exercises (lengthening the muscle while it contracts) are recognized as the most effective physical therapy treatment for Achilles tendinopathy, as they improve symptoms and restore function [246-249]. Eccentric-based exercises, such as the "heel drop" exercise, are achieved when the ankle of the affected limb moves through plantarflexion and dorsiflexion range of motion while the gastrocnemius muscle contracts. Several systematic reviews and clinical research studies support the efficacy of eccentric loading for the treatment of AT by reducing tendon hypertrophy, reducing pain, and improving the hierarchical structure of the tendon [250-252]. One study demonstrated reduced tendon thickness and symptomatic relief after performing the exercise routines [253]. When the foot/ankle is in plantarflexion, the muscle is in a concentric phase (muscle shortening while contracting). To correctly perform heel drop exercises some concentric loading is needed, but that has prompted a debate as to which (eccentric or concentric) phase is responsible for initiation of the healing response [234, 254]. Clinical evidence demonstrates similar healing times between eccentric and concentric loading groups; however, eccentric-based exercises improved

tendon thickness after loading compared to concentric loading, suggesting that eccentric loading is more influential for improved tendon structure [236, 255].

Despite promising outcomes, the mechanisms by which eccentric-based protocols result in healing and symptomatic relief are poorly understood. The heterogeneity of AT and its affected population further complicate the investigation of the pathology and accompanying healing interventions. Additionally, most studies of eccentric loading protocols involve athletes and do not often investigate the general population. One study demonstrated that 45% of non-athletic patients had no pain reduction or functional improvement [256]. Furthermore, several studies have implemented different clinical loading protocols with varied results and without identifying a single application that provides symptomatic relief and return of functional tendon properties [254, 257-261]. Loading intensity, frequency and the duration of treatments vary widely, and recovery is likely contingent on the patient's biometric factors such as age, body mass index, injury severity, and underlying health conditions [262, 263].

Chronic tendinopathy may be initiated by an accumulation of microdamage that alters the tissue structure and cellular composition [27, 71, 262]. The onset of tendinopathic changes is challenging to identify since early disease can be subclinical and a clear causative event is lacking in the patient history [177, 232]. A rigorous characterization of all stages of disease progression would aid in the identification of the changes between disease stages to better inform clinicians how to prescribe treatments that result in robust tissue healing while mitigating reinjury. The link between exercise and increases of regulators of type I collagen synthesis may provide key insights into how eccentric-based loading improves Achilles healing. Challenges remain in defining the underlying healing mechanisms induced from rehabilitative loading due to the range in treatment regimens and the unique tendon healing cascade. Identification of key molecular, cellular, and tissue responses to injury can be used to guide rehabilitative loading protocols to promote a robust healing response in tendons, ultimately improving functional outcomes. The goals of the studies described in the subsequent chapters are aimed at filling some of the current voids in our current understanding of tendinopathy and its treatment.

References:

1. Snedeker, J.G. and J. Foolen, Tendon injury and repair - A perspective on the basic mechanisms of tendon disease and future clinical therapy. Acta Biomater, 2017(1878-7568 (Electronic)).

2. Screen, H.R., et al., Tendon functional extracellular matrix. 2015(1554-527X (Electronic)).

3. Voleti, P.B., L.J. Buckley Mr Fau - Soslowsky, and L.J. Soslowsky, Tendon healing: repair and regeneration. Annual Review Biomed Eng, 2012. 14(1545-4274 (Electronic)).

4. Kannus, P., Structure of the tendon connective tissue. Scandinavian Journal of Medicine & Science in Sports, 2000. 10(6): p. 312-320.

5. Sharma, P. and N. Maffulli, Biology of tendon injury: healing, modeling and remodeling. Journal of Musculoskeletal Neuronal Interactions, 2006. 6(1108-7161 (Print)): p. 181-190.

6. Benjamin, M., E. Kaiser, and S. Milz, Structure-function relationships in tendons: a review. Journal of Anatomy, 2008. 212(3): p. 211-228.

7. Chen, B., et al., Tissue Engineering of Tendons: A Comparison of Muscle-Derived Cells, Tenocytes, and Dermal Fibroblasts as Cell Sources. Plastic Reconstructive Surgery, 2016(1529-4242 (Electronic)).

8. Gelse, K., E. Pöschl, and T. Aigner, Collagens—structure, function, and biosynthesis. Advanced Drug Delivery Reviews, 2003. 55(12): p. 1531-1546.

9. Özer Kaya, D., Chapter 9 - Architecture of tendon and ligament and their adaptation to pathological conditions, in Comparative Kinesiology of the Human Body, S. Angin and I.E. Şimşek, Editors. 2020, Academic Press. p. 115-147.

10. Jaworski, Ł., et al. Advances in Microscopic Studies of Tendinopathy: Literature Review and Current Trends, with Special Reference to Neovascularization Process. Journal of Clinical Medicine, 2022. 11, DOI: 10.3390/jcm11061572.

11. Sharma, P. and N. Maffulli, Tendon injury and tendinopathy: healing and repair. Journal of Bone and Joint Surgery, 2005(0021-9355 (Print)).

12. Gonçalves, A.I., et al., Exploring the Potential of Starch/Polycaprolactone Aligned Magnetic Responsive Scaffolds for Tendon Regeneration. Advanced Healthcare Materials, 2016(2192-2659 (Electronic)).

13. Kannus, P., L.G. Jozsa, and L. Josza, Human tendons: anatomy, physiology, and pathology. 1997, Human Kinetics Publishers Champaign.

14. Lin, T.W., L. Cardenas, and L.J. Soslowsky, Biomechanics of tendon injury and repair. Journal of biomechanics, 2004. 37(6): p. 865-877.

15. Kjaer, M., Role of extracellular matrix in adaptation of tendon and skeletal muscle to mechanical loading. Physiological reviews, 2004. 84(2): p. 649-698.

16. Taye, N., S.Z. Karoulias, and D. Hubmacher, The “other” 15–40%: the role of non-collagenous extracellular matrix proteins and minor collagens in tendon. Journal of Orthopaedic Research®, 2020. 38(1): p. 23-35.

17. Yoon, J.H. and J. Halper, Tendon proteoglycans: biochemistry and function. Journal of Musculoskeletal Neuronal Interactions, 2005. 5(1108-7161 (Print)).

18. Derwin, K.A., et al., Proteoglycans and glycosaminoglycan fine structure in the mouse tail tendon fascicle. Journal of Orthopedic Research, 2001. 19(0736-0266 (Print)): p. 260-277.

19. Ezura, Y., et al., Differential expression of lumican and fibromodulin regulate collagen fibrillogenesis in developing mouse tendons. Journal of Cell Biology, 2000. 151(0021-9525 (Print)): p. 779-788.

20. Robinson, K.A., et al., Decorin and biglycan are necessary for maintaining collagen fibril structure, fiber realignment, and mechanical properties of mature tendons. Matrix Biology, 2017. 64: p. 81-93.

21. Zhang, G., et al., Decorin regulates assembly of collagen fibrils and acquisition of biomechanical properties during tendon development. Journal of Cell Biology, 2006(0730-2312 (Print)).

22. Robbins, J.R., K.G. Evanko Sp Fau - Vogel, and K.G. Vogel, Mechanical loading and TGF-beta regulate proteoglycan synthesis in tendon. Archives of Biochemistry and Biophysics, 1997. 342(0003-9861 (Print)): p. 203-211.

23. Schaefer, L. and R.V. Iozzo, Biological functions of the small leucine-rich proteoglycans: from genetics to signal transduction. Journal of Biological Chemistry, 2008. 31(0021-9258 (Print)): p. 21305-21309.

24. Chakravarti, S., et al., Collagen fibril assembly during postnatal development and dysfunctional regulation in the lumican-deficient murine cornea. Developmental Dynamics, 2006. 235(1058-8388 (Print)): p. 2493-2506.

25. Chen, S. and D.E. Birk, The regulatory roles of small leucine-rich proteoglycans in extracellular matrix assembly. The FEBS Journal, 2013. 280(1742-4658 (Electronic)): p. 2120-2137.

26. Iozzo, R.V., Matrix proteoglycans: from molecular design to cellular function. Annual Review of Biochemistry, 1998. 67(0066-4154 (Print)): p. 609-652.

27. Lipman, K., et al., Tendinopathy: injury, repair, and current exploration. Drug Design, Development, and Therapy, 2018. 12(1177-8881 (Electronic)): p. 591-603.

28. Zhang, G., et al., Development of tendon structure and function: regulation of collagen fibrillogenesis. Journal of Musculoskeletal Neuronal Interactions, 2005. 5(1108-7161 (Print)): p. 5-21.

29. Chakravarti, S., Functions of lumican and fibromodulin: lessons from knockout mice. Glycoconjugate Journal, 2002. 19(0282-0080 (Print)): p. 287-293.

30. Al Makhzoomi, A.K., et al., Contribution of glycosaminoglycans to the structural and mechanical properties of tendons – A multiscale study. Journal of Biomechanics, 2021. 128: p. 110796.

31. Raman, R., R. Sasisekharan V Fau - Sasisekharan, and R. Sasisekharan, Structural insights into biological roles of protein-glycosaminoglycan interactions. Chemical Biology, 2005. 12(1074-5521 (Print)): p. 267-277.

32. Prydz , K. Determinants of Glycosaminoglycan (GAG) Structure. Biomolecules, 2015. 5, 2003-2022 DOI: 10.3390/biom5032003.

33. Ryan Cn Fau - Sorushanova, A., et al., Glycosaminoglycans in Tendon Physiology, Pathophysiology, and Therapy. Bioconjugate Chemistry, 2015. 26(1520-4812 (Electronic)): p. 1237-1251.

34. Melrose, J., et al., Chondroitin sulphate and heparan sulphate sulphation motifs and their proteoglycans are involved in articular cartilage formation during human foetal knee joint development. Histochemical and Cell Biology, 2012. 138(1432-119X (Electronic)): p. 461-475.

35. Kappler, J., et al., Single-molecule imaging of hyaluronan in human synovial fluid. Journal of biomedical optics, 2010. 15(6): p. 060504-060504.

36. Malda, J., et al., Of mice, men and elephants: the relation between articular cartilage thickness and body mass. PloS one, 2013. 8(2): p. e57683.

37. Katta, J., et al., Chondroitin sulphate: an effective joint lubricant? Osteoarthritis and cartilage, 2009. 17(8): p. 1001-1008.

38. Malcarney, H.L. and G.A.C. Murrell, The rotator cuff: biological adaptations to its environment. Sports Medicine, 2003. 33: p. 993-1002.

39. Stuart, K. and A. Panitch, Influence of chondroitin sulfate on collagen gel structure and mechanical properties at physiologically relevant levels. Biopolymers: Original Research on Biomolecules, 2008. 89(10): p. 841-851.

40. Kwok, J.C.F., P. Warren, and J.W. Fawcett, Chondroitin sulfate: a key molecule in the brain matrix. The international journal of biochemistry & cell biology, 2012. 44(4): p. 582-586.

41. Eekhoff, J.D., et al., Fascicular elastin within tendon contributes to the magnitude and modulus gradient of the elastic stress response across tendon type and species. Acta Biomaterialia, 2023. 163: p. 91-105.

42. Thorpe, C.T., et al., The interfascicular matrix enables fascicle sliding and recovery in tendon, and behaves more elastically in energy storing tendons. Journal of Mechnical Behavior of Biomedical Materials, 2015. 52(1878-0180 (Electronic)): p. 85-94.

43. Costa-Almeida, R., I. Calejo, and M.E. Gomes, Mesenchymal stem cells empowering tendon regenerative therapies. International journal of molecular sciences, 2019. 20(12): p. 3002.

44. Zhang, C., et al., Tendon stem/progenitor cells and their interactions with extracellular matrix and mechanical loading. Stem cells international, 2019. 2019(1): p. 3674647.

45. Schneider, M., et al., Rescue plan for Achilles: Therapeutics steering the fate and functions of stem cells in tendon wound healing. Advanced Drug Delivery Reviews, 2018. 129: p. 352-375.

46. Docheva, D., et al., Biologics for tendon repair. Advanced drug delivery reviews, 2015. 84: p. 222-239.

47. Yin, H., et al., Three-dimensional self-assembling nanofiber matrix rejuvenates aged/degenerative human tendon stem/progenitor cells. Biomaterials, 2020. 236: p. 119802.

48. Bi, Y., et al., Identification of tendon stem/progenitor cells and the role of the extracellular matrix in their niche. Nature medicine, 2007. 13(10): p. 1219-1227.

49. Zhang, J. and J.H.C. Wang, Characterization of differential properties of rabbit tendon stem cells and tenocytes. BMC musculoskeletal disorders, 2010. 11: p. 1-11.

50. Zelzer, E., et al., Tendon-to-bone attachment: From development to maturity. Birth Defects Research Part C: Embryo Today: Reviews, 2014. 102(1): p. 101-112.

51. Benjamin, M. and J.R. Ralphs, Fibrocartilage in tendons and ligaments—an adaptation to compressive load. The Journal of Anatomy, 1998. 193(4): p. 481-494.

52. Humphrey, J.D., E.R. Dufresne, and M.A. Schwartz, Mechanotransduction and extracellular matrix homeostasis. Nature reviews Molecular cell biology, 2014. 15(12): p. 802-812.

53. Müller, S.A., et al., Tendon healing: an overview of physiology, biology, and pathology of tendon healing and systematic review of state of the art in tendon bioengineering. Knee surgery, sports traumatology, arthroscopy, 2015. 23: p. 2097-2105.

54. Popov, C., et al., Mechanical stimulation of human tendon stem/progenitor cells results in upregulation of matrix proteins, integrins and MMPs, and activation of p38 and ERK1/2 kinases. BMC Molecular Biology, 2015. 16: p. 1-11.

55. Wang, J.H.C., M.I. Iosifidis, and F.H. Fu, Biomechanical basis for tendinopathy. Clinical Orthopaedics and Related Research (1976-2007), 2006. 443: p. 320-332.

56. Duenwald, S.E., R. Vanderby, and R.S. Lakes, Viscoelastic Relaxation and Recovery of Tendon. Annals of Biomedical Engineering, 2009. 37(6): p. 1131-1140.

57. Sensini, A. and L. Cristofolini, Biofabrication of electrospun scaffolds for the regeneration of tendons and ligaments. Materials, 2018. 11(10): p. 1963.

58. Shim, V., et al. Investigation of the role of crimps in collagen fibers in tendon with a microstructually based finite element model. 2012. IEEE.

59. de Campos Vidal, B., Image analysis of tendon helical superstructure using interference and polarized light microscopy. Micron, 2003. 34(8): p. 423-432.

60. Buehler, M.J., Nature designs tough collagen: explaining the nanostructure of collagen fibrils. Proceedings of the National Academy of Sciences, 2006. 103(33): p. 12285-12290.

61. Kastelic, J., A. Galeski, and E. Baer, The multicomposite structure of tendon. Connective tissue research, 1978. 6(1): p. 11-23.

62. Sasaki, N. and S. Odajima, Elongation mechanism of collagen fibrils and force-strain relations of tendon at each level of structural hierarchy. Journal of biomechanics, 1996. 29(9): p. 1131-1136.

63. Screen, H.R.C., Investigating load relaxation mechanics in tendon. Journal of the Mechanical Behavior of Biomedical Materials, 2008. 1(1): p. 51-58.

64. West, J.R., et al., Characterization of in vivo Achilles tendon forces in rabbits during treadmill locomotion at varying speeds and inclinations. Journal of biomechanics, 2004. 37(11): p. 1647-1653.

65. Dick, T.J.M., A.S. Arnold, and J.M. Wakeling, Quantifying Achilles tendon force in vivo from ultrasound images. Journal of Biomechanics, 2016. 49(14): p. 3200-3207.

66. Ishikawa, M., et al., Muscle-tendon interaction and elastic energy usage in human walking. Journal of Applied Physiology, 2005. 99(2): p. 603-608.

67. Maganaris, C.N., M.V. Narici, and N. Maffulli, Biomechanics of the Achilles tendon. Disability and Rehabilitation, 2008. 30(20-22): p. 1542-1547.

68. Wren, T.A.L., et al., Mechanical properties of the human achilles tendon. Clinical Biomechanics, 2001. 16(3): p. 245-251.

69. Ryan, E.D., et al., Viscoelastic creep in the human skeletal muscle–tendon unit. European Journal of Applied Physiology, 2010. 108(1): p. 207-211.

70. Peltonen, J., et al., Viscoelastic properties of the Achilles tendon in vivo. SpringerPlus, 2013. 2(1): p. 212.

71. Andarawis-Puri, N., E.L. Flatow, and L.J. Soslowsky, Tendon basic science: Development, repair, regeneration, and healing. Journal of Orthopaedic Research, 2015. 33(6): p. 780-784.

72. Andarawis-Puri, N., et al., The relationships between cyclic fatigue loading, changes in initial mechanical properties, and the in vivo temporal mechanical response of the rat patellar tendon. Journal of Biomechanics, 2012. 45(1): p. 59-65.

73. Wang, J.H.C., Q. Guo, and B. Li, Tendon Biomechanics and Mechanobiology—A Minireview of Basic Concepts and Recent Advancements. Journal of Hand Therapy, 2012. 25(2): p. 133-141.

74. Thomopoulos, S., et al., Mechanisms of tendon injury and repair. Journal of Orthopaedic Research, 2015. 33(6): p. 832-839.

75. Schizas, N., et al., Compression therapy promotes proliferative repair during rat Achilles tendon immobilization. Journal of Orthopaedic Research, 2010. 28(7): p. 852-858.

76. Killian, M.L., et al., The role of mechanobiology in tendon healing. Journal of Shoulder and Elbow Surgery, 2012. 21(2): p. 228-237.

77. Vogel, K.G., et al., Proteoglycans in the compressed region of human tibialis posterior tendon and in ligaments. Journal of Orthopaedic Research, 1993. 11(1): p. 68-77.

78. Molloy, T., Y. Wang, and G.A.C. Murrell, The Roles of Growth Factors in Tendon and Ligament Healing. Sports Medicine, 2003. 33(5): p. 381-394.

79. Veres, S.P., J.M. Harrison, and J.M. Lee, Repeated subrupture overload causes progression of nanoscaled discrete plasticity damage in tendon collagen fibrils. Journal of Orthopaedic Research, 2013. 31(5): p. 731-737.

80. Egerbacher, M., et al., Loss of Homeostatic Tension Induces Apoptosis in Tendon Cells: An In Vitro Study. Clinical Orthopaedics and Related Research®, 2008. 466(7).

81. Thornton, G.M., et al., Changes in mechanical loading lead to tendonspecific alterations in MMP and TIMP expression: influence of stress deprivation and intermittent cyclic hydrostatic compression on rat supraspinatus and Achilles tendons. British Journal of Sports Medicine, 2010. 44(10): p. 698.

82. Flint, J.H., et al., Defining the Terms Acute and Chronic in Orthopaedic Sports Injuries: A Systematic Review. The American Journal of Sports Medicine, 2013. 42(1): p. 235-241.

83. Nourissat, G., F. Berenbaum, and D. Duprez, Tendon injury: from biology to tendon repair. Nature Reviews Rheumatology, 2015. 11(4): p. 223-233.

84. T Sayegh, E., et al., Recent scientific advances towards the development of tendon healing strategies. Current Tissue Engineering (Discontinued), 2015. 4(2): p. 128-143.

85. Steinmann, S., et al., Spectrum of tendon pathologies: Triggers, trails and end-state. International journal of molecular sciences, 2020. 21(3): p. 844.

86. Leek, C.C., et al., Using tools in mechanobiology to repair tendons. Current tissue microenvironment reports, 2020. 1: p. 31-40.

87. Herod, T.W. and S.P. Veres, Development of overuse tendinopathy: a new descriptive model for the initiation of tendon damage during cyclic loading. Journal of Orthopaedic Research®, 2018. 36(1): p. 467-476.

88. Albers, I.S., et al., Incidence and prevalence of lower extremity tendinopathy in a Dutch general practice population: a cross sectional study. BMC Musculoskeletal Disorders, 2016. 17(1): p. 16.

89. Loiacono, C., et al. Tendinopathy: Pathophysiology, Therapeutic Options, and Role of Nutraceutics. A Narrative Literature Review. Medicina, 2019. 55, DOI: 10.3390/medicina55080447.

90. Millar, N.L., et al., Tendinopathy. Nature reviews Disease primers, 2021. 7(1): p. 1.

91. Walden, G., et al., A clinical, biological, and biomaterials perspective into tendon injuries and regeneration. Tissue Engineering Part B: Reviews, 2017. 23(1): p. 44-58.

92. Shen, H., et al., Flexor tendon injury and repair: the influence of synovial environment on the early healing response in a canine model. JBJS, 2021. 103(9): p. e36.

93. Voleti, P.B., M.R. Buckley, and L.J. Soslowsky, Tendon Healing: Repair and Regeneration. Annual Review of Biomedical Engineering, 2012. 14(Volume 14, 2012): p. 47-71.

94. Woo, S.L.-Y., et al., Injury and Repair of Ligaments and Tendons. Annual Review of Biomedical Engineering, 2000. 2(Volume 2, 2000): p. 83-118.

95. Howell, K., et al., Novel Model of Tendon Regeneration Reveals Distinct Cell Mechanisms Underlying Regenerative and Fibrotic Tendon Healing. Scientific Reports, 2017. 7(1): p. 45238.

96. Michel, P.A., et al., Microsurgical reconstruction affects the outcome in a translational mouse model for Achilles tendon healing. Journal of Orthopaedic Translation, 2020. 24: p. 1-11.

97. Notermans, T., et al., Tendon mechanobiology in small animal experiments during post-transection healing. European Cells and Materials, 2021. 42: p. 375-391.

98. Chen, C.H., et al., Tendon Healing In Vivo: Gene Expression and Production of Multiple Growth Factors in Early Tendon Healing Period. The Journal of Hand Surgery, 2008. 33(10): p. 1834-1842.

99. Theodossiou, S.K. and N.R. Schiele, Models of tendon development and injury. BMC Biomedical Engineering, 2019. 1(1): p. 32.

100. Theodossiou, S.K. and N.R. Schiele, Models of tendon development and injury. BMC biomedical engineering, 2019. 1: p. 1-24.

101. Tucker, J.J., et al., Effect of overuse-induced tendinopathy on tendon healing in a rat supraspinatus repair model. Journal of Orthopaedic Research, 2016. 34(1): p. 161-166.

102. Liu, H., et al., Pathogenesis and Development of Patellar Tendon Fibrosis in a Rabbit Overuse Model. The American Journal of Sports Medicine, 2020. 48(5): p. 1141-1150.

103. Parent, G., N. Huppé, and E. Langelier, Low Stress Tendon Fatigue is a Relatively Rapid Process in the Context of Overuse Injuries. Annals of Biomedical Engineering, 2011. 39(5): p. 1535-1545.

104. Backman, C., et al., Chronic achilles paratenonitis with tendinosis: An experimental model in the rabbit. Journal of Orthopaedic Research, 1990. 8(4): p. 541-547.

105. Abraham, T., G. Fong, and A. Scott, Second harmonic generation analysis of early Achilles tendinosis in response to in vivo mechanical loading. BMC Musculoskeletal Disorders, 2011. 12(1): p. 26.

106. Fung, D.T., et al., Early response to tendon fatigue damage accumulation in a novel in vivo model. Journal of Biomechanics, 2010. 43(2): p. 274-279.

107. Zhang, J. and J.H.C. Wang, The Effects of Mechanical Loading on Tendons - An In Vivo and In Vitro Model Study. PLOS ONE, 2013. 8(8): p. e71740.

108. Glazebrook, M.A., et al., Histological analysis of achilles tendons in an overuse rat model. Journal of Orthopaedic Research, 2008. 26(6): p. 840-846.

109. Ng, G.Y.-F., et al., Enforced Bipedal Downhill Running Induces Achilles Tendinosis in Rats. Connective Tissue Research, 2011. 52(6): p. 466-471.

110. Silva, R.D., et al., Achilles tendinosis–a morphometrical study in a rat model. International journal of clinical and experimental pathology, 2011. 4(7): p. 683.

111. Zhang, J., et al., Moderate and intensive mechanical loading differentially modulate the phenotype of tendon stem/progenitor cells in vivo. PLoS One, 2020. 15(12): p. e0242640.

112. Pingel, J., et al., Increased mast cell numbers in a calcaneal tendon overuse model. Scandinavian journal of medicine & science in sports, 2013. 23(6): p. e353-e360.

113. Heinemeier, K.M., et al., Uphill running improves rat Achilles tendon tissue mechanical properties and alters gene expression without inducing pathological changes. Journal of applied physiology, 2012. 113(5): p. 827-836.

114. Sereysky, J.B., et al., Structural and mechanical effects of in vivo fatigue damage induction on murine tendon. Journal of Orthopaedic Research, 2012. 30(6): p. 965-972.

115. Andarawis-Puri, N., et al., Molecular response of the patellar tendon to fatigue loading explained in the context of the initial induced damage and number of fatigue loading cycles. Journal of Orthopaedic Research, 2012. 30(8): p. 1327-1334.

116. Yuan, T., et al., Creating an Animal Model of Tendinopathy by Inducing Chondrogenic Differentiation with Kartogenin. PLOS ONE, 2016. 11(2): p. e0148557.

117. Solchaga, L.A., et al., Comparison of the effect of intra-tendon applications of recombinant human platelet-derived growth factor-BB, platelet-rich plasma, steroids in a rat achilles tendon collagenase model. Journal of Orthopaedic Research, 2014. 32(1): p. 145-150.

118. Lacitignola, L., et al., Survival of bone marrow mesenchymal stem cells labelled with red fluorescent protein in an ovine model of collagenase-induced tendinitis. Veterinary and Comparative Orthopaedics and Traumatology, 2014. 27(03): p. 204-209.

119. Chen, L., et al., Tendon derived stem cells promote platelet-rich plasma healing in collagenase-induced rat achilles tendinopathy. Cellular Physiology and Biochemistry, 2014. 34(6): p. 2153-2168.

120. Machova Urdzikova, L., et al., Human multipotent mesenchymal stem cells improve healing after collagenase tendon injury in the rat. Biomedical engineering online, 2014. 13: p. 1-15.

121. Bell, R., et al., Controlled treadmill exercise eliminates chondroid deposits and restores tensile properties in a new murine tendinopathy model. Journal of biomechanics, 2013. 46(3): p. 498-505.

122. Stone, D., et al., Cytokine-induced tendinitis: A preliminary study in rabbits. Journal of Orthopaedic Research, 1999. 17(2): p. 168-177.

123. Marsolais, D., et al., Inflammatory cells do not decrease the ultimate tensile strength of intact tendons in vivo and in vitro: protective role of mechanical loading. Journal of Applied Physiology, 2007. 102(1): p. 11-17.

124. Yoshida, R., et al., Murine supraspinatus tendon injury model to identify the cellular origins of rotator cuff healing. Connective tissue research, 2016. 57(6): p. 507-515.

125. Moser, H.L., et al., Genetic lineage tracing of targeted cell populations during enthesis healing. Journal of Orthopaedic Research®, 2018. 36(12): p. 3275-3284.

126. Fung, D.T., et al., Subrupture tendon fatigue damage. Journal of Orthopaedic Research, 2009. 27(2): p. 264-273.

127. Spiesz, E.M., et al., Tendon extracellular matrix damage, degradation and inflammation in response to in vitro overload exercise. Journal of Orthopaedic Research, 2015. 33(6): p. 889-897.

128. Arnoczky, S.P., M. Lavagnino, and M. Egerbacher, The mechanobiological aetiopathogenesis of tendinopathy: is it the over-stimulation or the under-stimulation of tendon cells? International journal of experimental pathology, 2007. 88(4): p. 217-226.

129. Maeda, T., et al., Conversion of mechanical force into TGF-β-mediated biochemical signals. Current Biology, 2011. 21(11): p. 933-941.

130. Dirks, R.C., et al., Uphill treadmill running does not induce histopathological changes in the rat Achilles tendon. BMC musculoskeletal disorders, 2013. 14: p. 1-5.

131. Reuther, K.E., et al., Effect of return to overuse activity following an isolated supraspinatus tendon tear on adjacent intact tendons and glenoid cartilage in a rat model. Journal of Orthopaedic Research, 2013. 31(5): p. 710-715.

132. Rezvani, S.N., Novel Preclinical Approaches to the Understanding and Treatment of Achilles Tendinopathy, in Biomedical Engineering. 2021, Virginia Tech.

133. Korcari, A., M.R. Buckley, and A.E. Loiselle, Characterization of scar tissue biomechanics during adult murine flexor tendon healing. Journal of the Mechanical Behavior of Biomedical Materials, 2022. 130: p. 105192.

134. Chisari, E., et al., Tendon healing is adversely affected by low-grade inflammation. Journal of Orthopaedic Surgery and Research, 2021. 16: p. 1-9.

135. Lichtnekert, J., et al., Changes in macrophage phenotype as the immune response evolves. Current opinion in pharmacology, 2013. 13(4): p. 555-564.

136. Sugg, K.B., et al., Changes in macrophage phenotype and induction of epithelial-to-mesenchymal transition genes following acute Achilles tenotomy and repair. Journal of Orthopaedic Research, 2014. 32(7): p. 944-951.

137. de la Durantaye, M., et al., Macrophage depletion reduces cell proliferation and extracellular matrix accumulation but increases the ultimate tensile strength of injured Achilles tendons. Journal of Orthopaedic Research, 2014. 32(2): p. 279-285.

138. Mantovani, A., et al., Macrophage polarization: tumor-associated macrophages as a paradigm for polarized M2 mononuclear phagocytes. Trends in immunology, 2002. 23(11): p. 549-555.

139. Hays, P.L., et al., The role of macrophages in early healing of a tendon graft in a bone tunnel. JBJS, 2008. 90(3): p. 565-579.

140. Qian, L.-W., et al., Exacerbated and prolonged inflammation impairs wound healing and increases scarring. Wound Repair and Regeneration, 2016. 24(1): p. 26-34.

141. Kim, H.M., et al., The role of transforming growth factor beta isoforms in tendon-to-bone healing. Connective tissue research, 2011. 52(2): p. 87-98.

142. Beredjiklian, P.K., et al., Regenerative versus reparative healing in tendon: a study of biomechanical and histological properties in fetal sheep. Annals of biomedical engineering, 2003. 31: p. 1143-1152.

143. Juneja, S.C., et al., Cellular and molecular factors in flexor tendon repair and adhesions: a histological and gene expression analysis. Connective tissue research, 2013. 54(3): p. 218-226.

144. Yang, G., B.B. Rothrauff, and R.S. Tuan, Tendon and ligament regeneration and repair: clinical relevance and developmental paradigm. Birth defects research part C: embryo today: reviews, 2013. 99(3): p. 203-222.

145. Rees, J.D., N. Maffulli, and J. Cook, Management of Tendinopathy. The American Journal of Sports Medicine, 2009. 37(9): p. 1855-1867.

146. Yasui, Y., et al., The Risk of Achilles Tendon Rupture in the Patients with Achilles Tendinopathy: Healthcare Database Analysis in the United States. BioMed Research International, 2017. 2017(1): p. 7021862.

147. Strocchi, R., et al., Human Achilles tendon: morphological and morphometric variations as a function of age. Foot & ankle, 1991. 12(2): p. 100-104.

148. Fahlström, M., R. Lorentzon, and H. Alfredson, Painful conditions in the Achilles tendon region: a common problem in middle-aged competitive badminton players. Knee Surgery, Sports Traumatology, Arthroscopy, 2002. 10: p. 57-60.

149. Holmes, G.B. and J. Lin, Etiologic factors associated with symptomatic achilles tendinopathy. Foot & Ankle International, 2006. 27(11): p. 952-959.

150. Ribard, P., et al., Seven Achilles tendinitis including 3 complicated by rupture during fluoroquinolone therapy. The Journal of rheumatology, 1992. 19(9): p. 1479-1481.

151. Lee, W.T. and J. Collins, Ciprofloxacin associated bilateral achilles tendon rupture. Australian and New Zealand journal of medicine, 1992. 22(5): p. 500-500.

152. Abate, M., et al., Occurrence of tendon pathologies in metabolic disorders. Rheumatology, 2013. 52(4): p. 599-608.

153. Gaida, J.E., J.L. Cook, and S. Bass, Adiposity and tendinopathy. Disability and rehabilitation, 2008. 30(20-22): p. 1555-1562.

154. Abate, M., et al., Achilles tendon and plantar fascia in recently diagnosed type II diabetes: role of body mass index. Clinical rheumatology, 2012. 31: p. 1109-1113.

155. Batista, F., et al., Achilles tendinopathy in diabetes mellitus. 2008.

156. Duffin, A., et al., Ultrasonography of plantar soft tissues thickness in young people with diabetes. Diabetic medicine, 2002. 19(12): p. 1009-1013.

157. Akturk, M., et al., Evaluation of Achilles tendon thickening in type 2 diabetes mellitus. Experimental and clinical endocrinology & diabetes, 2007. 115(02): p. 92-96.

158. Cook, J. and C.R. Purdam, Is tendon pathology a continuum? A pathology model to explain the clinical presentation of load-induced tendinopathy. British journal of sports medicine, 2009. 43(6): p. 409-416.

159. Cho, N.S., et al., Tendinosis-like Histologic and Molecular Changes of the Achilles Tendon to Repetitive Stress:A Pilot Study in Rats. Clinical Orthopaedics and Related Research®, 2011. 469(11): p. 3172-3180.

160. Tran, P.H.T., et al., Early development of tendinopathy in humans: Sequence of pathological changes in structure and tissue turnover signaling. The FASEB Journal, 2020. 34(1): p. 776-788.

161. de Jonge, S., et al., Incidence of midportion Achilles tendinopathy in the general population. British journal of sports medicine, 2011. 45(13): p. 1026-1028.

162. Tran, P.H.T., et al., Early development of tendinopathy in humans: Sequence of pathological changes in structure and tissue turnover signaling. The FASEB Journal, 2020. 34(1): p. 776-788.

163. Corrigan, P., et al., Tendon Morphology and Mechanical Properties Are Associated With the Recovery of Symptoms and Function in Patients With Achilles Tendinopathy. Orthopaedic Journal of Sports Medicine, 2020. 8(4): p. 2325967120917271.

164. Riley, G., et al., Tendon degeneration and chronic shoulder pain: changes in the collagen composition of the human rotator cuff tendons in rotator cuff tendinitis. Annals of the rheumatic diseases, 1994. 53(6): p. 359-366.

165. De Marchi, A., et al., In Achilles tendinopathy, the neovascularization, detected by contrast-enhanced ultrasound (CEUS), is abundant but not related to symptoms. Knee Surgery, Sports Traumatology, Arthroscopy, 2018. 26(7): p. 2051-2058.

166. Åström, M. and A. Rausing, Chronic Achilles tendinopathy: a survey of surgical and histopathologic findings mats. Clinical Orthopaedics and Related Research®, 1995(316): p. 151-164.

167. Maffulli, N., et al., Achilles tendinopathy. Foot and Ankle Surgery, 2020. 26(3): p. 240-249.

168. Attia, M., et al., HISTOCHEMICAL ANALYSIS OF GAGS IN ALTERED TENDON: A MEANS TO EVALUATE THE DEGREE OF PATHOLOGY. British Journal of Sports Medicine, 2013. 47(9): p. e2.

169. Hasan, S.A., et al., Epidemiology, etiology, and pathogenesis of tendinopathy among athletes. International Journal Of Community Medicine And Public Health, 2021. 9(1): p. 437-442.

170. Hijazi, K.M., K.L. Singfield, and S.P. Veres, Ultrastructural response of tendon to excessive level or duration of tensile load supports that collagen fibrils are mechanically continuous. Journal of the mechanical behavior of biomedical materials, 2019. 97: p. 30-40.

171. Marturano, J.E., et al., Characterization of mechanical and biochemical properties of developing embryonic tendon. Proceedings of the National Academy of Sciences, 2013. 110(16): p. 6370-6375.

172. Marqueti, R.C., et al., Androgenic-anabolic steroids associated with mechanical loading inhibit matrix metallopeptidase activity and affect the remodeling of the achilles tendon in rats. The American journal of sports medicine, 2006. 34(8): p. 1274-1280.

173. Pelled, G., et al., Smad8/BMP2-engineered mesenchymal stem cells induce accelerated recovery of the biomechanical properties of the Achilles tendon. Journal of orthopaedic research, 2012. 30(12): p. 1932-1939.

174. Langberg, H., et al., Time pattern of exercise-induced changes in type I collagen turnover after prolonged endurance exercise in humans. Calcified tissue international, 2000. 67: p. 41-44.

175. Langberg, H., L. Rosendal, and M. Kjær, Training-induced changes in peritendinous type I collagen turnover determined by microdialysis in humans. The Journal of physiology, 2001. 534(1): p. 297-302.

176. Heinemeier, K., et al., Role of TGF-β1 in relation to exercise-induced type I collagen synthesis in human tendinous tissue. Journal of Applied Physiology, 2003. 95(6): p. 2390-2397.

177. Del Buono, A., et al., Metalloproteases and tendinopathy. Muscles Ligaments Tendons, 2013. 3(2240-4554 (Print)): p. 51-71.

178. Thorpe, C.T., et al., The role of the non-collagenous matrix in tendon function. International Journal of Experimental Pathology, 2013. 94(4): p. 248-259.

179. Docking, S.I., C.C. Ooi, and D. Connell, Tendinopathy: Is Imaging Telling Us the Entire Story? Journal of Orthopaedic & Sports Physical Therapy, 2015. 45(11): p. 842-852.

180. Chen, Z., et al., Mechanical overload-induced release of extracellular mitochondrial particles from tendon cells leads to inflammation in tendinopathy. Experimental & Molecular Medicine, 2024. 56(3): p. 583-599.

181. Millar, N.L., et al., MicroRNA29a regulates IL-33-mediated tissue remodelling in tendon disease. Nature Communications, 2015. 6(1): p. 6774.

182. Morita, W., et al., Cytokines in tendon disease: a systematic review. Bone & joint research, 2017. 6(12): p. 656-664.

183. Ellis, I.M., L.V. Schnabel, and A.K. Berglund, Defining the profile: characterizing cytokines in tendon injury to improve clinical therapy. Journal of immunology and regenerative medicine, 2022. 16: p. 100059.

184. Manning, C.N., et al., The early inflammatory response after flexor tendon healing: a gene expression and histological analysis. Journal of Orthopaedic Research, 2014. 32(5): p. 645-652.

185. Millar, N.L., G.A.C. Murrell, and I.B. McInnes, Inflammatory mechanisms in tendinopathy – towards translation. Nature Reviews Rheumatology, 2017. 13(2): p. 110-122.

186. Dean, B.J.F., et al., Review: Emerging concepts in the pathogenesis of tendinopathy. The Surgeon, 2017. 15(6): p. 349-354.

187. Dakin, S.G., et al., Pathogenic stromal cells as therapeutic targets in joint inflammation. Nature Reviews Rheumatology, 2018. 14(12): p. 714-726.

188. Dakin, S.G., J. Dudhia, and R.K.W. Smith, Resolving an inflammatory concept: The importance of inflammation and resolution in tendinopathy. Veterinary Immunology and Immunopathology, 2014. 158(3): p. 121-127.

189. Millar, N.L., G.A.C. Murrell, and I.B. McInnes, Alarmins in tendinopathy: unravelling new mechanisms in a common disease. Rheumatology, 2013. 52(5): p. 769-779.

190. Crowe, L.A.N., et al., S100A8 & S100A9: Alarmin mediated inflammation in tendinopathy. Scientific Reports, 2019. 9(1): p. 1463.

191. Jouffroy, R., et al., Relationship between Exercise Intensity and IL-6 Increase during an 80 km Long-Distance Running Race. International Journal of Environmental Research and Public Health, 2022. 19(11): p. 6368.

192. Langberg, H., et al., Substantial elevation of interleukin-6 concentration in peritendinous tissue, in contrast to muscle, following prolonged exercise in humans. The Journal of Physiology, 2002. 542(3): p. 985-990.

193. Greenwel, P., et al., Tumor necrosis factor alpha inhibits type I collagen synthesis through repressive CCAAT/enhancer-binding proteins. Molecular and cellular biology, 2000.

194. Schmitz, J., et al., IL-33, an Interleukin-1-like Cytokine that Signals via the IL-1 Receptor-Related Protein ST2 and Induces T Helper Type 2-Associated Cytokines. Immunity, 2005. 23(5): p. 479-490.

195. Akbar, M., et al., Targeting danger molecules in tendinopathy: the HMGB1/TLR4 axis. RMD Open, 2017. 3(2): p. e000456.

196. Millar, N.L., et al., Hypoxia: a critical regulator of early human tendinopathy. Annals of the Rheumatic Diseases, 2012. 71(2): p. 302.

197. Tsai, S.L., M.-T. Nödl, and J.L. Galloway, Bringing tendon biology to heel: Leveraging mechanisms of tendon development, healing, and regeneration to advance therapeutic strategies. Developmental Dynamics, 2021. 250(3): p. 393-413.

198. Lim, W.L., et al., Current Progress in Tendon and Ligament Tissue Engineering. Tissue Engineering and Regenerative Medicine, 2019. 16(6): p. 549-571.

199. Heinemeier, K.M., et al., Effects of anti-inflammatory (NSAID) treatment on human tendinopathic tissue. Journal of Applied Physiology, 2017. 123(5): p. 1397-1405.

200. Thijs, K.M., et al., Effectiveness of shockwave treatment combined with eccentric training for patellar tendinopathy: a double-blinded randomized study. Clinical Journal of Sport Medicine, 2017. 27(2): p. 89-96.

201. Dragoo, J.L., et al., Platelet-rich plasma as a treatment for patellar tendinopathy: a double-blind, randomized controlled trial. The American journal of sports medicine, 2014. 42(3): p. 610-618.

202. Cardoso, T.B., et al., Current trends in tendinopathy management. Best Practice & Research Clinical Rheumatology, 2019. 33(1): p. 122-140.

203. Maffulli, N., U.G. Longo, and V. Denaro, Novel Approaches for the Management of Tendinopathy. JBJS, 2010. 92(15).

204. Bittermann, A., et al., Oral Ibuprofen Interferes with Cellular Healing Responses in a Murine Model of Achilles Tendinopathy. LID - 049 [pii] LID - 10.23937/2572-3243.1510049 [doi]. Journal of Musculoskeletal Disorders and Treatment, 2018. 4(2572-3243 (Electronic)): p. 49.

205. Loppini, M. and N. Maffulli, Conservative management of tendinopathy: an evidence-based approach. Muscles Ligaments Tendons, 2012. 1(2240-4554 (Print)): p. 134-137.

206. Chan, O., et al., High volume image guided injections in chronic Achilles tendinopathy. Disability and Rehabilitation, 2008. 30(20-22): p. 1697-1708.

207. Zhang, Y.-J., et al., Is Platelet-rich Plasma Injection Effective for Chronic Achilles Tendinopathy? A Meta-analysis. Clinical Orthopaedics and Related Research®, 2018. 476(8).

208. Madhi, M.I., et al., The use of PRP in treatment of Achilles Tendinopathy: A systematic review of literature. Study design: Systematic review of literature. Annals of Medicine and Surgery, 2020. 55: p. 320-326.

209. Rompe, J.D., J. Furia, and N. Maffulli, Eccentric Loading Compared with Shock Wave Treatment for Chronic Insertional Achilles Tendinopathy: A Randomized, Controlled Trial. JBJS, 2008. 90(1).

210. Rompe, J.D., J. Furia, and N. Maffulli, Eccentric Loading versus Eccentric Loading plus Shock-Wave Treatment for Midportion Achilles Tendinopathy: A Randomized Controlled Trial. The American Journal of Sports Medicine, 2008. 37(3): p. 463-470.

211. Best, T.M., et al., Low Intensity Ultrasound for Promoting Soft Tissue Healing: A Systematic Review of the Literature and Medical Technology. LID - 271 [pii] LID -

10.18103/imr.v2i11.271 [doi]. Internal Medicine Review, 2016. 2(2470-3524 (Print)): p. 271.

212. Dedes, V., et al., Comparison of radial extracorporeal shockwave therapy with ultrasound therapy in patients with lateral epicondylitis. Journal of Medical Ultrasonics, 2020. 47(2): p. 319-325.

213. Meduri, C., et al., Ultrasound Stimulation of Tendon Healing: Current Strategies and Opportunities for Novel Therapeutic Approaches, in Regenerative Rehabilitation: From Basic Science to the Clinic. 2022, Springer. p. 331-358.

214. de Lucas, B., et al., Application of low-intensity pulsed therapeutic ultrasound on mesenchymal precursors does not affect their cell properties. PLOS ONE, 2021. 16(2): p. e0246261.

215. Khanna, A., et al., The effects of LIPUS on soft-tissue healing: a review of literature. British Medical Bulletin, 2009. 89(1): p. 169-182.

216. Tanaka, E., et al., Effectiveness of low-intensity pulsed ultrasound on osteoarthritis of the temporomandibular joint: A review. Annals of Biomedical Engineering, 2020. 48(8): p. 2158-2170.

217. Zhang, N., et al., Ultrasound as a stimulus for musculoskeletal disorders. Journal of Orthopaedic Translation, 2017. 9: p. 52-59.

218. Darrieutort-Laffite, C., L.J. Soslowsky, and B. Le Goff, Molecular and structural effects of percutaneous interventions in chronic Achilles tendinopathy. International Journal of Molecular Sciences, 2020. 21(19): p. 7000.

219. Alfredson, H., Ultrasound and Doppler-guided mini-surgery to treat midportion Achilles tendinosis: results of a large material and a randomised study comparing two scraping techniques. British Journal of Sports Medicine, 2011. 45(5): p. 407.

220. Hsieh, Y.-L., et al., Percutaneous soft tissue release performed using a blunt cannula in rabbits with chronic collagenase-induced Achilles tendinopathy. Foot and Ankle Surgery, 2019. 25(2): p. 186-192.

221. Lin, M.-T., et al., Percutaneous soft tissue release for treating chronic recurrent myofascial pain associated with lateral epicondylitis: 6 case studies. Evidence-Based Complementary and Alternative Medicine, 2012. 2012(1): p. 142941.

222. Stoychev, V., A.S. Finestone, and L. Kalichman, Dry Needling as a Treatment Modality for Tendinopathy: a Narrative Review. Current Reviews in Musculoskeletal Medicine, 2020. 13(1): p. 133-140.

223. Darrieutort-Laffite, C., L.J. Soslowsky, and B. Le Goff Molecular and Structural Effects of Percutaneous Interventions in Chronic Achilles Tendinopathy. International Journal of Molecular Sciences, 2020. 21, DOI: 10.3390/ijms21197000.

224. Yeo, A., N. Kendall, and S. Jayaraman, Ultrasound-guided dry needling with percutaneous paratenon decompression for chronic Achilles tendinopathy. Knee Surgery, Sports Traumatology, Arthroscopy, 2016. 24(7): p. 2112-2118.

225. Abate, M., L. Di Carlo, and V. Salini, Platelet rich plasma compared to dry needling in the treatment of non-insertional Achilles tendinopathy. The Physician and Sportsmedicine, 2019. 47(2): p. 232-237.

226. Finnoff, J.T., et al., Treatment of Chronic Tendinopathy with Ultrasound-Guided Needle Tenotomy and Platelet-Rich Plasma Injection. PM&R, 2011. 3(10): p. 900-911.

227. Maffulli, N. and D. Kader, TENDINOPATHY OF TENDO ACHILLIS. The Journal of Bone & Joint Surgery British Volume, 2002. 84-B(1): p. 1-8.

228. Paavola, M., et al., Achilles Tendinopathy. JBJS, 2002. 84(11).

229. Maffulli, N., et al., Surgical Decompression of Chronic Central Core Lesions of the Achilles Tendon. The American Journal of Sports Medicine, 1999. 27(6): p. 747-752.

230. Longo, U.G., M. Ronga, and N. Maffulli, Achilles Tendinopathy. Sports Medicine and Arthroscopy Review, 2009. 17(2).

231. Maffulli, N., A.G. Via, and F. Oliva, Chronic Achilles Tendon Disorders: Tendinopathy and Chronic Rupture. Clinics in Sports Medicine, 2015. 34(1556-228X (Electronic)): p. 607-624.

232. Silbernagel, K.G., S. Hanlon, and A. Sprague, Current Clinical Concepts: Conservative Management of Achilles Tendinopathy. Journal of Athletic Training, 2020. 55(1938-162X (Electronic)): p. 438-447.

233. Malliaras, P., et al., Achilles and Patellar Tendinopathy Loading Programmes. Sports Medicine, 2013. 43(4): p. 267-286.

234. Kongsgaard, M., et al., Corticosteroid injections, eccentric decline squat training and heavy slow resistance training in patellar tendinopathy. Scandinavian Journal of Medicine & Science in Sports, 2009. 19(6): p. 790-802.

235. Yu, J., D. Park, and G. Lee, Effect of Eccentric Strengthening on Pain, Muscle Strength, Endurance, and Functional Fitness Factors in Male Patients with Achilles Tendinopathy. American Journal of Physical Medicine & Rehabilitation, 2013. 92(1).

236. Mafi, N., R. Lorentzon, and H. Alfredson, Superior short-term results with eccentric calf muscle training compared to concentric training in a randomized prospective multicenter study on patients with chronic Achilles tendinosis. Knee Surgery, Sports Traumatology, Arthroscopy, 2001. 9(1): p. 42-47.

237. Fahlström, M., et al., Chronic Achilles tendon pain treated with eccentric calf-muscle training. Knee Surgery, Sports Traumatology, Arthroscopy, 2003. 11(5): p. 327-333.

238. Magnusson, S.P. and M. Kjaer, The impact of loading, unloading, ageing and injury on the human tendon. The Journal of Physiology, 2019. 597(5): p. 1283-1298.

239. Murrell, G.A.C., et al., Effects of immobilization on achilles tendon healing in a rat model. Journal of Orthopaedic Research, 1994. 12(4): p. 582-591.

240. Palmes, D., et al., Achilles tendon healing: Long-term biomechanical effects of postoperative mobilization and immobilization in a new mouse model. Journal of Orthopaedic Research, 2002. 20(5): p. 939-946.

241. Hillin, C.D., et al., Effects of immobilization angle on tendon healing after achilles rupture in a rat model. Journal of Orthopaedic Research, 2019. 37(3): p. 562-573.

242. Grävare Silbernagel, K. and K.M. Crossley, A Proposed Return-to-Sport Program for Patients With Midportion Achilles Tendinopathy: Rationale and Implementation. Journal of Orthopaedic & Sports Physical Therapy, 2015. 45(11): p. 876-886.

243. Färnqvist, K., S. Pearson, and P. Malliaras, Adaptation of Tendon Structure and Function in Tendinopathy With Exercise and Its Relationship to Clinical Outcome. Journal of Sport Rehabilitation, 2020. 29(1): p. 107-115.

244. Beyer, R., et al., Heavy slow resistance versus eccentric training as treatment for Achilles tendinopathy: a randomized controlled trial. The American journal of sports medicine, 2015. 43(7): p. 1704-1711.

245. Tan, S.C. and O. Chan, Achilles and patellar tendinopathy: Current understanding of pathophysiology and management. Disability and Rehabilitation, 2008. 30(20-22): p. 1608-1615.

246. Irby, A., et al., Clinical management of tendinopathy: A systematic review of systematic reviews evaluating the effectiveness of tendinopathy treatments. Scandinavian Journal of Medicine & Science in Sports, 2020. 30(10): p. 1810-1826.

247. Kingma, J.J., et al., Eccentric overload training in patients with chronic Achilles tendinopathy: a systematic review. British Journal of Sports Medicine, 2007. 41(6): p. e3.

248. Murphy, M., M. Travers, and W. Gibson, Is heavy eccentric calf training superior to wait-and-see, sham rehabilitation, traditional physiotherapy and other exercise interventions for pain and function in mid-portion Achilles tendinopathy? Systematic Reviews, 2018. 7(1): p. 58.

249. Vander Doelen, T. and W. Jelley, Non-surgical treatment of patellar tendinopathy: A systematic review of randomized controlled trials. Journal of Science and Medicine in Sport, 2020. 23(2): p. 118-124.

250. O'Neill, S., S. Barry, and P. Watson, Plantarflexor strength and endurance deficits associated with mid-portion Achilles tendinopathy: The role of soleus. Physical Therapy in Sport, 2019. 37: p. 69-76.

251. O'Neill, S., P.J. Watson, and S. Barry, WHY ARE ECCENTRIC EXERCISES EFFECTIVE FOR ACHILLES TENDINOPATHY? nternational journal of sports physical therapy, 2015. 10,4(2159-2896 (Print)): p. 552-562.

252. Öhberg, L., R. Lorentzon, and H. Alfredson, Eccentric training in patients with chronic Achilles tendinosis: normalised tendon structure and decreased thickness at follow up. British Journal of Sports Medicine, 2004. 38(1): p. 8.

253. Grigg, N.L., S.C. Wearing, and J.E. Smeathers, Eccentric calf muscle exercise produces a greater acute reduction in Achilles tendon thickness than concentric exercise. British Journal of Sports Medicine, 2009. 43(4): p. 280.

254. Couppé, C., et al., Eccentric or concentric exercises for the treatment of tendinopathies? journal of orthopaedic & sports physical therapy, 2015. 45(11): p. 853-863.

255. Woodley, B.L., R.J. Newsham-West, and G.D. Baxter, Chronic tendinopathy: effectiveness of eccentric exercise. British Journal of Sports Medicine, 2007. 41(4): p. 188.

256. Sayana, M.K. and N. Maffulli, Eccentric calf muscle training in non-athletic patients with Achilles tendinopathy. Journal of science and medicine in sport, 2007. 10(1440-2440 (Print)): p. 52-8.

257. Alfredson, H., et al., Heavy-Load Eccentric Calf Muscle Training For the Treatment of Chronic Achilles Tendinosis. The American Journal of Sports Medicine, 1998. 26(3): p. 360-366.

258. Habets, B., et al., No difference in clinical effects when comparing alfredson eccentric and silbernagel combined concentric-eccentric loading in achilles tendinopathy: a randomized controlled trial. Orthopaedic journal of sports medicine, 2021. 9(10): p. 23259671211031254.

259. Murphy, M., et al., Rate of improvement of pain and function in mid-portion Achilles tendinopathy with loading protocols: a systematic review and longitudinal meta-analysis. Sports Medicine, 2018. 48: p. 1875-1891.

260. Stanish, W.D., R.M. Rubinovich, and S. Curwin, Eccentric exercise in chronic tendinitis. Clinical Orthopaedics and Related Research®, 1986. 208: p. 65-68.

261. Thomee, P., J. Karlsson, and R. Thomee, Eccentric overload training for patients with chronic Achilles tendon pain–a randomised controlled study with reliability testing of the evaluation methods. Scand J Med Sci Sports, 2001. 11: p. 197-206.

262. Scott, A., et al., Sports and exercise-related tendinopathies: a review of selected topical issues by participants of the second International Scientific Tendinopathy Symposium (ISTS) Vancouver 2012. British Journal of Sports Medicine, 2013. 47(9): p. 536.

263. Silbernagel, K.G., Does One Size Fit All When It Comes to Exercise Treatment for Achilles Tendinopathy? Journal of Orthopaedic & Sports Physical Therapy, 2014. 44(2): p. 42-44.

Chapter 3 - Treatment Duration and Load Magnitude Differentially Affect Biomechanical Properties in a Preclinical Model of Achilles

3.1 Introduction

3.1.1 Achilles Tendinopathy and Treatments

Achilles tendinopathy (AT) is a common, debilitating disorder affecting people of all ages and lifestyles [1, 2]. Achilles tendinopathy develops in response to accumulation of damage from repetitive overloading and age-related factors such as decreased cellular renewal and differentiation [1, 3-7]. It is clinically defined by pain, swelling, and loss of physical function. If left untreated, AT results in increased risk for tendon rupture [4-6]. Current treatment methods remain limited, with poor long-term efficacy [8-10]. When administered during early recovery and the inflammatory phase of healing, common pain medications can be deleterious to tendon healing. In a murine model of tendinopathy, oral ibuprofen (a common nonsteroidal anti-inflammatory drug) administration resulted in decreased tendon stiffness and elastic modulus and inhibited the remodeling phase [10]. Surgical treatment, consisting of the removal of the degraded and immediately adjacent tissue often prolongs healing times and results in an increased risk of developing infection, rupture, tissue necrosis, and fibrotic scar-tissue formation, which could require additional surgeries [11-13]. Other conservative treatments, such as platelet rich plasma injection, dry needling, and ultrasound stimulation have shown mixed results [14-16]. Physical therapy regimens have, however, been shown to effectively provide symptomatic relief and improve tissue architecture [17-21].

3.1.2 Muscle Loading Therapies

Physical therapy exercises employ both eccentric (lengthening of the gastrocnemius muscle while it contracts) and concentric (shortening of the gastrocnemius muscle while it contracts) loading phases (Figure 3.1) and provide symptomatic relief of human AT [19, 22-26]. To perform these eccentric exercises, the patient is positioned with the ball of the foot on the edge of a step with the heel off the step. The heel is then extended slowly downward, creating dorsiflexion of the ankle, and the position is briefly maintained. The heel is then slowly raised into plantarflexion. This cycle of motion is then repeated multiple times per session as prescribed by the physiotherapist. The

underlying mechanisms by which these muscle loading routines achieve tendon healing have yet to be elucidated [17, 24]**.** Clinical evidence is inconclusive. For example, one study reported that eccentric muscle loading reestablished normal tendon architecture (tendon geometry and collagen orientation) [21]while other studies have shown that eccentric exercises increase tendon cross sectional area [27, 28]. These inconclusive outcomes suggest that structural improvements are not solely responsible for the positive functional outcomes [29, 30]**.** Extrinsic factors (body mass and severity of tendinopathy) influence the patient's healing capacity. The identification and an adequate physical therapy regime (loading magnitude and duration of therapy) to achieve functional tendon healing is imperative to improve patient outcomes [18, 31]. The heterogeneity of the affected population creates an opportunity for further investigation into the underlying mechanisms that facilitate tendon healing.

Figure 3.4: Human heel drop loading exercises. Range of motion dorsiflexion (left), plantarflexion (middle), and return to dorsiflexion (right).

3.1.3 Pre-clinical Exercise Models

Several studies have investigated the efficacy of mechanostimulation to improve tendon healing by comparing muscle loading to immobilized muscle-tendon units. Both canine and rat models demonstrated the benefits of muscle stimulation on healthy and injured tendon biomechanical properties such as maximum load and strain [32-34]. Prolonged immobilization negatively impacts the biomechanical properties (maximum load and modulus) of tendons [35-39]. Muscle loading has been shown to stimulate healing in rodent transection and repair models, and eccentric-based

exercises improved the maximum load of partially transected rat patellar tendons [40, 41]. Furthermore, muscle loading resulted in the enhancement of the biomechanical properties of naïve tendons after 2-3 weeks of loading [41, 42]. Treadmill running and voluntary wheel running are common muscle loading models and are readily implemented in rodent models [43-46]; however, they lack specificity in muscle stimulation and do not simulate clinical physical therapy routines [47, 48]. This lack of specificity makes the identification of loading intensity and frequency difficult to replicate and does not translate to clinical exercises. To mimic clinical rehabilitative muscle loading routines, we used an established tissue-targeted preclinical mouse model of Achilles tendinopathy to investigate the effects of different loading magnitudes and treatment durations on tendon healing. We hypothesized that as eccentric muscle loading magnitude and treatment duration increased there would be significant improvements in the biomechanical properties of injured Achilles tendons and morphological improvements.

3.2 Materials and Methods

3.2.1 Experimental Design

A modification of a previously described transforming growth factor (TGF)-β1 mouse Achilles tendon injury model [10, 12, 48-50] was used to study the effects of loading magnitude for 1, 2 and 4 weeks (Figure 3.3). Loading parameters and electrical stimulation tolerance (dorsiflexion range of motion, footplate speed, number of repetitions, sets of repetitions, and treatment frequency to best imitate clinical practices) were previously described by Rezvani et al. [49]. For tendon biomechanical analyses, 3 different loading magnitudes (50%, 75%, and 100% bodyweight (BW)) were investigated, while histologic and transcriptomic evaluations were carried out at 50% and 100% BW loading magnitudes (Table 3.1). *In vivo* muscle strength quantifications were performed as detailed below on all mice included in the study (n=8). Naïve mice and injured but unexercised mice served as controls.

3.2.2 Animals

Under Virginia Tech IACUC approval (protocol #21-239, 21-125), 12-week-old C57BL/6 male mice (Jackson Laboratories, Bar Harbor, ME; Stock No. 000664) were used for all studies. 11-week-old mice were delivered and entered a 1-week acclimation period prior to any

experimentation. All animals were housed on a 12-hour light/dark cycle and fed standard mouse diet and water *ad libitum* and allowed unrestricted cage activity (5 mice/cage). Upon the conclusion of *in vivo* experiments, mice were euthanized using carbon dioxide inhalation for a minimum of 4 minutes followed by cervical dislocation. Tissues were then harvested for analyses as detailed below.

3.2.3 Tendinopathy Induction

Achilles tendinopathy was induced using a modification of an established TGF-β1 mouse model [10, 48-50]. Lyophilized active recombinant human TGF-β1 (Peprotech, Inc, Rocky Hill, NJ) was reconstituted in filter sterilized 0.1% sterile bovine serum albumin in phosphate buffered saline and frozen and stored in 75µL aliquots at -20ºC in sterile 1mL microfuge tubes until use. On the day of model induction, a frozen TGF-β1 aliquot was thawed on ice, mixed gently by inversion, aliquoted in uniform 8 µl droplets onto a sterile petri dish, and 6 µL of 100 ng active rhTGF- β1 was drawn into a sterile 0.5 ml insulin syringe using a 0.5" 28G needle. This technique ensured consistent injection volumes. Mice were deeply anesthetized using 3% isoflurane in oxygen in a sealed anesthesia chamber and the hindlimb was prepared using aseptic technique. Two sets of paired injections of 100 ng of active rhTGF-β1 in 6 µL PBS were delivered 48 hours apart into the mid- and distal portions of the Achilles tendon of 12-week-old C57Bl/6 male mice (Figure 3.2). The 0.5" 28G needle was inserted into the gastrocnemius muscle complex and directed distally (~3 mm) into the midportion of the Achilles tendon, where the first injection was delivered (Figure 3.2). The second injection, using a new needle and fresh TGF-β1 aliquot, was directed through the gastrocnemius complex and guided more distally into the tendon near the calcaneus (~4-5 mm) to deliver the TGF-β1 [51]. Mice were allowed to recover in a clean cage with a heating pad or heat lamp. Injections were repeated 48 hours later in the same manner and under general anesthesia. These injections were well tolerated and did not result in lameness, soreness, or difficulty with ambulating.

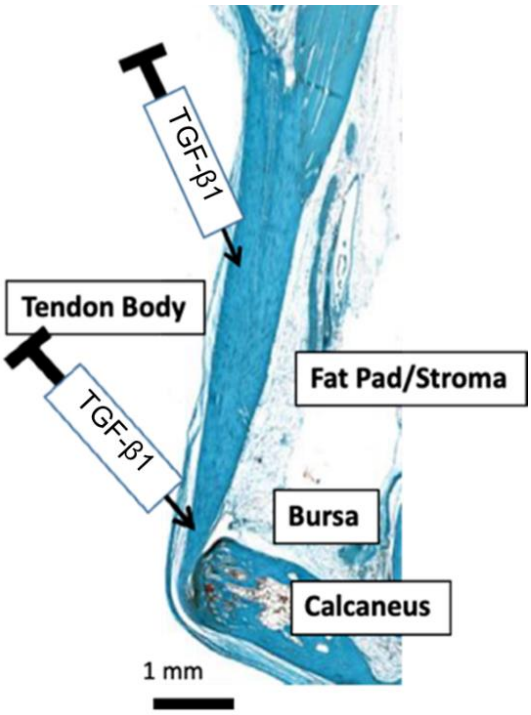

Figure 3.5: Locations of the TGF-β1 injections in the Achilles tendon (midportion and distal) [51].

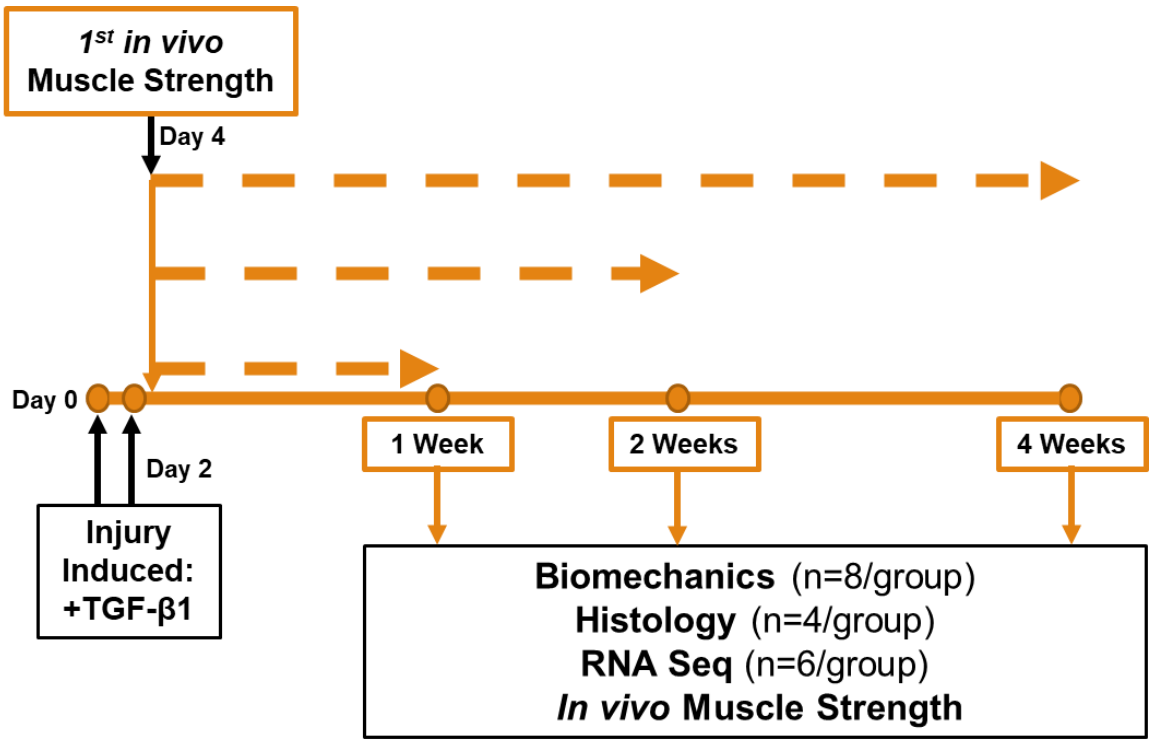

Figure 3.6: Tendinopathy induction and treatment timeline. Mice in treatment groups received treatment twice weekly for either 1-, 2-, or 4-weeks. Upon the conclusion of the treatment duration, mice were euthanized, and tendons harvested for biomechanical testing (50%, 75% and 100% BW) and histology (50% and 100% BW).

3.2.3 Tissue Targeted Muscle Loading and *In Vivo* Muscle Strength Measures

Two days following the second TGF-β1 injection, mice were deeply anesthetized using 3% isoflurane maintained in oxygen in a sealed anesthesia chamber for 3 minutes, weighed, then transferred to the temperature-controlled (37º) testing platform of the 305C-5N Dual-Mode Muscle Lever System (Aurora Scientific; Aurora, ON, Canada). While on the platform, anesthesia was delivered via a nose cone and maintained between 1.5-3% isoflurane [52]. The hair of the hind right limb was clipped and chemical depilatory cream was applied. Petroleum-based ophthalmic ointment was applied to both eyes to prevent corneal drying and irritation during anesthesia. The right hind foot was placed and secured into the foot pedal and the limb was adjusted so that the femur was oriented 90º to the tibia and the tibia 90º to the foot (Figure 3.4). The upper portion of the hindlimb was prepared using aseptic technique and stimulating electrodes (Natus

Manufacturing Ltd.; Galaway, Ir) were placed subcutaneously and parallel along the tibial nerve on the lateral aspect of the gastrocnemius muscle (~1 mm distal to the knee) at a depth between 0.5-1.0 mm. *In vivo* muscle strength assessments were performed immediately prior to each initial loading session and 24 hours after the final loading session following the methods outlined by Rezvani *et al*. and using the Aurora system [49, 53, 54]. Muscle strength profiles (torque-frequency) were established using a range of 11 frequencies (1, 10, 30, 50, 65, 80, 100, 120, 150, 180, and 200 Hz) with the stimulation being delivered for 0.5 seconds at 30 second intervals until all frequencies were completed. Torque output was measured at each of the 11 frequencies with each output being normalized to the body mass of each mouse to generate a torque-frequency relationship (n=8/group). Electrical stimulations were computer controlled (Aurora Scientific; Aurora, ON, Canada) while the foot pedal moved through the ankle joint's range of motion (±18º), mimicking the clinical heel drop exercise. Mice were maintained under anesthesia for the entire duration of the treatment (~20 minutes) until placed in a recovery cage following each treatment session. Identical measures were used to establish muscle strength profiles in age-matched naïve and injured/untreated groups.

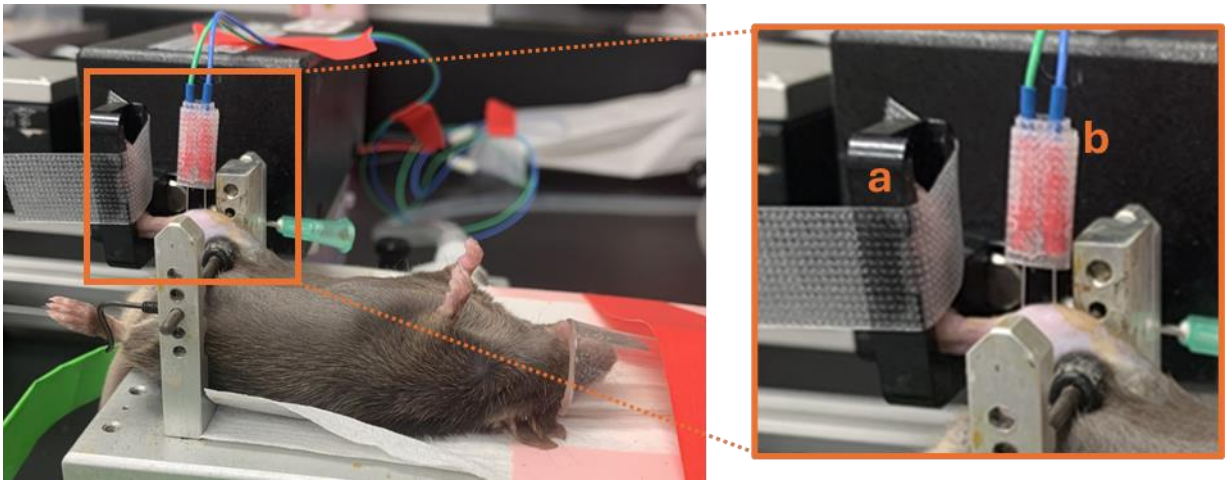

Figure 3.7*: In vivo* murine muscle loading set up. Insert to the right shows the (a) footplate to rotate the ankle through its range of motion and (b) electrodes to stimulate the tibial nerve to produce muscle contraction.

Isometric twitch torque profiles were generated for each mouse and optimized by identifying the ideal current (between 25-55 mÅ to maximize muscle stimulation). These were then used throughout the session and identified for each new session. Each repetition of the exercise began with the foot pedal in neutral position (90º between the foot and the tibia) and moved into (18º) dorsiflexion, followed by (18º) plantarflexion, then returned to the neutral (90º) starting position (Figure 3.4)[49, 55]. During the dorsi- and plantar- flexion phases specifically, electrical stimulation was delivered constantly at the determined current and assigned magnitude of frequency.

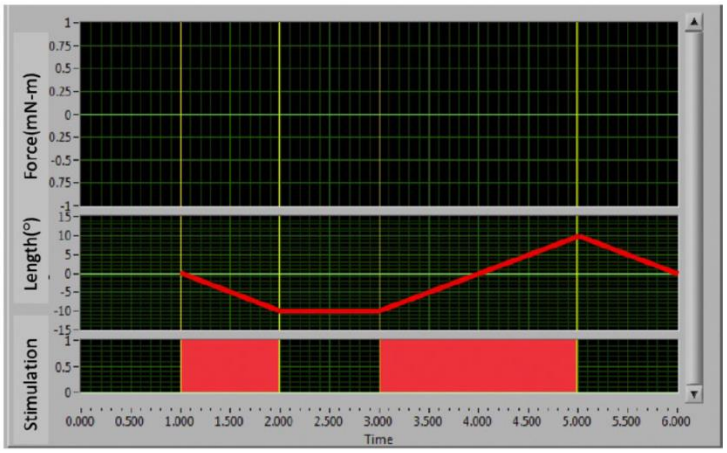

Figure 3.8: Overview of electrode stimulation pattern and footplate movement through one repetition of the exercise routine. Electrodes were stimulated in conjunction with the footplate movement to mimic physical therapy exercises. Length corresponds to the movement of the footplate, with a negative values denoting dorsiflexion and positive values denoting plantarflexion.

Age-matched naïve and injured/untreated (IU) groups served as controls at each time point. Injured/untreated mice were placed under anesthesia and fitted into the testing platform and foot pedal, as described above. The electrodes were placed in a manner identical to the loaded groups, but no muscle stimulation or ankle flexion was induced. Following the *in vivo* exercises, mice were placed in a clean recovery cage, equipped with a heating pad or heating lamp, and allowed to recover completely (fully ambulatory and alert) before being transferred to their original cage. All

mice were monitored for 24 hours after treatments to ensure there were no signs of distress, alterations to appetite, and activity level. These exercises were well tolerated and did not result in lameness, soreness, or difficulty with ambulating.

3.2.4 Eccentric Loading Protocols

Muscle loading protocols based on clinical methods that provide symptomatic relief [26, 49, 56] were developed in a previous preclinical *in vivo* study [51, 57]. Several iterations of these protocols were investigated to determine the tolerance and translation to an *in vivo* model of AT from the previous, uninjured model. The preclinical protocol was set at 3 sets of 10 repetitions of muscle loading treatments, 2 times per week using the full range of motion for the ankle joint (±18º), and a footplate speed of 5 mm/sec (Figure 3.5) [49]. The stimulation frequency (loading magnitude) is correlated to body mass according the following equation [57] to ensure that Aurora System stimulation frequencies of 50 Hz, 75 Hz, and 100 Hz corresponded to 50%, 75% and 100% BW loading represented in clinical practice when a patient targets the injured leg to complete the exercises with different degrees of support from either uninjured limb or the upper limbs.

$$Body\ Mass\ (g) = (Torque\ Output\ (mN * m)\ \times \frac{100cm}{1m} \times \frac{1N}{1000mN}\ \times \frac{1kg}{9.8N} \times \frac{1000g}{1kg})/ 2\ cm(foot\ pedal\ length))$$

The different loading magnitude protocols were performed for 1-, 2- or 4-weeks (Table 3.1).

Table 3.1: Experimental design outlining treatment groups, treatment duration, and outcome measures with the associated number of mice included per group.

Experimental Design			
Treatment Duration	Treatment Group	Outcome Measures	
		Biomechanics & Muscle Strength	Histology
1 Week	Naïve	8	0
	Injured/untreated	8	4
	50% Loading	8	4
	75% Loading	8	0
	100% Loading	8	4
2 Weeks	Naïve	8	4
	Injured/untreated	8	4
	50% Loading	8	4
	75% Loading	8	0
	100% Loading	8	4
4 Weeks	Naïve	8	0
	Injured/untreated	8	4
	50% Loading	8	4
	75% Loading	8	0
	100% Loading	8	4
	Total Mice	120	40

3.2.7 Biomechanical Testing

Tendon tensile properties were the primary quantitative measures used to assess how treatment protocols influenced tendon healing (n=8). Whole carcasses were frozen following euthanasia and maintained at -20ºC for 3-6 months before testing. On the day of testing, whole carcasses were thawed in a warm water bath for 20-25 minutes then the skin was removed from the right hind limb, the Achilles tendon was carefully separated from the fat pad/stroma, and excess muscle was dissected away from the remaining gastrocnemius complex. The foot with the attached tendon was then removed from the tibia by making a single cut anteriorly to the ankle joint, and the plantaris tendon was carefully dissected away from the Achilles tendon. The Achilles tendon/calcaneus complex was left fully intact. Finally, the remaining muscle was gently scraped away using the back of a scalpel blade[49, 58, 59]. The tendon-bone unit was then submerged in 0.9% saline and transferred for measurements. Tendon thickness was measured using a laser displacement sensor (Model #LK-G2; Keyence Corp., Itasca IL) and width was measured using precision digital calipers (resolution 0.01 mm; Model: CD-4" ASX; Mitutoyo American Corp. Aurora, IL) with measurements collected in 3 separate locations (proximal, midportion, and distal identified by the same anatomical landmarks) for width and thickness and the mean calculated for each. Cross-sectional area (CSA) was calculated assuming an elliptical geometry.

$$CSA\ (mm^2) = \frac{\pi}{4} \times mean\ thickness(mm) \times mean\ width(mm)$$

The dissected foot was then potted into a brass tube (6 mm diameter x 20 mm length), leaving the insertion site above the potting, and the dental cement (Stoelting Co., Wood Dale, IL) was allowed to cure for 25-30 minutes [57]. While curing, the tendon was wrapped in saline-soaked gauze. Once fully cured, the proximal portion of the tendon was blotted dry with a general-purpose cellulose wipe, secured into 20 mm wide thin film grips (Imada Inc., Northbrook, IL) with a gauge length based on the 6:1 length to width ratio for that tendon, and mounted into a mechanical testing system (MTS Insight 10, Eden Prairie, MN) (Figure 3.6).

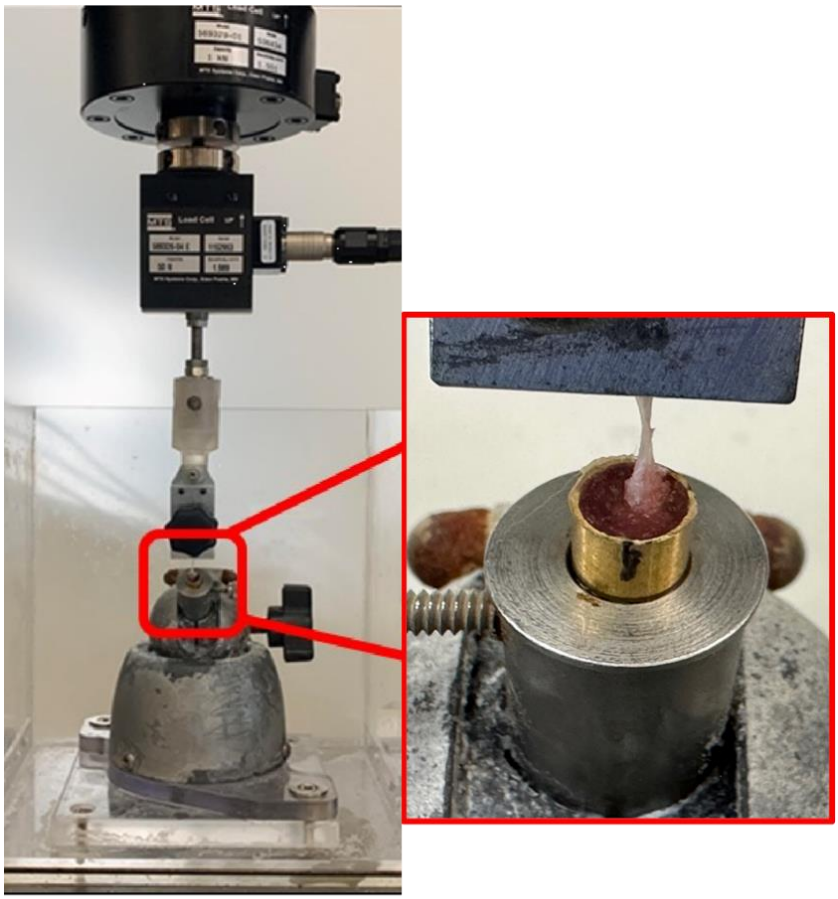

Figure 3.9: Dissected Achilles tendon-calcaneus unit set into MTS Insight 10 for biomechanical testing. Inset at right shows potted foot and attached Achilles tendon under preload.

Uniaxial tensile testing consisted of a preload to 0.5 N, a 2-minute rest period at the same extension as the preload, and a preconditioning protocol (20 cycles from 0.05 N to 0.55 N at 0.05 mm/sec),

concluding with a load to failure test at a rate of 0.05 mm/sec. A detailed protocol for uniaxial testing is outlined in Appendix A.

Tendon biomechanical property outcomes from tensile load-to-failure testing were divided into 2 main categories: structural (maximum load, stiffness) and material (stress, modulus) properties (Table 3.2). Maximum load was the upper limit of force before the tissue was irreversibly deformed (mimicking tendon rupture). Stiffness represents the ability of the tissue to resist deformation. Stiffness (representing the ability of the tissue to resist deformation) was calculated as the steepest part of the load-deformation curve spanning 30% of all data points collected between initiation of the test and the failure point [59]. After normalizing the gauge length by initial length (to calculate grip-to-grip strain) and load values to the CSA (to calculate stress), material properties were similarly computed using a custom MATLAB (Mathworks; Natick, MA) code unless stated otherwise (Outlined in Appendix C).

Table 3.2: List of biomechanical properties and respective units.

Biomechanical Properties		
Category	**Property**	**Units**
Geometric	Width	mm
	Thickness	mm
	Cross Sectional Area	mm^2
Structural	Maximum Load	Newtons (N)
	Stiffness	Newtons/millimeter (N/mm)
	Yield Load	N
Material	Maximum Stress	Megapascals (MPa)
	Elastic Modulus	MPa
	Yield Stress	MPa

3.2.8 Histology

Following completion of the treatment duration (1-, 2-, and 4-weeks), mice (n=4) from naïve, injured/untreated, and 50% and 100% BW groups were dissected immediately following euthanasia and prepared for histology [10, 12, 49, 58]. The skin was removed from the right hind limb and the limb was disarticulated at the hip joint and placed in a tissue cassette with the knee and ankle joints positioned at 90º angles. Tissues were fixed in 10% neutral buffered formalin for 5-7 days at room temperature, then decalcified using 5% ethylenediaminetetraacetic acid (EDTA) for 4-5 weeks with solution changes every 3 days. Decalcified tissues were embedded using a custom hydrophobic resin, sectioned at 5 μm, and stained with Toluidine blue (Tol Blue) and Safranin-O/Fast Green (Saf-O) [60]. Tissue sections were deidentified and scored blindly by 3 investigators trained in evaluation of tendon histology (DCE and LAD) on a scale of 0-3 (Table 3.3).

Table 3.3: Histology grading scale used to identify morphological and cellular changes in response to TGF-β1 injury induction and muscle loading treatments.

Histology Grading System				
	Score			
	0	**1**	**2**	**3**
Collagen Orientation	Normal: continuous, parallel fibers	Slightly abnormal: partially disorganized fibers	Abnormal: Moderately disorganized, crossed, wavy fiber	Severely abnormal: completely disorganized and non-identifiable pattern
Cell Density	Normal	Slightly Increased	Moderately increased	Severely Increased
Cellular Appearance	Spindle, cigar, or rectangularly shaped (mostly nucleus with little cytoplasm)	Slightly rounded	Moderately Rounded	Drastically Rounded
Saf-O (Intensity of staining immediately adjacent to cells)	Normal	Mild	Moderate	High

3.2.9 Statistical Analysis

Tendon geometric and biomechanical outcomes measures were assessed for normal distribution and analyzed using a 2-way ANOVA with Tukey's post-hoc tests (SAS Cary, NC). Histologic scores from the 2 investigators were averaged and the mean scores used for statistical analysis. Individual histologic parameters as well as the sum of the parameters for each sample were analyzed. Non-parametric methods with generalized estimating equations were used to analyze histologic scoring. Multivariate analysis was performed to determine correlations between muscle strength and tendon geometric and biomechanical properties (CSA, maximum load, maximum stress, and elastic modulus). Pooled data from injured and uninjured were analyzed separately for exercised and unexercised mice. A correlation coefficient >0.7 was considered a strong correlation, between 0.5 and 0.7 considered moderate correlation and <0.5 a weak correlation. Statistical significance was set at $p<0.05$.

3.3 Results

3.3.1 Muscle Strength Evaluations

Muscle strength quantified pre and post therapeutic exercise enabled documentation of the effect of exercise over time. The initial muscle strength at 100 Hz at 2 weeks the IU had significantly lower muscle strength compared to the naïve group ($p=0.017$). No other significant differences were observed with the remaining initial muscle strength assessments for any treatment group for any timepoint (Figure 3.7) at 100 Hz. After 1-week muscle strength was significantly lower in the 50% and 100% BW loading groups compared to the naïve group ($p<0.001$ for both) (Figure 3.8A). After 2 weeks of exercise muscle strength in the 75% and 100% BW loading groups was significantly decreased compared to the naïve group ($p<0.001$ for both) (Figure 3.8B). Muscle strength was significantly decreased after 4-weeks of exercise in the 50% ($p=0.021$) and 75% BW ($p<0.001$) groups compared to the naïve group (Figure 3.8C). Muscle strength at 100 Hz differential effects muscle strength from each treatment group (Figure 3.8D).

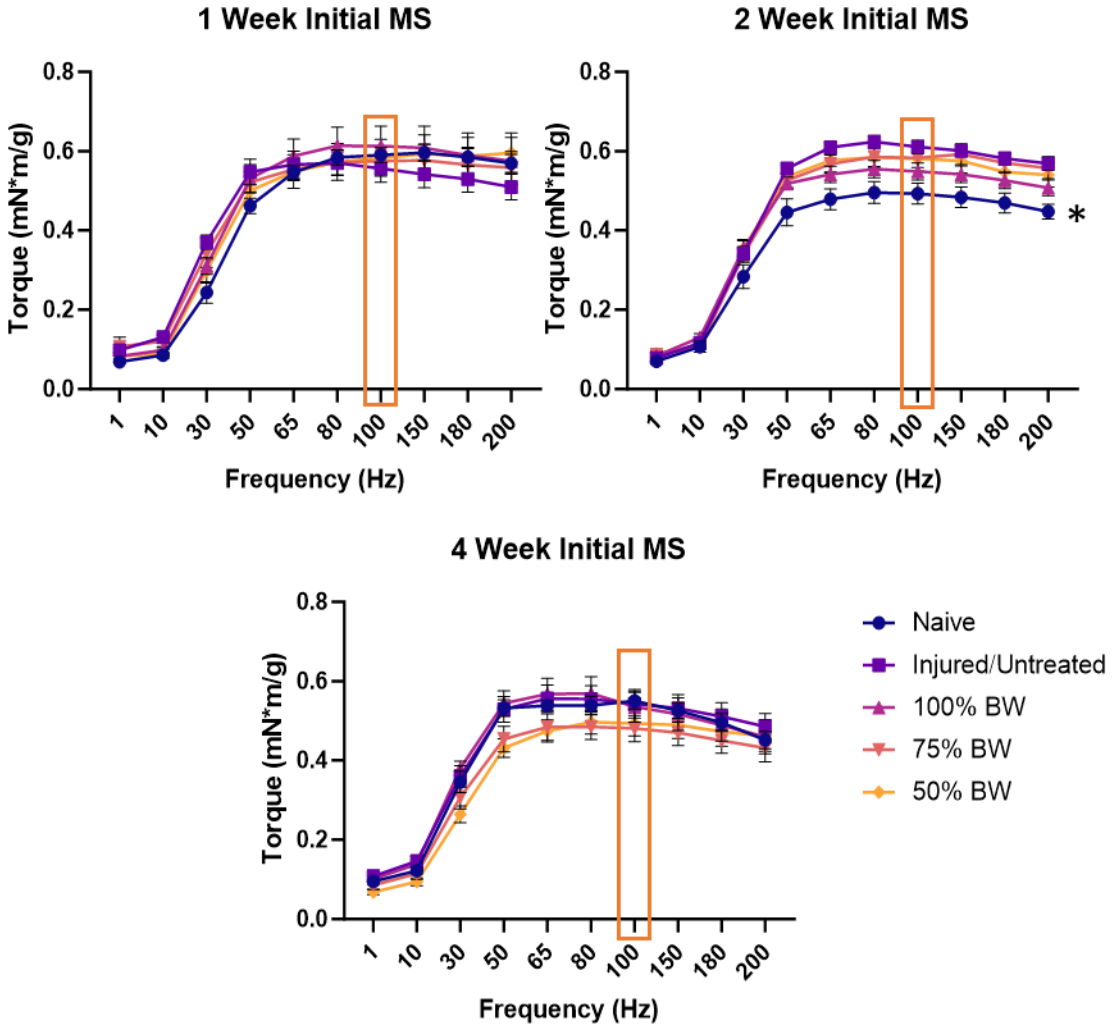

Figure 3.10: Initial *in vivo* muscle strength collected prior to experimental muscle stimulation. 100 Hz outlined in the orange rectangle. * denotes a significant difference from the naïve group. Mean ± SD.

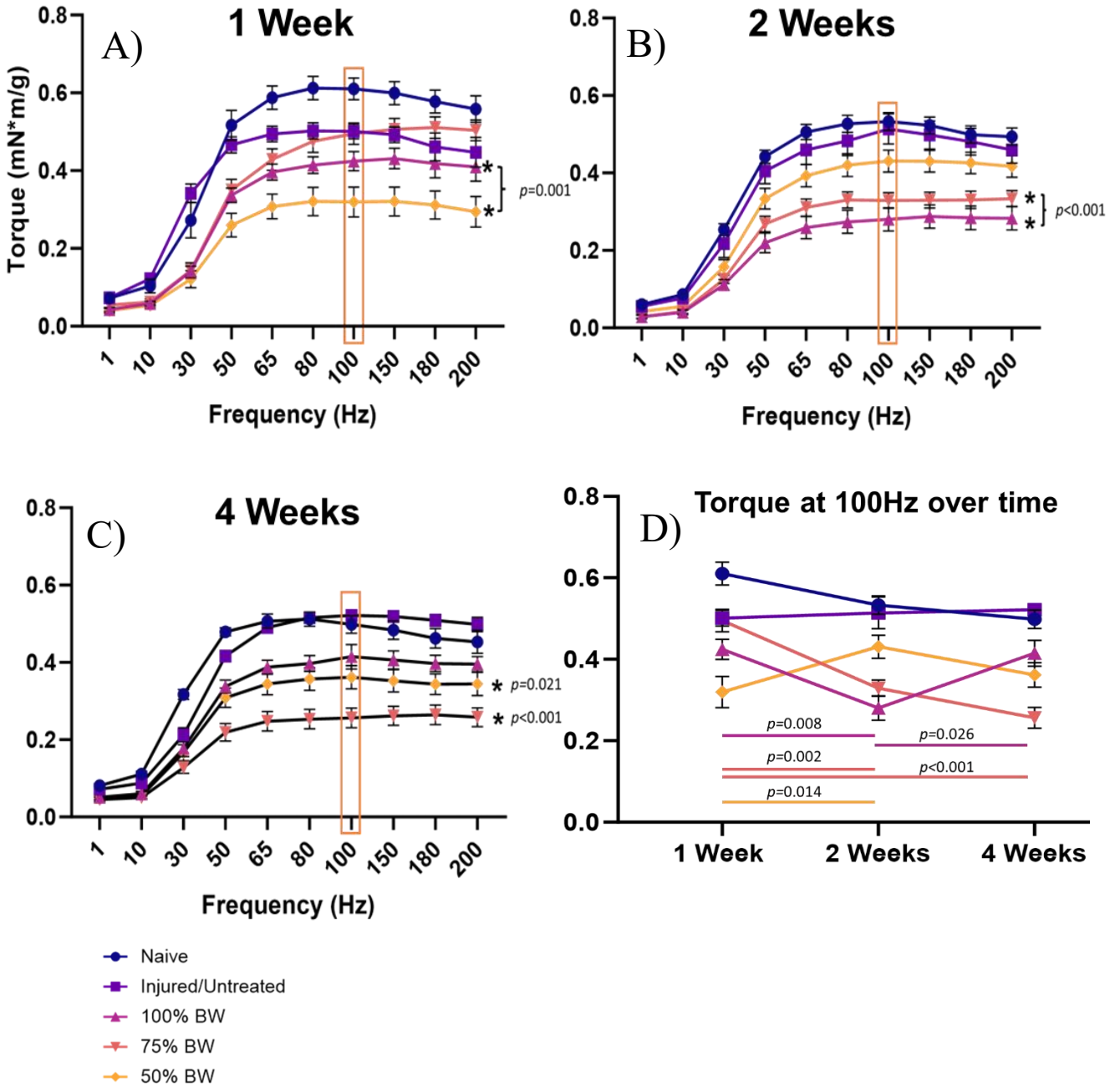
A)
1 Week
Torque (mN*m/g)
Frequency (Hz)
p=0.001
B)
2 Weeks
Frequency (Hz)
p<0.001
C)
4 Weeks
Frequency (Hz)
p=0.021
p<0.001
D)
Torque at 100Hz over time
p=0.008
p=0.026
p=0.002
p<0.001
p=0.014
1 Week
2 Weeks
4 Weeks
Naive
Injured/Untreated
100% BW
75% BW
50% BW

Figure 3.11: *In vivo* muscle strength after 1 (A), 2 (B), and 4 (C) weeks of treatment and over time within treatments (at 100 Hz). Muscle strength decreased significantly when measured at 100 Hz for all 3 treatment durations compared to the naïve group as indicated by * (highlighted by orange box). Significant differences over time within a single treatment group (D) indicated by colored lines. A) The 50% BW, 100% BW, and IU groups muscle strength was significantly lower than the naïve group at 1 week. B) The 75% BW and 100% BW was significantly lower than the naïve group at 2 weeks. C) The 50% and 75% BW groups were significantly lower than the naive group at 4 weeks. Mean ± SD.

3.3.1 Effects of Eccentric Loading Magnitude and Duration on Tendon Healing

After 1 week of loading (Figure 3.9), there was no significant difference in CSA between any of the groups, but maximum load of the IU group was significantly lower compared to the naïve (p<0.001) and 100% BW (p=0.008) groups. The maximum stress of the IU group was significantly decreased compared to the naïve (p=0.001) and 100% BW (p=0.009) groups and the elastic modulus of the IU group was significantly decreased compared to the naïve group (p=0.004).

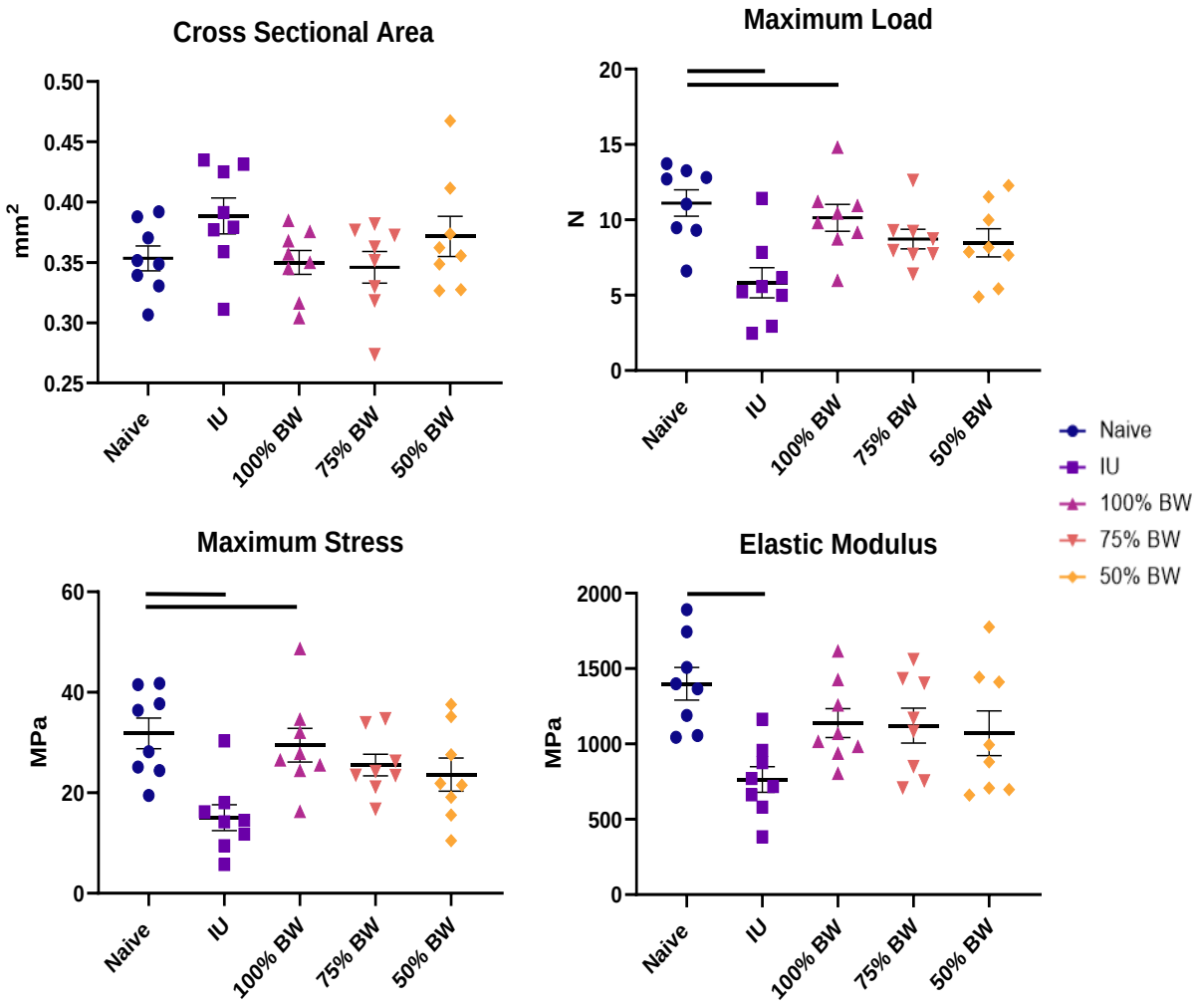

Figure 3.12: Biomechanical properties of healing Achilles tendons following 1 week of muscle loading. Horizontal lines denote significant differences between two groups ($p<0.05$).

Following 2 weeks of loading (Figure 3.10), the CSA of the IU group was significantly increased compared to all other groups ($p<0.001$). There were no significant differences in maximum load between groups. The maximum stress of the IU group was significantly lower than the 50% BW group ($p=0.038$). The elastic modulus of the IU group was significantly decreased compared to the 75% BW group ($p=0.032$).

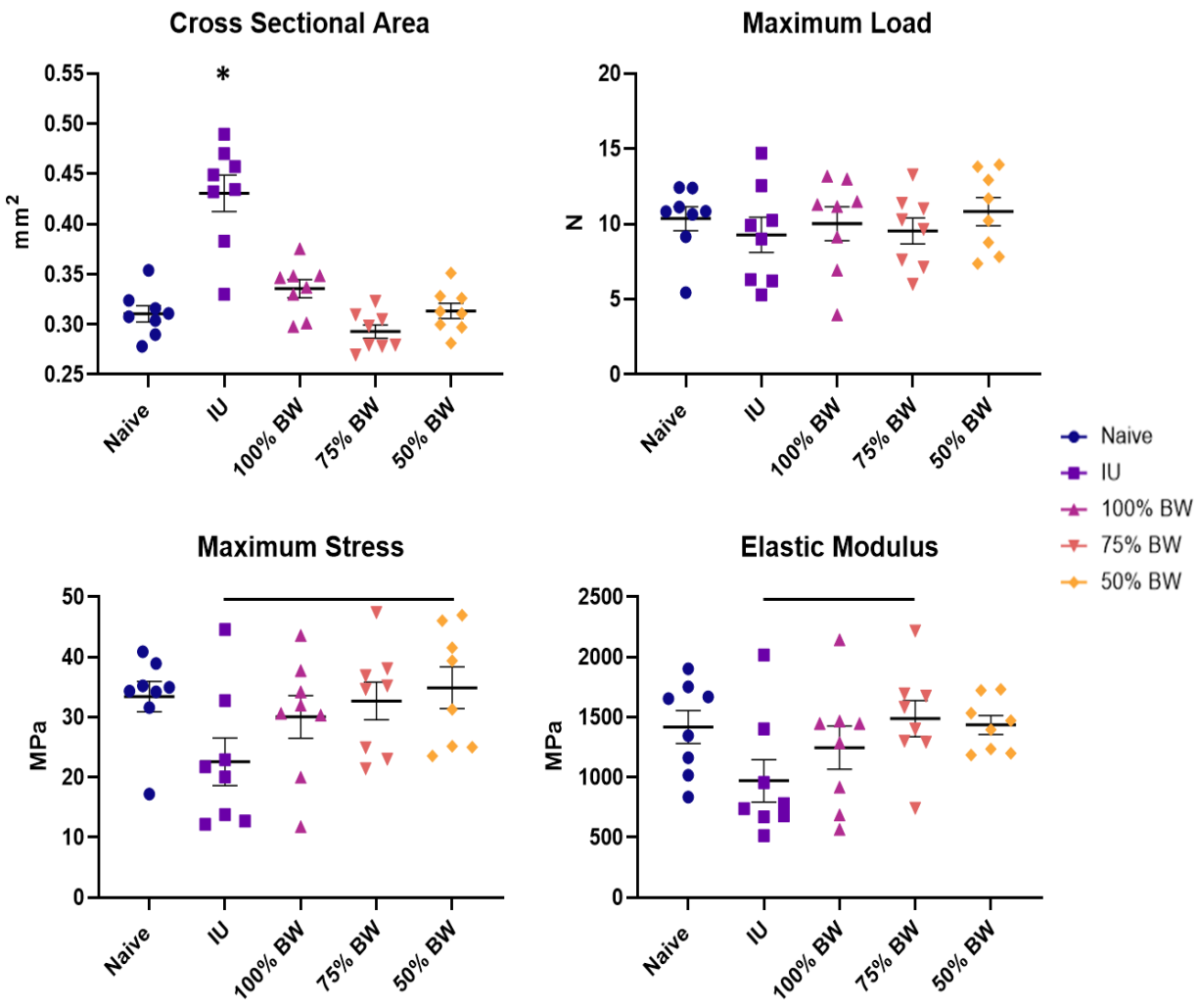

Figure 3.13: Biomechanical properties of healing Achilles tendons following 2 weeks of muscle loading. Symbols above groups denote differences from the naïve group ($p<0.05$). Horizontal lines denote significant differences between two groups ($p<0.05$).

After 4 weeks of loading (Figure 3.11), the CSA of the IU group was significantly increased compared to the naïve and all loading groups (p<0.001 for all) and the 100% BW group was significantly increased to the naïve group (p=0.020). There were no significant differences for maximum load between groups. The maximum stress of the IU group was significantly lower than the naïve (p=0.026), 100% BW (p=0.020), 75% BW (p=0.004), and 50% BW (p=0.006) groups. The elastic modulus of the IU group was significantly decreased compared to the naïve (p=0.017) and 75% BW (p=0.026) groups.

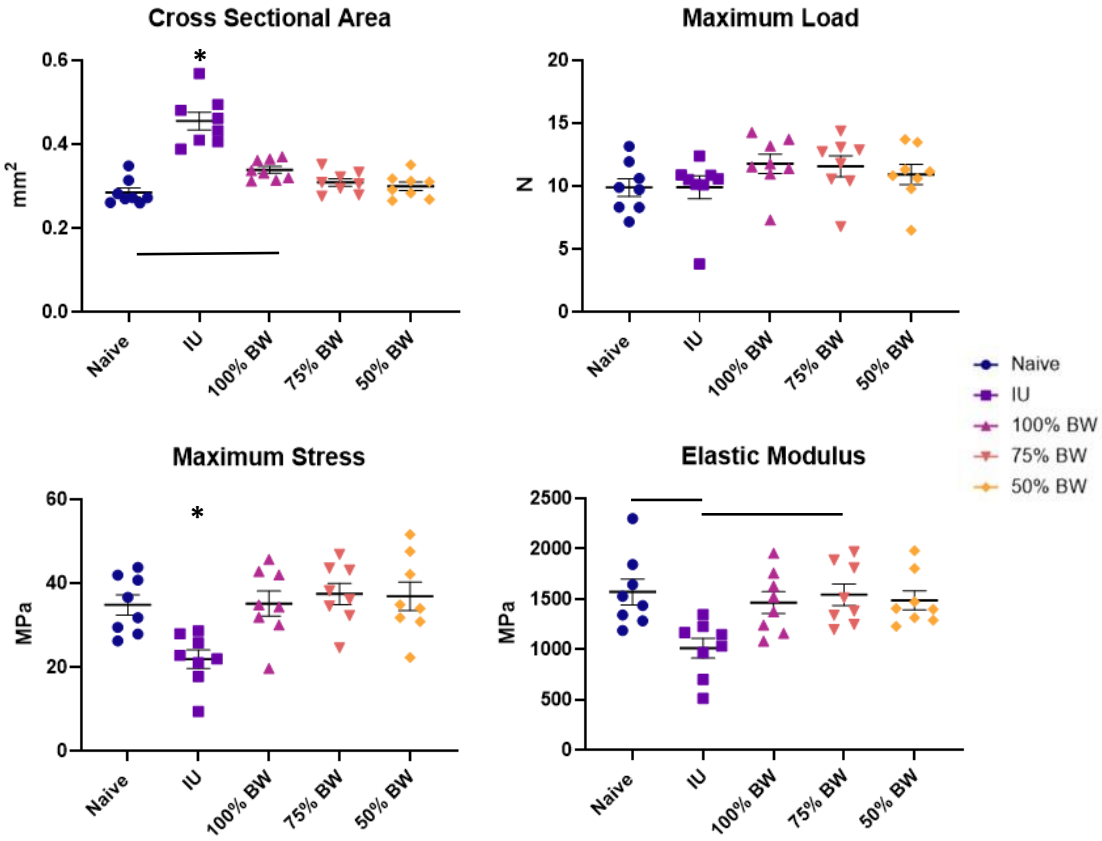

Figure 3.14: Biomechanical properties of healing Achilles tendons following 4 weeks of muscle loading. Symbols above groups denote differences from the naïve group (p<0.05). Horizontal lines denote significant differences between two groups (p<0.05).

When considered over the duration of the study (Figure 3.12), the CSA of the IU group was significantly increased at 2 and 4 weeks (p<0.001) compared to all other groups at the respective

time points. At 4 weeks the CSA of the 100% BW group was significantly increased compared to the naïve group (p<0.020. Maximum stress of the IU group was significantly decreased (p=0.025) compared to the naive and all loading groups after 4 weeks of loading. Similarly, the elastic modulus of the IU group was significantly decreased (p<0.001) after 4 weeks compared to the naïve and 75% BW groups. No statistically significant differences were observed in maximum load over time.

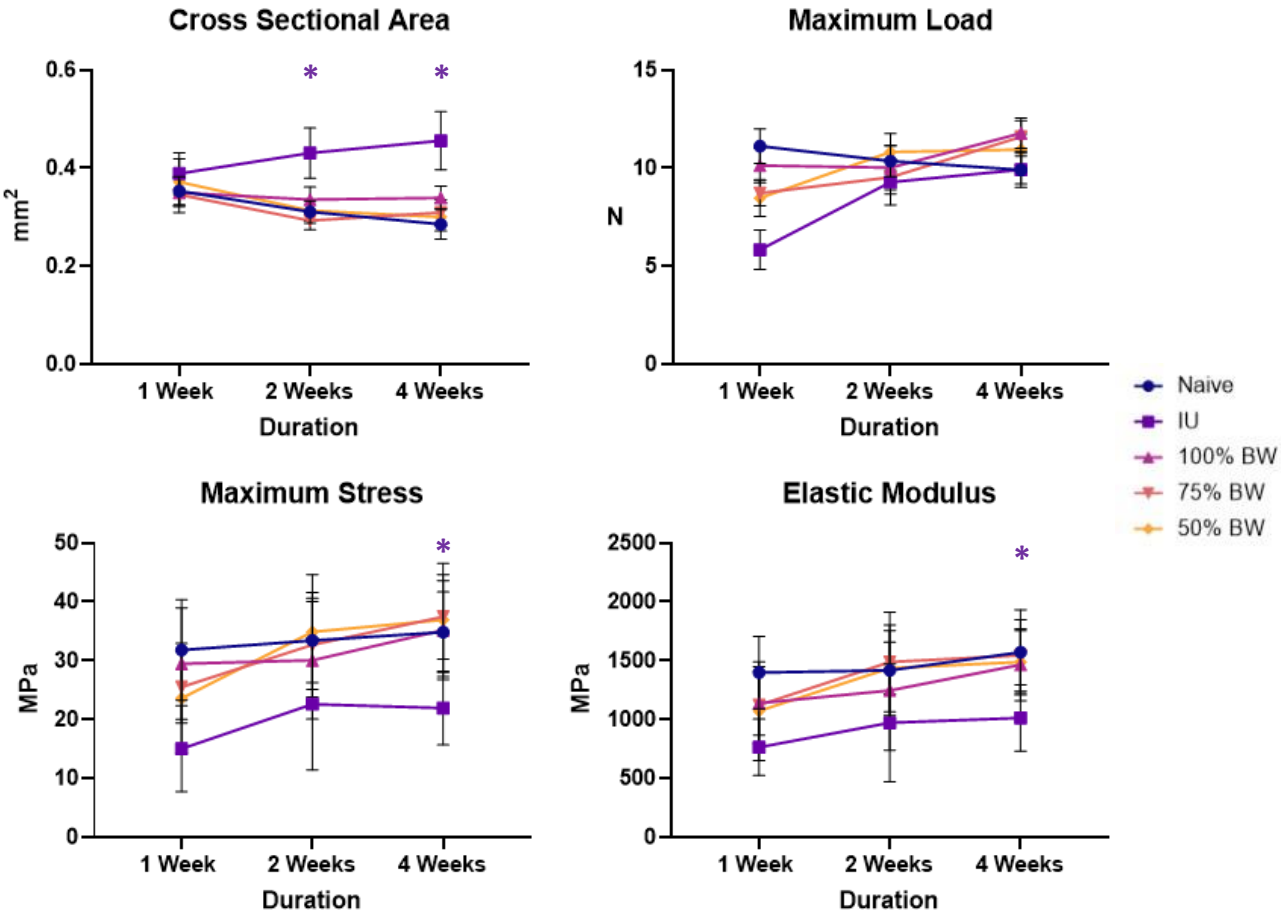

Figure 3.15: Biomechanical properties of healing Achilles tendons over time. * Indicates significant differences between groups at that time point (p<0.05). Mean ± SD.

The correlation analysis data showed a weak or no correlation between muscle strength and tendon CSA (0.04), maximum load (-0.002), maximum stress (0.016), and elastic modulus (-0.0003).

3.3.2 Histological Evaluation of Tendon from Different Eccentric Loading Protocols

There were no significant differences in any of the scored parameters or the sum of the scores for any treatment group at any time point or over time within a treatment group (Table 3.4). Interobserver agreement was determined by Kappa statistical measures for each of our histologic grading categories: collagen orientation (0.82), cellular density (0.86), cellular appearance (0.76), and safranin-o staining intensity (0.82). A Kappa score greater than 0.8 was considered a strong agreement, between 0.8 and 0.6 was considered good agreement, 0.6 to 0.4 was moderate agreement, and below 0.4 was considered little agreement. A number of subjective observations of note were observed. Along the interface between the tendon body and the deep adipose tissue increased cellularity was observed at 1 week in the loading groups (Figure 3.14). In the IU group, localized areas of chondroid metaplasia were more visible in the midportion of the tendon at 4 weeks compared to the two exercised groups (Figure 3.16). The 50% and 100% BW loading groups exhibited a more linear collagen fiber orientation than the IU group and exhibited increased cellularity at the myotendinous junction compared to naïve tendons at 4 weeks (Figure 3.15). Collagen alignment improved, cellularity increased, and reduced areas of sulphated glycosaminoglycans were observed as loading magnitude and treatment duration increased.

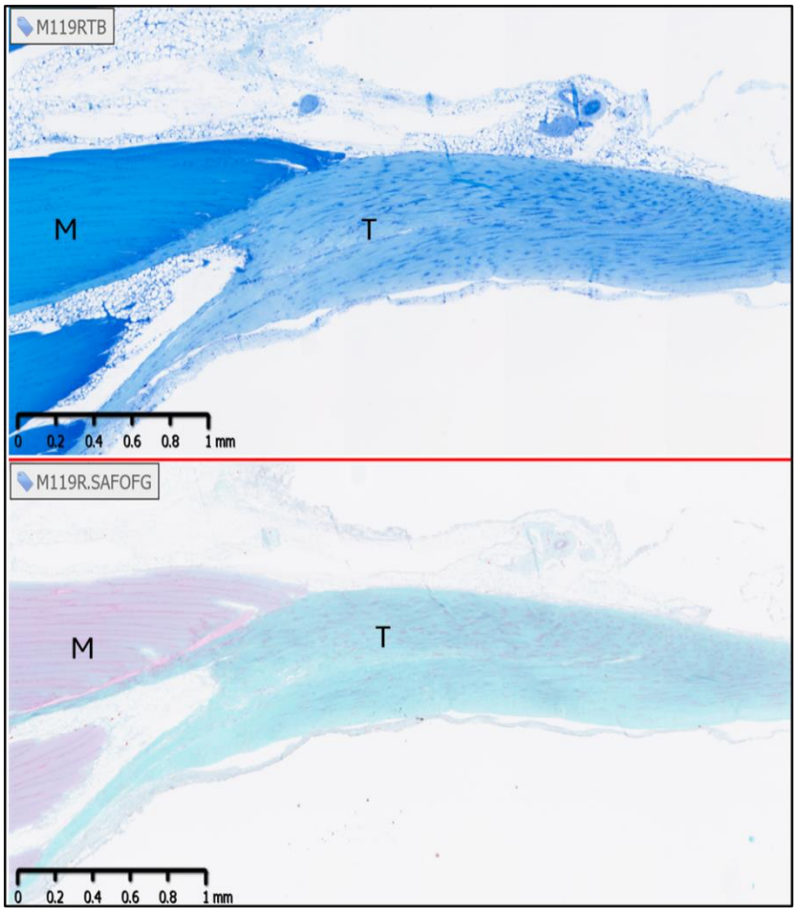

Figure 3.16: Representative low magnification images of Toluidine Blue- (Top) and Safranin-O/Fast Green-stained (Bottom) naïve Achilles tendon showing cellularity in muscle and tendon and collagen orientation. M: Muscle, T: Tendon. Left of images is proximal.

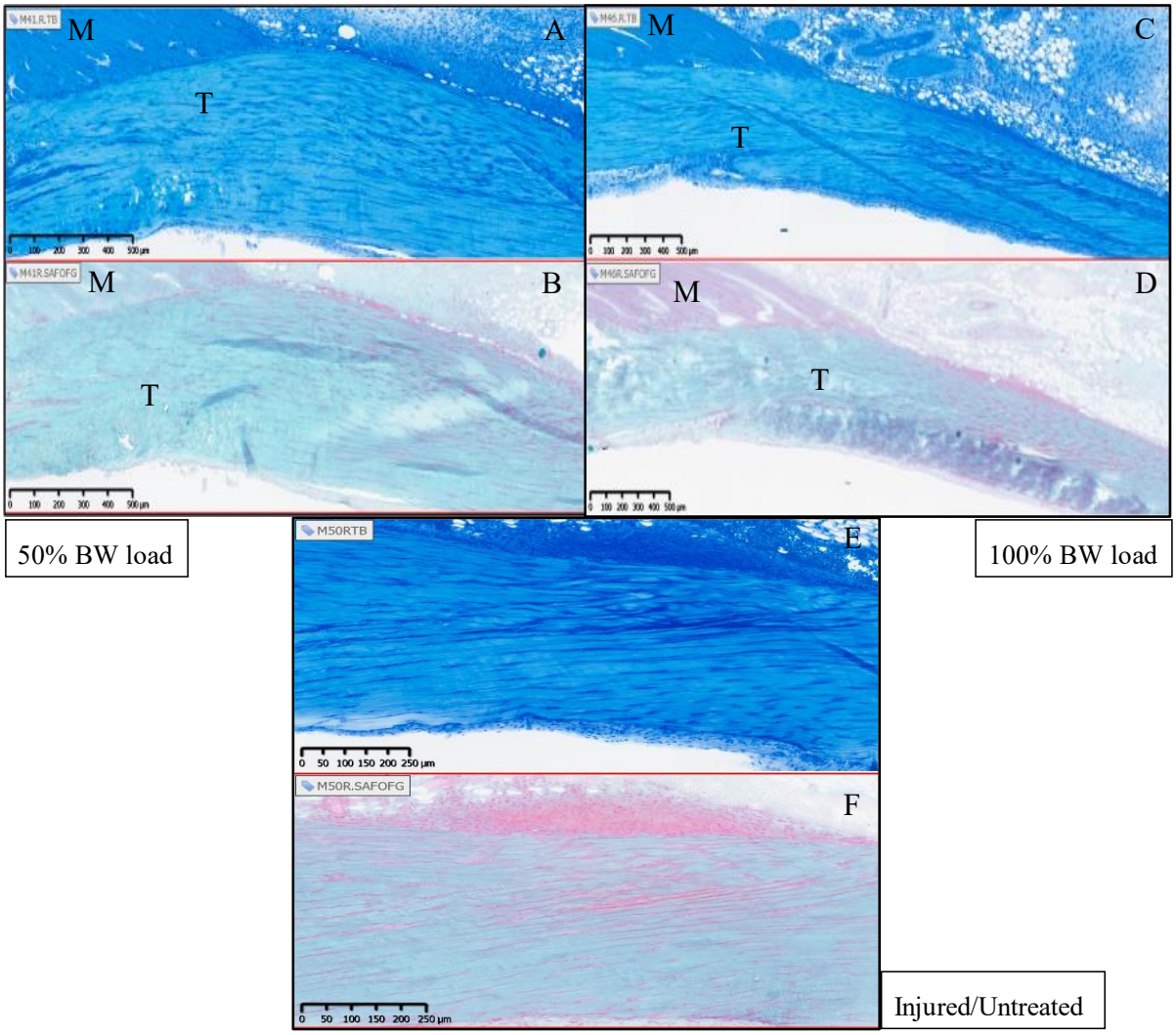

Figure 3.17: Representative Toluidine Blue- (A, C, E) and Safranin-O/Fast Green-stained (B, D, F) Achilles tendons after 1 week of exercise showing increased cellularity, collagen orientation, and Safranin-O staining intensity between the 50% BW, 100% BW and Injured/Untreated groups. Top left: 50% BW, Top right: 100% BW, Bottom Injured/Untreated. M: Muscle, T: Tendon. Left side of each image is proximal.

After 2 weeks of loading, large areas of increase cellularity throughout the tendons midportion and increased cellularity between the adipose and tendon tissue in the IU, 50%, and 100% BW groups were noted compared to naïve tendon. Consistent with the 1 week observations, 50% and 100% BW loading groups displayed more normally aligned collagen fibers and increased cellularity at the myotendinous junction and between the tendon and the adipose tissue of the fat pad. The cells

that infiltrate the tendon/adipose tissue border congregate in a stacked and aligned fashion and over time they become more organized with a more elongated morphology.

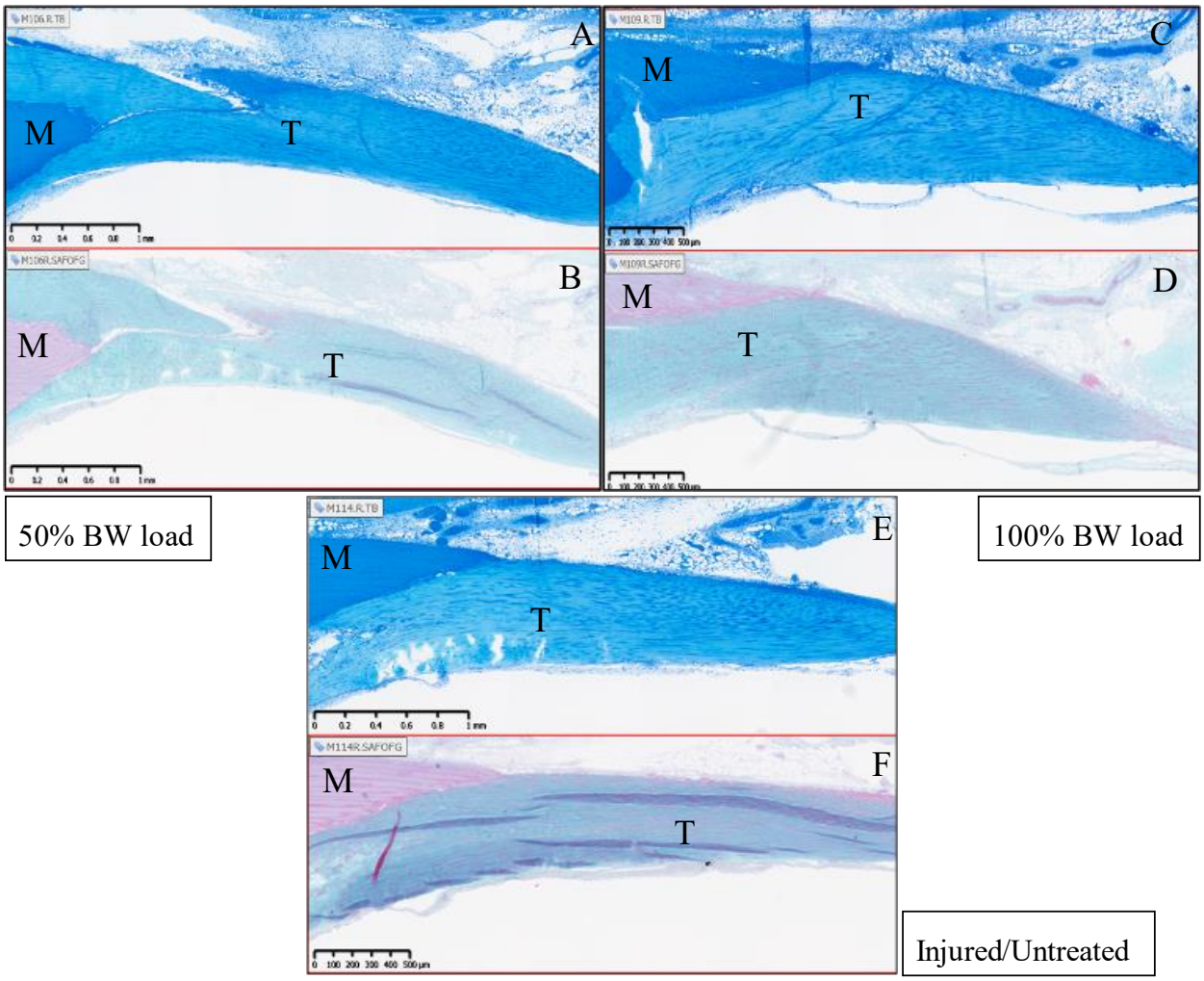

Figure 3.18*:* Representative Toluidine Blue (A., C., & E.) and Safranin-O/Fast Green (B., D., & F.) stained tissues at 2 weeks of exercise showing increased cellularity, collagen orientation, and Safranin-O staining intensity between the 50% BW, 100% BW and Injured/Untreated groups. Top left: 50% BW, Top right: 100% BW, Bottom Injured/Untreated. M: Muscle, T: Tendon. Left of side of images is proximal.

Exercised groups (50% and 100% BW) displayed an increase in cellularity at the muscle tendon interface and the 100% BW group had a marked increase over the 50% group after 4-weeks of exercise. Both the 50% and 100% BW groups increased the amount of rounded cells in the tendon

body. There was also an increase in cellularity between the tendon and adipose tissue, but not as pronounced as at 2-weeks. Additionally, the IU groups displayed more chondrocyte like cells and had larger areas of sectioning artifacts, which could be indicative of compromised tissue integrity (Figure 3.17). The IU group also contained more areas of wavy and disorganized collagen fibers (Figure 3.15, 3.16, 3.17).

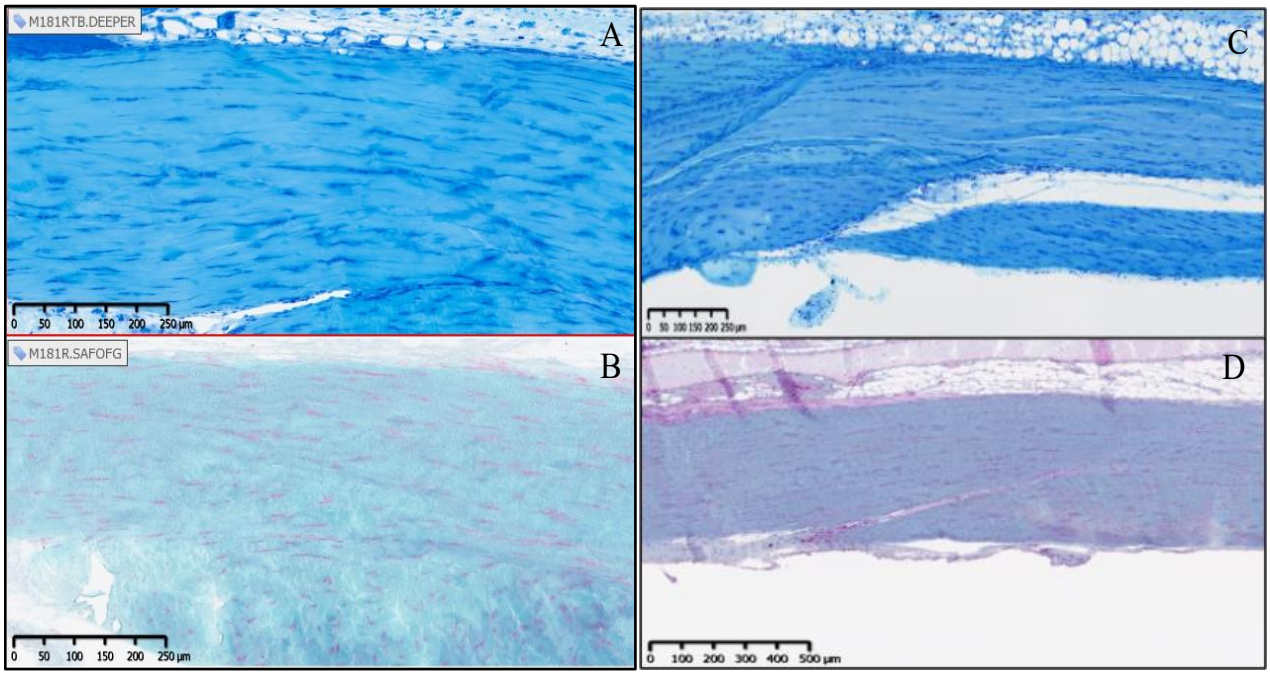

Figure 3.19: Representative Toluidine Blue (A. & C.) and Safranin-O/Fast Green (B. & D.) stained tissues at 4 weeks of exercise showing increased cellularity, collagen orientation, and Safranin-O staining intensity between the 50% BW and 100% BW groups. Top left: 50% BW, Top right: 100% BW, Bottom Injured/untreated. Left of images is proximal.

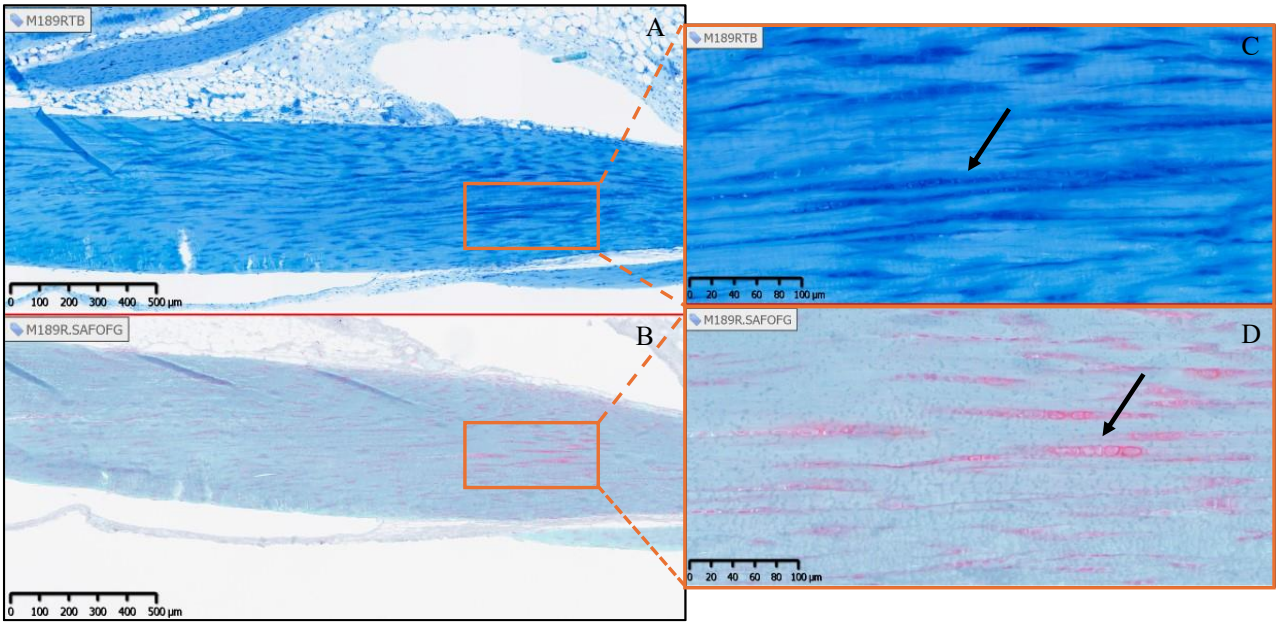

Figure 3.20: Representative Toluidine Blue (A. & C.) and Safranin-O/Fast Green (B. & D.) of the injured untreated tendons at 4 weeks. Left: Midportion of Achilles tendon. Right: Insert showing intense Safranin-O staining highlighting sulfated GAG concentration. Left of images is proximal.

3.4 Discussion

The objective of this research was to determine the effects of different eccentric magnitudes and treatment durations for improved Achilles tendinopathy healing. Our results indicate that treatment duration is more impactful than individual loading magnitudes and any eccentric loading proved beneficial on tendon CSA and biomechanical properties. Consistent with preclinical and clinical findings, CSA, maximum stress, and elastic modulus of injured tendons were restored towards naïve levels following eccentric-based exercises [57, 61, 62]. Training and exercise often increase tendon CSA and allow for the tendon to better dissipate forces, tendinopathic tissues have increased collagen fiber disruption and GAG deposits weakening compromising tendon function. Muscle strength was differentially impacted by muscle loading treatments, but did improve as loading intensity increased at 4 weeks.

Exercise at all 3 loading levels resulted in tendon CSA similar to naïve Achilles tendon, whereas the CSA of IU tendons was significantly increased at 2 weeks and remained elevated at 4 weeks.

CSA was maintained similar to that of naïve Achilles tendon in all 3 muscle loading groups. In clinical studies, high intensity running and exercise routines increase healthy tendon CSA allowing for better capacity to dissipate loading forces [63, 64]. Increased CSA can be a positive adaptation on uninjured tendon to exercise, but this model demonstrates a decreased CSA after exercise in injured tendon. The material properties of tendons are normalized to its geometry, so it is reasonable to believe that an increase in CSA would decrease the maximum stress and elastic modulus of the tendons. The maximum stress of the IU group was significantly decreased compared to all the loading groups after 4 weeks of loading but was significantly lower at 2 weeks than the 50% BW group and at 1 week it was significantly decreased compared to the naïve and 100% BW group.

Our results indicate that individual loading magnitude (50%, 75%, or 100% BW) was not as influential on tendon geometry or biomechanical properties over time points. However, the data suggest that any eccentric loading is beneficial for improving tendon outcomes and that treatment duration is more instrumental for tendon healing. Furthermore, any eccentric loading is beneficial to tendon healing compared to cage activity alone. The majority of clinical results focus on symptomatic relief and tendon size; our data demonstrated improvements in CSA [20, 21, 56, 65, 66]. Kaux *et al.* reported no differences in maximum load of Achilles tendons after uphill running exercise [40]. Similarly, Rezvani *et al.*, reported no difference in maximum load after eccentric loading, but did demonstrate CSA, maximum stress, and modulus of injured tendons returned to naïve levels after eccentric muscle loading protocols [57]. Taken together, eccentric loading has clear benefits for improving AT; however, the role of load magnitude is less clear.

In contrast to the biomechanical data, our muscle strength data suggest that loading magnitudes do differentially affect muscle strength. At 50% BW loading, muscle strength was initially reduced at 1 week, recovered closer to naïve levels at 2 weeks, and decreased again after 4 weeks of loading. Conversely, muscle strength in the 100% BW group was significantly degreased compared to naïve levels after 1 week of loading, significantly decreased after two weeks, then recovered to naïve levels after 4 weeks. In untrained muscle, eccentric loading may initially cause muscle damage, but once accustomed to training, muscle strength improves [67-69]. These results as a whole are consistent with clinical finding that demonstrated that repetitive low-load ($\leq$60% maximum

muscle capacity) training does not increase muscle strength, whereas high-load (≥60% muscle capacity) does increase muscle strength [70-72].

Histologic observations showed that exercised groups showed improvements in collagen alignment and restoration of CSA compared to injured tendons and reduced instances of chondroid metaplasia. Exercise resulted in improved collagen matrix organization and reduced chondroid metaplasia in *in vivo* rodent models [48, 73, 74]. Our histologic observations suggest an increase in fibroblast activation and collagen alignment in exercised groups compared to injured/untreated groups.

Our modified TGFβ-1 injury model, designed to prolong the injury period compared to the original single injection model, mirrors the clinical hallmarks of AT, including loss of matrix organization, increased CSA, increased cellularity, and a transition of cell phenotype away from normal tendon cell to more rounded chondrocyte-like [48, 75, 76]. The IU groups had increased safranin-O staining around cuboidal cells, which is indicative of chondroid metaplasia, a key hallmark in human Achilles tendinopathy [75, 77, 78]. This model allowed us to follow the temporal changes that supported injury resolution in response to exercise. We saw fewer instances of chondroid metaplasia and collagen disorganization in the exercised groups as treatment duration increased compared to the IU groups at the same timepoint. The preclinical muscle loading regimes used in our study effectively replicated the clinical rehabilitative exercise (heel drop) by mimicking the muscle-tendon interactions during plantar- and dorsiflexion motions. Electrical stimulation ensured quantifiable muscle contraction during the eccentric and concentric phases of these exercises, which is not achievable in other running-based exercise models. *In vivo* muscle stimulation is most frequently used as a diagnostic evaluation of muscle function in disease states [52, 53, 79, 80]. Furthermore, these stimulations are extremely well tolerated The Aurora software is amenable to other applications that can mimic human gait or therapeutic exercises [49, 81]. Alternative applications could be particularly useful for isolating eccentric and concentric effects on musculoskeletal tissues. This would be achieved by implementing exercises that mimic those respective phases. These models are amenable to the investigation of focused ultrasound or biocompatible hydrogels using the injury and treatment models, particularly early implementation of these techniques followed by the introduction of controlled muscle loading could define the

benefits of less intense therapeutic options preceding more intense rehabilitative muscle loading exercises.

While our models facilitates the investigation of AT, this study did have some limitations. The injury model does mimic the clinical hallmarks of human AT, but TGF-β1, does not fully emulate the causative overuse of the tendon to induce the disease. Furthermore, we are translating our findings from a quadruped animal which have different anatomical loading than humans. This study utilized a small number of mice, and a relatively short timeframe, which could hinder the elucidation of key finding.

3.5 Conclusions

The muscle loading protocols tested in our study improved CSA, maximum stress, and elastic modulus compared to IU tendons. Muscle strength was differentially affected by our loading protocols with 100% BW loading resulting in muscle strength closest to naïve levels compared to the other two loading protocols after 4 weeks. Repeated eccentric loading protocols from 50 to 100% BW improved tendon biomechanical properties compared to age-matched IU mice and returned these properties to those of naïve Achilles tendons. Similarly, these exercises elicited positive cellular and structural changes. Our muscle strength, biomechanical and histologic results support the application of eccentric based physical therapy exercises to improve functional outcomes following Achilles tendon injury.

Tendon is slow to heal and return to normal function. Additional studies extending treatment durations beyond just 4 weeks to 8, 12, and 16 weeks are required to investigate the long-term effects of these protocols. Transcriptomic studies will further advance our understanding of the mechanisms by which tendon healing may be improved following eccentric loading protocols. Our data highlight the benefits of eccentric loading as a therapeutic intervention for chronic Achilles tendinopathy. Eccentric-based loading restores tendon CSA and biomechanical properties (maximum stress and elastic modulus) of injured Achilles tendons.

3.6 Acknowledgements

This work was supported by The Edward Via College of Osteopathic Medicine / Virginia-Maryland College of Veterinary Medicine Center for One Health Research Seed Grant and the Interdisciplinary Graduate Education Program in Regenerative Medicine at Virginia Tech (DCE). The authors thank Shelby Hamm and Claire Yuan (Grange Lab) and Matt Brisendine (Drake Lab), for their assistance with the Aurora system, and Kyle Cooper, Megan Gulian, Gianna Manzo, and Jacob Holsopple for their assistance with *in vivo* experiments. The authors extend special thanks to Emily Rogers for her MTS and mechanical testing guidance, and Damien Laudier for his excellent histology services.

References:

1. Obst, S.J., et al., Are the Mechanical or Material Properties of the Achilles and Patellar Tendons Altered in Tendinopathy? A Systematic Review with Meta-analysis. Sports Medicine, 2018. **48**(9): p. 2179-2198.

2. Colbert, L.H., J.M. Hootman, and C.A. Macera, Physical Activity-Related Injuries in Walkers and Runners in the Aerobics Center Longitudinal Study. Clinical Journal of Sport Medicine, 2000. **10**(4).

3. Tu, P., Heel Pain: Diagnosis and Management. American Family Physician, 2018. **97,2**(1532-0650 (Electronic)): p. 86-93.

4. Yasui, Y., et al., The Risk of Achilles Tendon Rupture in the Patients with Achilles Tendinopathy: Healthcare Database Analysis in the United States. BioMed Research International, 2017. **2017**(1): p. 7021862.

5. Maffulli, N., Current Concepts Review - Rupture of the Achilles Tendon*. JBJS, 1999. **81**(7).

6. Abate, M. and V. Salini, Mid-portion Achilles tendinopathy in runners with metabolic disorders. European Journal of Orthopaedic Surgery & Traumatology, 2019. **29**(3): p. 697-703.

7. Zhou, Z., et al., Tendon-derived stem/progenitor cell aging: defective self-renewal and altered fate. Aging cell, 2010. **9**(5): p. 911-915.

8. Dean, B.J.F., et al. The risks and benefits of glucocorticoid treatment for tendinopathy: a systematic review of the effects of local glucocorticoid on tendon. in Seminars in arthritis and rheumatism. 2014. Elsevier.

9. Coladonato, C., et al., Risk Factors Associated With Poor Outcomes After Quadriceps Tendon Repair. Orthopaedic Journal of Sports Medicine, 2024. **12**(2): p. 23259671241229105.

10. Bittermann, A., et al., Oral Ibuprofen Interferes with Cellular Healing Responses in a Murine Model of Achilles Tendinopathy. LID - 049 [pii] LID - 10.23937/2572-3243.1510049 [doi]. Journal of Musculoskeletal Disorders and Treatment, 2018. **4**(2572-3243 (Electronic)): p. 49.

11. Paavola, M., et al., Chronic Achilles Tendon Overuse Injury: Complications after Surgical Treatment: An Analysis of 432 Consecutive Patients. The American Journal of Sports Medicine, 2000. **28**(1): p. 77-82.

12. Sikes, K.J., et al., TGF-b1 or hypoxia enhance glucose metabolism and lactate production via HIF1A signaling in tendon cells. Connective Tissue Research, 2018. **59**(5): p. 458-471.

13. Saxena, A., et al., Wound Complications from Surgeries Pertaining to the Achilles Tendon: An Analysis of 219 Surgeries. Journal of the American Podiatric Medical Association, 2008. **98**(2): p. 95-101.

14. Stoychev, V., A.S. Finestone, and L. Kalichman, Dry Needling as a Treatment Modality for Tendinopathy: a Narrative Review. Current Reviews in Musculoskeletal Medicine, 2020. **13**(1): p. 133-140.

15. Abate, M., L. Di Carlo, and V. Salini, Platelet rich plasma compared to dry needling in the treatment of non-insertional Achilles tendinopathy. Phys Sportsmed, 2019. **47**(2): p. 232-237.

16. Finnoff, J.T., et al., Treatment of chronic tendinopathy with ultrasound-guided needle tenotomy and platelet-rich plasma injection. PM R, 2011. **3**(10): p. 900-11.

17. O'Neill, S., P.J. Watson, and S. Barry, WHY ARE ECCENTRIC EXERCISES EFFECTIVE FOR ACHILLES TENDINOPATHY? nternational journal of sports physical therapy, 2015. **10,4**(2159-2896 (Print)): p. 552-562.

18. van der Plas, A., et al., A 5-year follow-up study of Alfredson's heel-drop exercise programme in chronic midportion Achilles tendinopathy. British Journal of Sports Medicine, 2012. **46**(3): p. 214.

19. Fahlström, M., et al., Chronic Achilles tendon pain treated with eccentric calf-muscle training. Knee Surgery, Sports Traumatology, Arthroscopy, 2003. **11**(5): p. 327-333.

20. Mafi, N., R. Lorentzon, and H. Alfredson, Superior short-term results with eccentric calf muscle training compared to concentric training in a randomized prospective multicenter study on patients with chronic Achilles tendinosis. Knee Surgery, Sports Traumatology, Arthroscopy, 2001. **9**(1): p. 42-47.

21. Öhberg, L., R. Lorentzon, and H. Alfredson, Eccentric training in patients with chronic Achilles tendinosis: normalised tendon structure and decreased thickness at follow up. British Journal of Sports Medicine, 2004. **38**(1): p. 8.

22. Frizziero, A., et al., Efficacy of eccentric exercise in lower limb tendinopathies in athletes. JOURNAL OF SPORTS MEDICINE AND PHYSICAL FITNESS, 2016. **56**(11): p. 1352-1358.

23. Habets, B. and R.E.H. van Cingel, Eccentric exercise training in chronic mid-portion Achilles tendinopathy: A systematic review on different protocols. Scandinavian Journal of Medicine & Science in Sports, 2015. **25**(1): p. 3-15.

24. O'Neill, S., S. Barry, and P. Watson, Plantarflexor strength and endurance deficits associated with mid-portion Achilles tendinopathy: The role of soleus. Physical Therapy in Sport, 2019. **37**: p. 69-76.

25. McAuliffe, S., et al., Altered Strength Profile in Achilles Tendinopathy: A Systematic Review and Meta-Analysis. Journal of Athletic Training, 2019. **54**(8): p. 889-900.

26. Alfredson, H., et al., Heavy-Load Eccentric Calf Muscle Training For the Treatment of Chronic Achilles Tendinosis. The American Journal of Sports Medicine, 1998. **26**(3): p. 360-366.

27. Geremia, J.M., et al., Effects of high loading by eccentric triceps surae training on Achilles tendon properties in humans. European Journal of Applied Physiology, 2018. **118**(8): p. 1725-1736.

28. Fouré, A., A. Nordez, and C. Cornu, Effects of eccentric training on mechanical properties of the plantar flexor muscle-tendon complex. Journal of Applied Physiology, 2012. **114**(5): p. 523-537.

29. de Vos, R.J., et al., Tendon Structure's Lack of Relation to Clinical Outcome After Eccentric Exercises in Chronic Midportion Achilles Tendinopathy. Journal of Sport Rehabilitation, 2012. **21**(1): p. 34-43.

30. Scott, A., et al., Sports and exercise-related tendinopathies: a review of selected topical issues by participants of the second International Scientific Tendinopathy Symposium (ISTS) Vancouver 2012. British Journal of Sports Medicine, 2013. **47**(9): p. 536.

31. Silbernagel, K.G., Does One Size Fit All When It Comes to Exercise Treatment for Achilles Tendinopathy? Journal of Orthopaedic & Sports Physical Therapy, 2014. **44**(2): p. 42-44.

32. Thomopoulos, S., et al., The effect of muscle loading on flexor tendon-to-bone healing in a canine model. Journal of Orthopaedic Research, 2008. **26**(12): p. 1611-1617.

33. Ma, J., et al., Bioprotection of Tendon Repair: Adjunctive Use of Botulinum Toxin A in Achilles Tendon Repair in the Rat. JBJS, 2007. **89**(10).

34. Hettrich, C.M., et al., The effect of muscle paralysis using Botox on the healing of tendon to bone in a rat model. Journal of Shoulder and Elbow Surgery, 2011. **20**(5): p. 688-697.

35. Galatz, L.M., et al., Complete removal of load is detrimental to rotator cuff healing. Journal of Shoulder and Elbow Surgery, 2009. **18**(5): p. 669-675.

36. Boyer, M.I., C.A. Goldfarb, and R.H. Gelberman, Recent Progress in Flexor Tendon Healing: The Modulation of Tendon Healing with Rehabilitation Variables. Journal of Hand Therapy, 2005. **18**(2): p. 80-85.

37. Gelberman, R.H., et al., Effects of early intermittent passive mobilization on healing canine flexor tendons. The Journal of Hand Surgery, 1982. **7**(2): p. 170-175.

38. Killian, M.L., et al., The role of mechanobiology in tendon healing. Journal of Shoulder and Elbow Surgery, 2012. **21**(2): p. 228-237.

39. Hillin, C.D., et al., Effects of immobilization angle on tendon healing after achilles rupture in a rat model. Journal of Orthopaedic Research, 2019. **37**(3): p. 562-573.

40. Kaux, J.-F., et al., Eccentric training improves tendon biomechanical properties: A rat model. Journal of Orthopaedic Research, 2013. **31**(1): p. 119-124.

41. Kaux, J.-F., et al., Eccentric Training for Tendon Healing After Acute Lesion: A Rat Model. The American Journal of Sports Medicine, 2017. **45**(6): p. 1440-1446.

42. Galloway, M.T., A.L. Lalley, and J.T. Shearn, The Role of Mechanical Loading in Tendon Development, Maintenance, Injury, and Repair. JBJS, 2013. **95**(17).

43. Szczodry, M., et al., Treadmill running exercise results in the presence of numerous myofibroblasts in mouse patellar tendons. Journal of Orthopaedic Research, 2009. **27**(10): p. 1373-1378.

44. Thampatty, B.P. and J.H.C. Wang, Mechanobiology of young and aging tendons: In vivo studies with treadmill running. Journal of Orthopaedic Research®, 2018. **36**(2): p. 557-565.

45. Zhang, J., et al., Mouse treadmill running enhances tendons by expanding the pool of tendon stem cells (TSCs) and TSC-related cellular production of collagen. Journal of orthopaedic research, 2010. **28**(9): p. 1178-1183.

46. Zhang, J., T. Yuan, and J.H. Wang, Moderate treadmill running exercise prior to tendon injury enhances wound healing in aging rats. Oncotarget, 2016. **7**(8): p. 8498.

47. Hammerman, M., et al., Different gene response to mechanical loading during early and late phases of rat Achilles tendon healing. Journal of Applied Physiology, 2017. **123**(4): p. 800-815.

48. Bell, R., et al., Controlled treadmill exercise eliminates chondroid deposits and restores tensile properties in a new murine tendinopathy model. Journal of biomechanics, 2013. **46**(3): p. 498-505.

49. Rezvani, S.N., Novel Preclinical Approaches to the Understanding and Treatment of Achilles Tendinopathy, in Biomedical Engineering. 2021, Virginia Tech.

50. Bell, R., et al., ADAMTS5 is required for biomechanically-stimulated healing of murine tendinopathy. Journal of Orthopaedic Research, 2013. **31**(10): p. 1540-1548.

51. Rezvani, S.N., Novel Preclinical Approaches to the Understanding and Treatment of Achilles Tendinopathy, in Biomedical Engineering. 2021, Virginia Tech. p. 208.

52. Capogrosso, R.F., et al., Contractile efficiency of dystrophic mdx mouse muscle: in vivo and ex vivo assessment of adaptation to exercise of functional end points. Journal of Applied Physiology, 2017. **122**(4): p. 828-843.

53. Au - Childers, M.K., R.W. Au - Grange, and J.N. Au - Kornegay, In Vivo Canine Muscle Function Assay. JoVE, 2011(50): p. e2623.

54. Hamm, S.E., et al., Voluntary wheel running complements microdystrophin gene therapy to improve muscle function in mdx mice. Molecular Therapy - Methods & Clinical Development, 2021. **23**: p. 460.

55. Ashton-Miller, J.A., et al., An apparatus to measure in vivo biomechanical behavior of dorsi- and plantarflexors of mouse ankle. Journal of Applied Physiology, 1992. **72**(3): p. 1205-1211.

56. Silbernagel, K.G., A. Brorsson, and M. Lundberg, The Majority of Patients With Achilles Tendinopathy Recover Fully When Treated With Exercise Alone: A 5-Year Follow-Up. The American Journal of Sports Medicine, 2010. **39**(3): p. 607-613.

57. Rezvani, S.N., et al., A novel murine muscle loading model to investigate Achilles musculotendinous adaptation. Journal of Applied Physiology, 2021. **130**(4): p. 1043-1051.

58. Rezvani, S.N., et al., In-Vivo Efficacy of Recombinant Human Hyaluronidase (rHuPH20) Injection for Accelerated Healing of Murine Retrocalcaneal Bursitis and Tendinopathy. Journal of Orthopaedic Research, 2020. **38**(1): p. 59-69.

59. Wang, V.M., et al., Murine tendon function is adversely affected by aggrecan accumulation due to the knockout of ADAMTS5. Journal of Orthopaedic Research, 2012. **30**(4): p. 620-626.

60. Laudier, D., et al., Novel procedure for high-fidelity tendon histology. Journal of Orthopaedic Research, 2007. **25**(3): p. 390-395.

61. Arya, S. and K. Kulig, Tendinopathy alters mechanical and material properties of the Achilles tendon. Journal of Applied Physiology, 2010. **108**(3): p. 670-675.

62. Kader, D., et al., Achilles tendinopathy: some aspects of basic science and clinical management. British journal of sports medicine, 2002. **36**(4): p. 239-249.

63. Sponbeck, J.K., et al., Achilles tendon cross sectional area changes over a division I NCAA cross country season. International journal of exercise science, 2017. **10**(8): p. 1226.

64. Radovanović, G., et al., Evidence-Based High-Loading Tendon Exercise for 12 Weeks Leads to Increased Tendon Stiffness and Cross-Sectional Area in Achilles Tendinopathy: A Controlled Clinical Trial. Sports Medicine - Open, 2022. **8**(1): p. 149.

65. Kingma, J.J., et al., Eccentric overload training in patients with chronic Achilles tendinopathy: a systematic review. British Journal of Sports Medicine, 2007. **41**(6): p. e3.

66. Rompe, J.D., J. Furia, and N. Maffulli, Eccentric Loading versus Eccentric Loading plus Shock-Wave Treatment for Midportion Achilles Tendinopathy: A Randomized Controlled Trial. The American Journal of Sports Medicine, 2008. **37**(3): p. 463-470.

67. Friden, J. and R.L. Lieber, Structural and mechanical basis of exercise-induced muscle injury. Medicine & Science in Sports & Exercise, 1992. **24**(5): p. 521-530.

68. Fridén, J., et al., Adaptive response in human skeletal muscle subjected to prolonged eccentric training. International journal of sports medicine, 1983. **4**(03): p. 177-183.

69. NOSAKA, K. and M. NEWTON, Difference in the Magnitude of Muscle Damage Between Maximal and Submaximal Eccentric Loading. The Journal of Strength & Conditioning Research, 2002. **16**(2): p. 202-208.

70. Popov, D., et al., Hormonal adaptation determines the increase in muscle mass and strength during low-intensity strength training without relaxation. Human Physiology, 2006. **32**: p. 609-614.

71. Tanimoto, M., et al., Effects of whole-body low-intensity resistance training with slow movement and tonic force generation on muscular size and strength in young men. The Journal of Strength & Conditioning Research, 2008. **22**(6): p. 1926-1938.

72. Van Roie, E., et al., Strength training at high versus low external resistance in older adults: effects on muscle volume, muscle strength, and force–velocity characteristics. Experimental gerontology, 2013. **48**(11): p. 1351-1361.

73. Johnson, S.A., et al., Fast, non-eccentrically loaded exercise worsens tendinopathic healing responses in a murine model. American Journal of Veterinary Research, 2023. **84**(6): p. ajvr.23.01.0018.

74. Kovanen, V., Effects of ageing and physical training on rat skeletal muscle. An experimental study on the properties of collagen, laminin, and fibre types in muscles serving different functions. Acta Physiologica Scandinavica. Supplementum, 1989. **577**: p. 1-56.

75. Khan, K.M., et al., Histopathology of common tendinopathies: update and implications for clinical management. Sports medicine, 1999. **27**: p. 393-408.

76. Pingel, J., et al., Increased mast cell numbers in a calcaneal tendon overuse model. Scandinavian journal of medicine & science in sports, 2013. **23**(6): p. e353-e360.

77. Corps, A.N., et al., Changes in matrix protein biochemistry and the expression of mRNA encoding matrix proteins and metalloproteinases in posterior tibialis tendinopathy. Annals of the rheumatic diseases, 2012. **71**(5): p. 746-752.

78. Scott, A., et al., Increased versican content is associated with tendinosis pathology in the patellar tendon of athletes with jumper's knee. Scandinavian journal of medicine & science in sports, 2008. **18**(4): p. 427-435.

79. Tegeler, C.J., et al., Eccentric contractions induce rapid isometric torque drop in dystrophin-deficient dogs. Muscle & Nerve, 2010. **42**(1): p. 130-132.

80. Au - Gerlinger-Romero, F., et al., Non-invasive Assessment of Dorsiflexor Muscle Function in Mice. JoVE, 2019(143): p. e58696.

81. Bukovec, K.E., et al., A novel ex vivo protocol to mimic human walking gait: implications for Duchenne muscular dystrophy. Journal of Applied Physiology, 2020. **129**(4): p. 779-791.

Chapter 4 - Transcriptional Adaptations to Muscle Loading in a Murine Model of Achilles Tendinopathy

4.1 Introduction

4.1.1 Achilles Tendinopathy and Current Treatments

Achilles tendinopathy (AT) is a painful and debilitating disorder often caused by chronic overuse, affecting ~6% of the US population [1-3]. The progression and severity of AT can be exacerbated by intrinsic and extrinsic factors, including genetics, age, and activity level [4]. Symptoms of Achilles tendinopathy include pain and swelling, which result in loss of functionality and negatively impact daily work and recreational activities [2, 5-7]. Without treatment, AT can lead to further tissue degeneration and eventually tendon rupture [2, 3, 8]. Current treatment options, such as surgery, pain management (nonsteroidal anti-inflammatory drugs), injectable orthobiologic therapies (platelet rich plasma), and non-invasive treatments (ultrasound, electrical stimulation and ice and heat routines) have limited efficacy, with 30% of athletes not able to return to competition [9-11].

4.1.2 Rehabilitative Exercises

Clinical rehabilitative exercises (physical therapy) are effective at improving tendon function and muscle strength after acute injury [12, 13]. Recent reviews emphasize the efficacy of eccentric-based exercises (lengthening of the gastrocnemius muscle while it contracts) for providing symptomatic relief of AT; however, the underlying healing mechanisms remain poorly defined [14, 15]. Several of the same intrinsic and extrinsic factors that affect disease development also determine the effectiveness of tendon healing; body weight, age, activity level, genetics, and disease severity [16-20]. The multifactorial nature of AT makes it challenging to define an exercise routine that is advantageous for tendon healing and tolerable for a variety of patients. The heterogeneity of disease further hinders identification of the healing mechanisms involved and the discovery of robust therapeutic options.

Preclinical models of muscle stimulation have examined the effects of exercise, but do not utilize exercise models that are consistent with rehabilitative approaches used clinically [21]. Treadmill

running is a common exercise model, but muscle activation is variable during running [21-23]. The inability to apply precise muscle stimulation during treadmill running makes replication challenging [21-25]. Previously, we developed a tissue-targeted muscle loading approach that simulates clinical eccentric-based exercises: muscle contractions while the ankle moves through its physiologic range of motion [26]. We demonstrated that muscle stimulation is not deleterious to naïve muscle and tendon tissue and that eccentric-based exercises improved biomechanical properties of injured Achilles tendon [26]. Utilization of the combination of tissue-targeted muscle loading and rehabilitative exercises provides an opportunity to rigorously characterize the cellular adaptations of tendon tissue to enhance the understanding of the underlying tendon healing mechanisms.

4.1.3 Tendon Cellular Response to Mechanical Loading

Tendons require mechanostimulation to maintain homeostasis [27-29]. Stimulation above or below physiologic levels may result in adverse effects on tendon tissue, causing tendon fibroblasts to respond by altering their metabolic output. Under normal physiological loading, tensile strain ranges between 2-6% for murine tendons. During physiologic conditions *in vitro*, tendon cells produce collagen type 1 and inhibit interstitial collagenase (MMP-1) production [30, 31]. When tendon explants were "underloaded" (strain <1%), MMP-1 expression increased [31]. Immobilization of the tendon had negative effects on healing, including inhibition of blood circulation and innervation, resulting in inferior biomechanical properties [32-34]. When overloaded, tendon fibroblasts increase production of the inflammatory mediators prostaglandin E_2 and cyclooxygenase -1 and -2, regulators of prostaglandin E_2, and apoptotic markers [35, 36]. Furthermore, overloaded (9% strain) murine tendon constructs *in vitro* produced the proinflammatory cytokines interleukin (IL)-6, IL-18, and chemokine ligand-1 [37]. After injury, tendon can become hypoxic, which causes inflammation and further tissue damage [38, 39]. Dysregulation of cellular components due to under- or over-loading tendons may prolong the inflammatory phase of healing and delay the remodeling/healing response [35-37, 39, 40].

The cellular adaptations of muscle tissue in response to eccentric-based muscle loading has been well characterized. Eccentric loading promoted an increase transcriptional response compared to concentric loading and eccentric loading upregulated macrophage and neutrophil immune

responses [41-45]. However, information about tendon tissue adaptations to loading remains sparse. Increased optogenetic-induced muscle contraction in young, uninjured mice resulted in increased glycolysis, focal adhesions, and cell matrix interactions within Achilles tendons [46]. In a mouse model of patellar tendinopathy, expression of scleraxis and collagen types I, II, and III was increased after isometric muscle loading compared to the contralateral (control) limb [47]. In a murine transforming growth factor (TGF)-β1 tendinopathy model, flat-fast treadmill running elevated serum levels of collagen type X breakdown product and inferior tendon healing [48]. To our knowledge, there has been no investigation into the cellular adaptations in tendon in response to eccentric-based muscle loading on tendinopathic Achilles tendons. This gap in knowledge led us to explore tendon transcriptomic changes in response to different eccentric-based muscle loading regimes. We hypothesized that eccentric muscle loading will upregulate signaling and metabolic networks associated with extracellular matrix production and organization, focal adhesions and oxidative stress compared to naïve and injured/untreated groups.

4.2 Materials and Methods

4.2.1 Animals

Under Virginia Tech IACUC approval (protocol #21-239 and #21-125), 12-week-old C57BL/6 male mice (Jackson Laboratories, Bar Harbor, ME; Stock No. 000664) were used for all studies. 11-week-old mice were delivered and entered a 1-week acclimation period prior to experimentation. All animals were housed on a 12-hour light/dark cycle and fed standard mouse diet and water *ad libitum* and allowed unrestricted cage activity (5 mice/cage). Upon the conclusion of *in vivo* experiments, mice were euthanized using carbon dioxide inhalation for a minimum of 4 minutes, followed by cervical dislocation. Tissues were harvested and isolated for RNA sequencing immediately post-euthanasia.

4.2.2 Experimental Design

Eccentric muscle loading parameters and stimulation tolerance were previously identified by Rezvani et al., which determined dorsiflexion range of motion, footplate speed, number of repetitions, sets of repetitions, and treatment frequency to best imitate clinical practices [49]. For tendon transcriptomic analyses, loading magnitudes of 50% and 100% bodyweight (BW) were

investigated over the course of 1, 2, and 4 weeks using a previously developed preclinical murine model of Achilles tendinopathy [26, 50-53]. Naïve mouse tendon (normal tendon) and injured/untreated (IU) tendon served as controls.

4.2.3 Tendinopathy Induction

To determine the effects of loading parameters on tendon healing, AT was induced unilaterally using a modification of an established TGF-β1 mouse model [26, 50-52]. Lyophilized active human recombinant TGF-β1 (Peprotech, Inc, Rocky Hill, NJ) was reconstituted in 0.1% sterile bovine serum albumin in phosphate buffered saline and stored in 75µL aliquots at -20ºC in sterile 1 mL microfuge tubes until use. On the day of model induction, a frozen TGF-β1 aliquot was thawed on ice, mixed gently, aliquoted in uniform 8 ul droplets onto a sterile petri dish, and 6 µL drawn into a sterile 0.5 ml insulin syringe using a 0.5" 28G needle. This technique ensured consistent injection volumes. Animals were deeply anesthetized using 3% isoflurane in oxygen for the duration of the injection procedure and the hindlimb was prepared using aseptic technique. Two sets of paired injections of 100 ng of active rhTGF-β1 in 6 µL PBS were delivered 48 hours apart into the mid and distal portions of the Achilles tendon of 12-week-old mice. The needle was inserted into and through the gastrocnemius muscle complex and directed distally into the midportion of the Achilles tendon, where the injection was delivered. Similarly, the second injection, using a new needle and fresh aliquot of TGF-β1, was directed through the gastrocnemius complex and guided more distally into the tendon near the enthesis site [26]. Mice were allowed to recover in a clean cage with a heating pad or heat lamp. The paired injections were repeated 48 hours later in the same manner.

Table 4.1 Treatment groups, treatment durations, and animal usage for each group.

Experimental Design			
Treatment Duration	**Treatment Group**	**RNA Sequencing**	
		In vivo **# of mice**	**# of Samples**
1 Week	Injured/Untreated	12	5
	50% BW Loading	12	6
	100% BW Loading	12	4
2 Weeks	Naïve	28	6
	Injured/Untreated	12	5
	50% BW Loading	12	6
	100% BW Loading	12	5
4 Weeks	Injured/Untreated	12	6
	50% BW Loading	12	6
	100% BW Loading	12	6
	Total number	**136**	**55**

4.2.4 Tissue Targeted Muscle Loading

Two days following the second TGF-β1 injection, mice were deeply anesthetized using 3% isoflurane in oxygen in a sealed anesthesia chamber for 3 minutes, then transferred to the temperature-controlled (37º) testing platform of a 305C-5N Dual-Mode Muscle Lever System (Aurora Scientific). While on the platform, anesthesia was delivered via a nose cone and maintained between 1.5-3% isoflurane in oxygen [54]. For each mouse, the hair of the hind right limb was clipped, then chemical depilatory cream was applied. Petroleum-based ophthalmic ointment was applied to both eyes to prevent corneal drying and irritation during anesthesia. The foot was placed and secured into the foot pedal and the hind limb was adjusted so the femur was oriented 90º to the tibia and the tibia 90º to the foot. The limb was prepared using aseptic technique and stimulating electrodes (Natus Manufacturing Ltd.; Galaway, Ir) were placed subcutaneously and parallel along the tibial nerve on the lateral aspect of the gastrocnemius muscle (~1 mm distal to the knee) at a depth between 0.5-1.0 mm. Electrical stimulations were computer-controlled (Aurora Scientific; Aurora, ON, Canada) while the foot pedal moved through the ankle joint's range of motion (±18º), mimicking the clinical heel drop exercise [26, 55]. Mice were maintained under anesthesia for the entire duration of the treatment (~20 minutes) until placed in a recovery cage after each treatment session.

4.2.5 Eccentric Loading Protocol

Previously, a preclinical *in vivo* model of eccentric-based muscle loading was developed to simulate clinical methods that are effective at providing symptomatic relief of AT [26, 56, 57]. Several iterations of these protocols were investigated to determine the tolerance of eccentric muscle loading in uninjured tendons and translation to an *in vivo* model of AT [26]. An effective preclinical protocol was set at 3 sets of 10 repetitions of muscle loading treatments, 2 times per week, using the full range of motion for the ankle joint (±18º), and a footplate speed of 5 mm/sec [26]. The stimulation frequencies (loading magnitude) of 50 Hz and 100 Hz correspond to 50% and 100% of BW loading, respectively. These different loading magnitudes were performed for 1-, 2- or 4-week periods to determine the effects of muscle loading on tendon healing over time (Table 4.1). Age-matched naïve and injured/untreated (IU) groups served as controls at each time

point. Injured/untreated mice were placed under anesthesia and fitted into the testing platform and foot pedal, as described above. The electrodes were placed in a manner identical to the loaded groups, but no muscle stimulation or ankle flexion was induced. Following the *in vivo* exercises, mice were placed in a clean recovery cage, equipped with a heating pad or heating lamp, and allowed to recover completely (fully ambulatory and alert) before being transferred to their original cage. All mice were monitored for 24 hours after treatments to ensure there were no signs of distress, alterations to appetite, and activity level. These exercises were well tolerated and did not result in lameness, soreness, or difficulty with ambulating.

4.2.6 RNA sequencing in Isolated Achilles Tendons

Mice were euthanized 24 hours after the final muscle loading session. All utensils and surfaces were cleaned with 70% EtOH and RNAase away (ThermoFisher, Durham, NC). Immediately following euthanasia, hindlimbs were thoroughly sprayed with 70% EtOH, the skin was dissected away from the tendon-muscle-bone complex, taking care to avoid any hair contaminating the exposed tendon. Once exposed and separated from the connected muscle and adipose tissue, the plantaris tendon was removed and the Achilles tendon (including peritenon) was sharply transected from the bone and muscle tissues using micro-scissors. The isolated Achilles tendon was placed directly into a prefilled BeadBeater tube (Genesee Scientific, Cat #D1032-15, Morrisville, NC) with 600 µl TRIzol® reagent (Invitrogen, Carlsbad, CA). Two tendons per sample were pooled for each exercise and IU groups (n=6/group). Naïve tendons (6-10 tendons per sample) were pooled per sample to ensure adequate RNA concentration. Once both tendons were dissected out and placed in TRIzol® reagent, the sample was immediately snap-frozen in liquid nitrogen and stored at -80ºC. Tendon samples were thawed on ice before being secured in a tissue homogenizer (BeadBug, Benchmark Scientific Inc., Edison, NJ) and processed for 4 sets of 45 second cycles with 2 minute rest periods on ice between each cycle, then column purified, including DNase digest (Direct-zol MicroPrep, Zymo Research, Irvine, CA) [58]. Eluted RNA samples were stored at -80ºC until shipped for RNA quality assessment (bioanalyzer 2100, Alignent Technologies, Santa Clara, CA) and cDNA library preparation using TruSeq DNA Library Preparation kits (Illumina,

Inc. San Diego, CA). A detailed description of each step used in the RNA isolation process is provided in Appendix A.

4.2.7 RNA Sequencing Pipeline and Statistical Analysis

Following RNA isolation, samples underwent initial quality control screening NanoDrop™ (Thermo Scientific) to determine concentration (ng/μL) and purity ratios (260/280 $\geq$ 2.0 and 260/230 $\geq$ 2.0). Samples that passed initial quality control underwent final quality control to determine final concentration and ensure RNA integrity number $\geq$ 4.0 (minimum 200 ng total RNA in a volume $\geq$ 10μL; Novogene), and purity. Samples with low RNA concentrations but adequate quality were either combined with a sample from the same treatment group or excluded completely, resulting in n<6 in some groups (Table 4.1). RNA-Seq was performed using Illumina NovaSeq 6000 S4, reads were trimmed for quality and adapters with TrimGalore 0.4.3 and mapped to the murine reference genome using STAR algorithm (version 2.7.2a), and read counts and expression values were determined using gene length corrected trimmed mean of M-values (GeTMM) [59, 60]. Differentially expressed genes were identified using DESeq2 (FDR< 0.05 and represented by a principal component analysis using JMP Pro 13. Weighted gene co-expression network analysis (WGCNA) was used to build co-expression networks from the entire transcriptome. To normalize the GeTMM values, each gene was log2 transformed [61]. A topological overlap matrix was created and used as input for the clustering analysis. Then, a dynamic tree cutting algorithm was used to identify gene clusters or modules (i.e., genes with high topological overlap) in an unsupervised fashion. A heatmap plot (TOMplot) was used to visualize the clusters of the topological overlap. Association between gene modules and traits were tested by correlating module eigengenes to traits of interest. Module-trait correlations were considered significant with R^2>0.7 or R^2<-0.7 and p<0.05 and used for further analysis. Gene clusters with associations with traits from samples from related research were investigated [53, 62]. Gene ontology (GO) was used to analyze the whole list of genes within each cluster and annotated with the database for annotation, visualization, and integrated discovery (DAVID) Bioinformatics Resources version 6.8 [61, 63]. Upstream regulators were identified with ingenuity pathway analysis (IPA) and the interactions and associations between activated and inhibited upstream regulators assessed using STRING [61]. Expression levels from the naïve, IU, and exercised (50% and 100% BW muscle loading) groups were compared across the 3 time points and between

groups. IPA was also used to determine activated and inactivated signaling pathways, considering significance at $P < 0.05$ and activation Z-score >2 (activated) or or<-2 (inhibited) and a -log(p-value > 1.3, which corresponds to p>0.05). For cases in which a large list of pathways met this criterion, those with a -log(p-value > 3 (FDR <0.01) were given priority attention.

4.3 Results

Differential Gene Expression

The Principal Component Analysis (PCA) of differentially expressed genes (DEG) demonstrated relatively tight clustering within each treatment group at each time point (Figure 4.1). Of particular note was the very tight clustering of the naïve samples within a single quadrant. The IU group progressively converged toward the naïve group, with the 4 -week IU samples clustering with the naïve samples. Samples in the 50% and 100% BW loading groups start in different quadrants and converge over time such that they are loosely clustered at 4 weeks. The slope of the vector line for the 100% BW groups is steeper than the 50% BW groups. Finally, gene expression in the exercised groups (50% and 100% BW loading) diverges from the naïve and IU groups over 4 weeks. The 100% BW loading groups are clustered with the IU groups at 1 and 2 weeks and are not clustered with the 50% BW loading group.

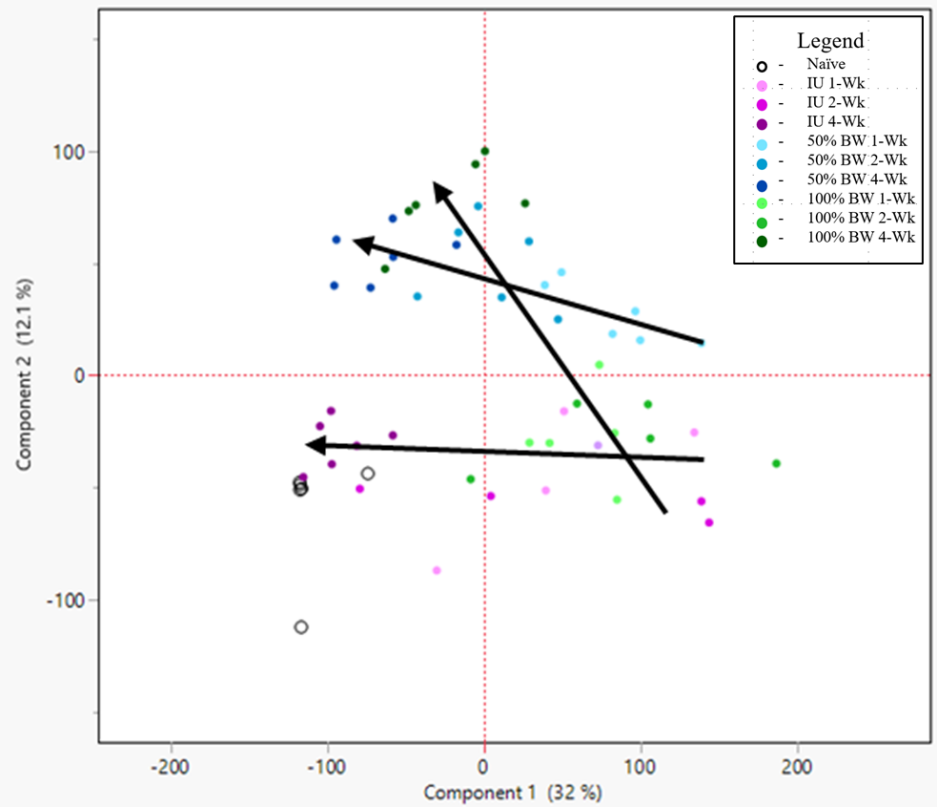

Figure 4.1: Principal component analysis from the entire transcriptome (49,437 genes) showing the different patterns of gene expression in response to TGF-β1 model induction and muscle loading over 4 weeks in response to no exercise (IU) and 50% and 100% body weight loading. Naïve tendons served as baseline gene expression controls. Each dot represents an individual sample.

Horizontal (across time within a treatment group) and vertical comparisons (between treatment groups at a single time point) were made and the numbers of up-and downregulated genes reported for each comparison. Naïve samples served as the baseline of expression in normal tendon. In response to model induction, counts of up- and downregulated genes were high for both loading groups and the IU group compared to naïve tendon (Figure 4.2 and Table 4.2). Counts of upregulated genes were most notable between 2 and 4 week durations for all three groups. Horizontally, the IU and 100% BW loading groups displayed the largest counts of up- and downregulated genes between weeks 2 and 4, whereas the numbers of up- and down-regulated

genes at 50% BW loading was more evenly distributed between 1 and 2 and 2 and 4 weeks. The numbers of DEG between 100% BW loading and IU occurred at 4 weeks were strongly concentrated at 4 weeks. Numbers of DEG between 50% BW loading and IU was somewhat evenly distributed across time. Although there was a moderate difference in up- and downregulated genes between 50% and 100% BW loading at 1 week, the largest numbers of the DEG were at 2 weeks.

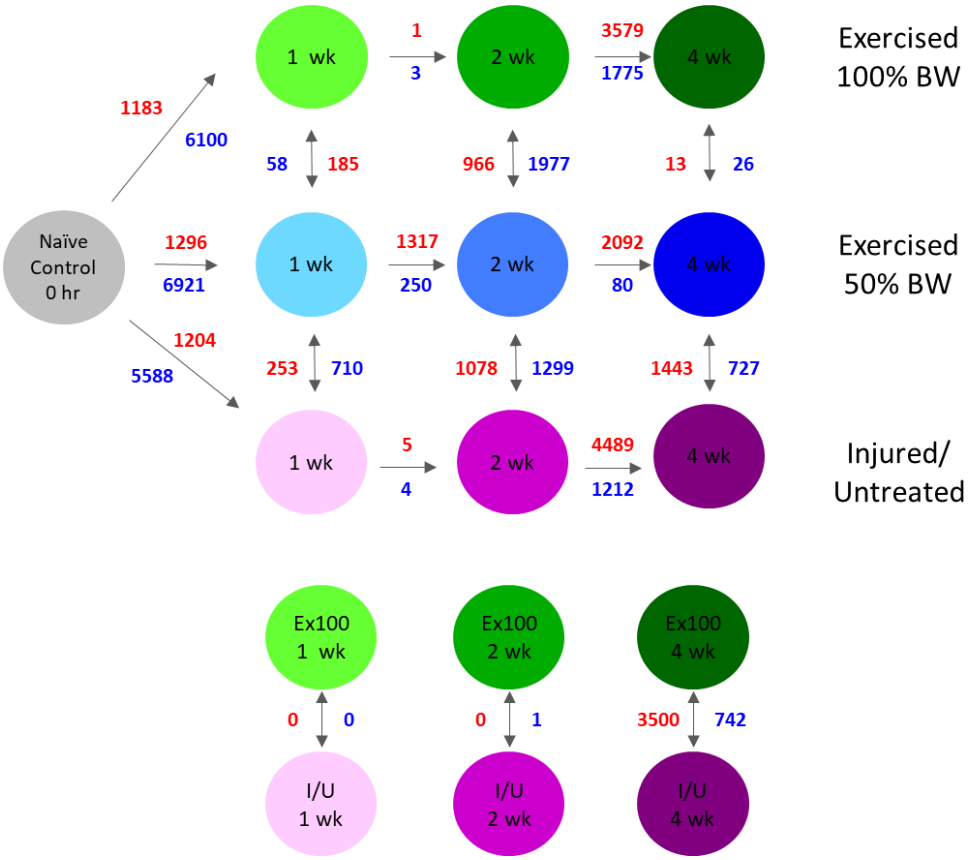

Figure 4.2: Numbers of differentially expressed genes between treatment groups over time and between treatment groups at each time point. Naïve controls served as normal tendon and a basis for comparison following induction of the injury model and exercise at 50% or 100% BW loading or IU controls. Numbers of upregulated genes are in shown in red and numbers of downregulated genes in blue.

Table 4.2 Number of differentially expresses genes (upregulated and downregulated) for each comparison of interest.

Group 1	Group 2	# Upregulated Genes	# Downregulated Genes
UnExer_Wk1	Naive	1204	5588
Exer_Wk1_50	Naive	1296	6921
Exer_Wk1_100	Naive	1183	6100
Exer_Wk2_100	Exerc_Wk1_100	1	3
Exer_Wk4_100	Exer_Wk2_100	3579	1775
UnExer_Wk2	UnExer_Wk1	5	4
UnExer_Wk4	UnExer_Wk2	4489	1212
Exer_Wk2_50	Exer_Wk1_50	1317	250
Exer_Wk4_50	Exer_Wk2_50	2092	80
Exer_Wk1_50	UnExer_Wk1	253	710
Exer_Wk2_50	UnExer_Wk2	1078	1299
UnExer_Wk4	Exer_Wk4_50	1443	1212
Exer_Wk1_100	Exer_Wk1_50	185	58
Exer_Wk2_100	Exer_Wk2_50	966	1977
Exer_Wk4_100	Exer_Wk4_50	13	26
Exer_Wk1_100	UnExer_Wk1	0	0
Exer_Wk2_100	UnExer_Wk2	0	1
Exer_Wk4_100	UnExer_Wk4	3500	742

Co-Expression Network Analysis from Tendon in Response to Exercise

WGCNA of 22,904 genes identified 8 module eigengene (ME) of which 3 were positively associated ($R^2 \geq 0.7$, $p \leq 0.05$) and 1 was negatively associated ($R^2 \leq -0.7$, $p \leq 0.05$) with the timeline (Figure 4.3 and Table 4.1). The brown module was significantly associated with 50% BW loading at 2 weeks and the red and yellow modules significantly associated with 100% BW loading at 2 weeks. The grey module was significantly negatively associated with the injured/untreated group, also at 2 weeks. To consider the effects of exercise over time, mean GeTMM from all genes for each significant module (50% BW and 100% BW) were plotted (Figure 4.4) and for injured/unexercised for the grey module (Figure 4.5). The red module displayed 39 significant biological processes with fold enrichment as from 137 to 3 fold and involved with cellular response, cell to cell signaling, and cell migration (Table 4.4). The 82 significant biological processes identified in the yellow module (106-to-2-fold enrichment) were response to prostaglandin E, neutrophil chemotaxis, extracellular matrix organization, and the inflammatory response (Table 4.5). Both the grey and the brown modules displayed large groups of genes associated with as-yet unspecified biological processes (Tables 4.6 and 4.7).

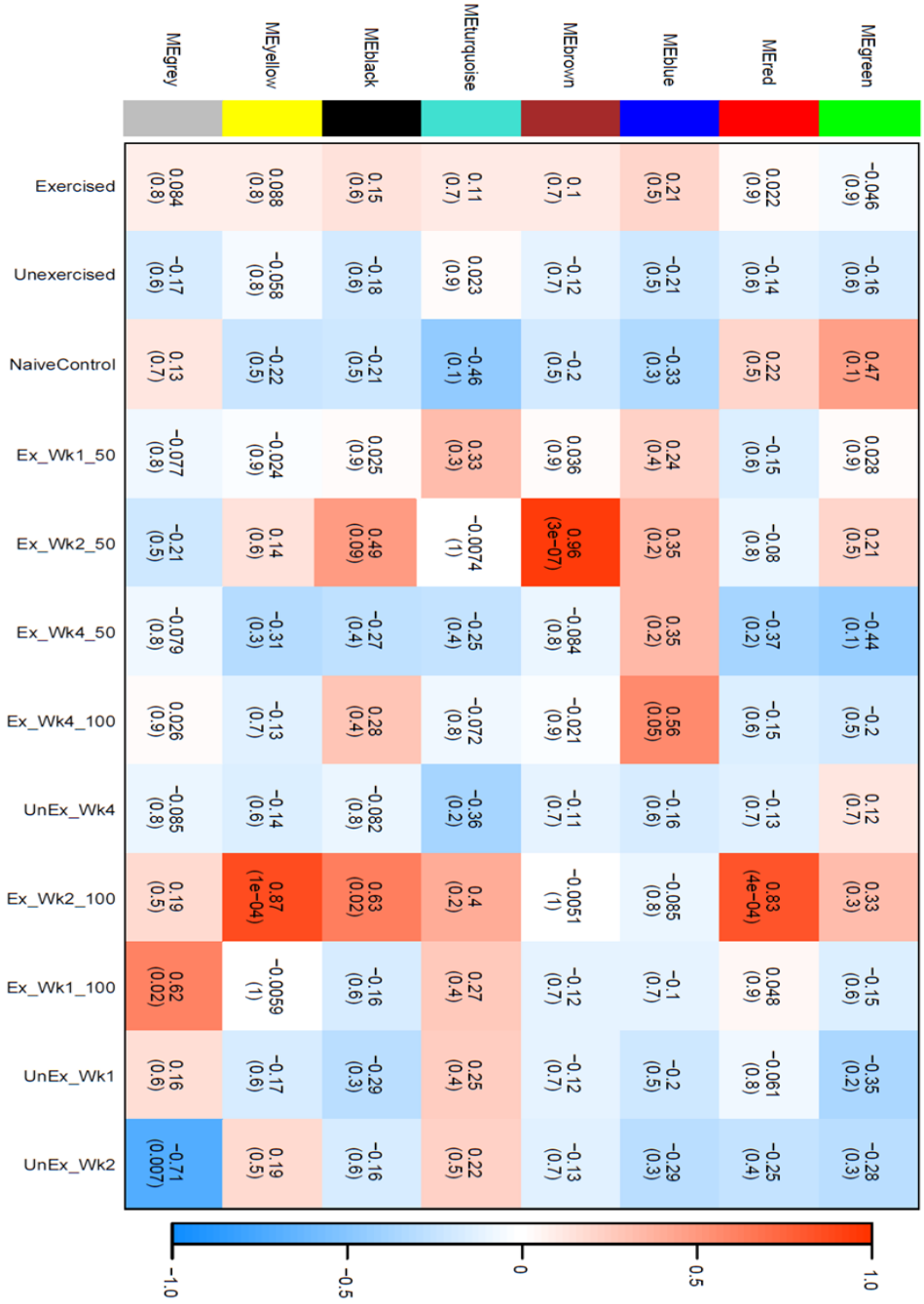

Figure 4.3: Heatmap of weighted gene co-expression network analysis (WGCNA) module-trait relationships. Top number is R^2 with the associated p value below for each module-trait relationship. The brown (50% BW), and red and yellow (100% BW) modules were significantly positively associated with loading at 2 weeks and the grey module was significantly negatively associated with the injured/untreated group at 2 weeks.

Table 4.3: Significantly expressed modules and associated treatment group.

Module Membership				
	Associated Module			
	Red	**Yellow**	**Brown**	**Grey**
Treatment Group	Exercised Week 2 100% BW	Exercised Week 2 100% BW	Exercised Week 2 50% BW	Unexercised Week 2
Correlation Coefficient	0.83	0.87	0.96	-0.71
p-value	$4x10^{-4}$	$1x10^{-4}$	$3x10^{-7}$	0.007

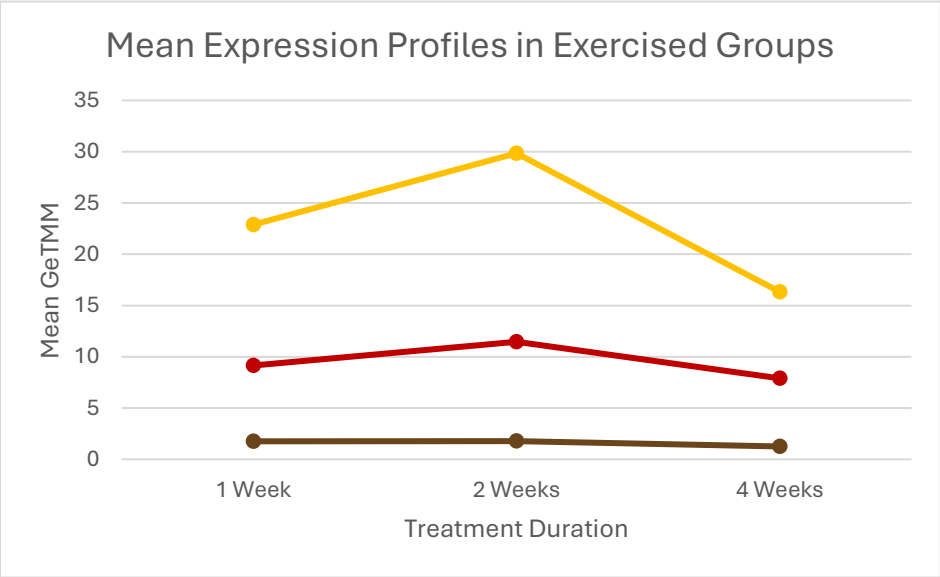

Figure 4.4: Mean expression profile (mean GeTMM values for all genes) for each significant eigengene module positively associated with exercise plotted over time for both exercise groups (50% and 100% BW). Expression in the yellow module was highest, increased from 1 to 2 weeks then decreased by 4 weeks. Expression of the red module was intermediate and showed a similar pattern with a lower magnitude of differential expression. Expression in the brown module was much lower and more static over time.

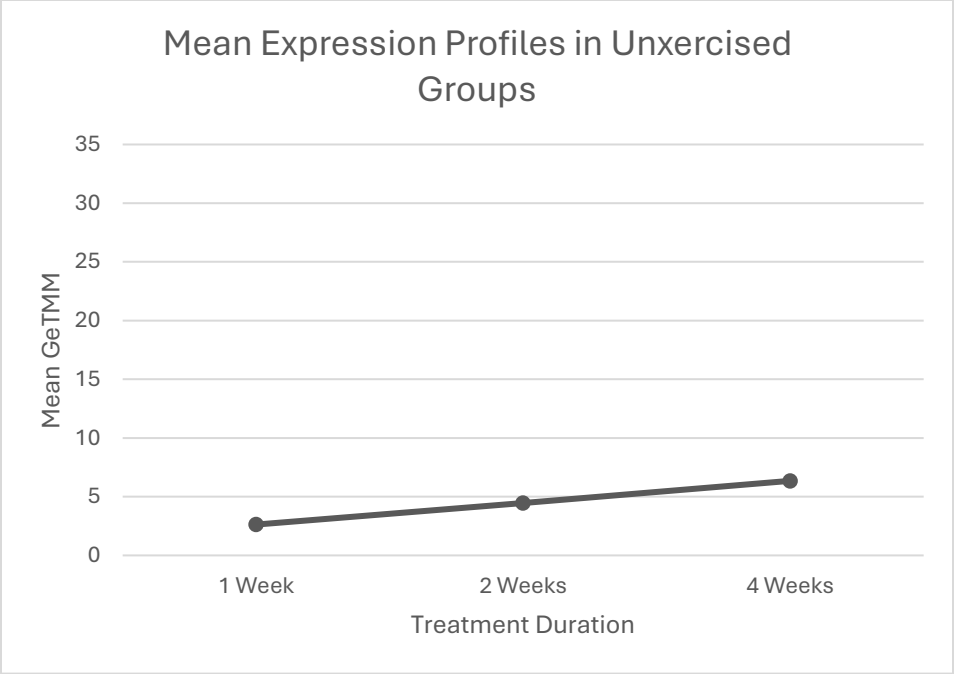

Figure 4.5: Mean expression profile (mean GeTMM values for all genes) of significant eigengene module negatively associated with the injured/untreated group showing relatively low expression and a steady increase in expression over time.

Table 4. 4: Overrepresented biological processes in the red module and their corresponding fold enrichment and p-value.

Red Module			
Term	PValue	Genes	Fold Enrichment
GO:0034696~response to prostaglandin F	0.0144	EDN1, HMGCS2	137
GO:0070649~formin-nucleated actin cable assembly	0.0144	SPIRE2, FMN2	137
GO:0006682~galactosylceramide biosynthetic process	0.0003	FA2H, GAL3ST1, UGT8A	103
GO:0032290~peripheral nervous system myelin formation	0.0191	PRX, NCMAP	103
GO:0002175~protein localization to paranode region of axon	0.0239	UGT8A, MAL	82
GO:0051295~establishment of meiotic spindle localization	0.0286	SPIRE2, FMN2	69
GO:0019530~taurine metabolic process	0.0333	GHR, PHGDH	59
GO:0040038~polar body extrusion after meiotic divisions	0.0379	SPIRE2, FMN2	52
GO:0035633~maintenance of blood-brain barrier	0.0017	MBP, TSPAN12, MFSD2A	48
GO:0032229~negative regulation of synaptic transmission, GABAergic	0.0426	HTR1B, SLC6A1	46
GO:0032287~peripheral nervous system myelin maintenance	0.0426	FA2H, PRX	46
GO:0003406~retinal pigment epithelium development	0.0426	TMEM135, MFSD2A	46
GO:0022010~central nervous system myelination	4.27E-06	MAG, PLP1, MAL, SOX10, ASPA	45
GO:0042552~myelination	9.62E-13	MAG, GJC3, GAL3ST1, UGT8A, DHH, PLLP, MPZ, PLP1, MAL, MAL2, MBP, BCAS1	27
GO:0031643~positive regulation of myelination	0.0092	MAG, NCMAP, SOX10	21
GO:0051384~response to glucocorticoid	0.0002	SULT1A1, GHR, BCL2, HNMT, CPN1	17
GO:0007154~cell communication	0.0145	GJC3, GJB1, ENPP5	16
GO:0051924~regulation of calcium ion transport	0.0160	P2RX1, BCL2, ADRB1	15
GO:0045665~negative regulation of neuron differentiation	4.63E-05	DISP3, MAG, ZFP536, NBN, GPR37L1, BMP7	15
GO:0009636~response to toxic substance	0.0001	TTPA, BCL2, HTR1B, MBP, SLC6A1, CLDN1	14
GO:0006665~sphingolipid metabolic process	0.0199	FA2H, GAL3ST1, UGT8A	14
GO:2000781~positive regulation of double-strand break repair	0.0199	FAM178B, SPIRE2, FMN2	14
GO:0042220~response to cocaine	0.0208	HTR1B, HNMT, SLC6A1	13
GO:0007193~adenylate cyclase-inhibiting G protein-coupled receptor signaling pathway	0.0252	EDN1, HTR1B, GPR37L1	12
GO:0007405~neuroblast proliferation	0.0300	NBN, GATA2, SOX10	11
GO:0007267~cell-cell signaling	0.0074	EDN1, GJC3, GJB1, DHH	10
GO:0007157~heterophilic cell-cell adhesion via plasma membrane cell adhesion molecules	0.0394	TENM2, AMIGO2, L1CAM	10
GO:0035725~sodium ion transmembrane transport	0.0098	SLC9A3, ASIC4, SLC6A15, SLC6A1	9
GO:0071805~potassium ion transmembrane transport	0.0036	SLC9A3, KCNH6, KCNMB1, KCNA2, KCNA6	8
GO:0032355~response to estradiol	0.0140	GHR, DHH, SLC6A1, BMP7	8
GO:0007010~cytoskeleton organization	0.0218	STRIP2, CCL11, UGT8A, SYNE2	7
GO:0045471~response to ethanol	0.0262	BCL2, HTR1B, HMGCS2, CLDN1	6
GO:0006813~potassium ion transport	0.0299	KCNH6, KCNMB1, KCNA2, KCNA6	6
GO:0071456~cellular response to hypoxia	0.0321	EDN1, KCNMB1, BCL2, FMN2	6
GO:0007156~homophilic cell adhesion via plasma membrane adhesion molecules	0.0123	CADM2, AMIGO2, PLXNB3, L1CAM, CDH19	6
GO:0030335~positive regulation of cell migration	0.0430	EDN1, CCL11, PLP1, CLDN1, SYNE2	4
GO:0016192~vesicle-mediated transport	0.0464	ARL4D, SPIRE2, KIF1A, FMN2, CHML	4
GO:0034220~monoatomic ion transmembrane transport	0.0237	ASIC4, PLLP, P2RX1, KCNMB1, KCNA2, KCNA6	4
GO:0006811~monoatomic ion transport	0.0092	SLC9A3, ASIC4, PLLP, SLCO1A4, P2RX1, KCNMB1, SLC6A15, KCNA2, KCNA6	3

Table 4. 5: Overrepresented biological processes in yellow module and their corresponding fold enrichment and p-value.

Yellow Module			
Term	PValue	Genes	Fold Enrichment
GO:0072272~proximal/distal pattern formation involved in metanephric nephron development	0.019	IRX1, IRX2	106
GO:0071409~cellular response to cycloheximide	0.028	KLF4, KLF2	71
GO:0140973~positive regulation of AIM2 inflammasome complex assembly	0.028	GBP5, GBP2	71
GO:0002002~regulation of angiotensin levels in blood	0.037	CPA3, MCPT4	53
GO:0072086~specification of loop of Henle identity	0.037	IRX1, IRX2	53
GO:0060435~bronchiole development	0.046	MMP12, HOXA5	43
GO:0003150~muscular septum morphogenesis	0.046	TGFBR3, HEY2	43
GO:0060977~coronary vasculature morphogenesis	0.046	TGFBR3, HEY2	43
GO:0003184~pulmonary valve morphogenesis	0.001	BMP4, ADAMTS5, HEY2, STRA6	24
GO:0003084~positive regulation of systemic arterial blood pressure	0.008	ACE, CAMK2N1, RARRES2	21
GO:0045576~mast cell activation	0.001	MRGPRX2, MRGPRB1, NDRG1, MRGPRB2	20
GO:0006518~peptide metabolic process	0.010	ACE, CMA1, CPZ	20
GO:0001913~T cell mediated cytotoxicity	0.001	H2-T23, PRF1, GZMB, SERPINB9B	19
GO:0060441~epithelial tube branching involved in lung morphogenesis	0.002	SOX2, BMP4, DAG1, HOXA5	17
GO:0034695~response to prostaglandin E	0.013	TGFBR3, CCL19-PS3, CCL21A	17
GO:0001702~gastrulation with mouth forming second	0.002	UGDH, NAT8F3, NAT8F5, AMOT	16
GO:0048745~smooth muscle tissue development	0.016	BMP4, PTCH1, STRA6	15
GO:0003180~aortic valve morphogenesis	0.002	BMP4, ADAMTS5, HEY2, SLIT3	15
GO:0051481~negative regulation of cytosolic calcium ion concentration	0.018	NPY1R, IL6ST, KCNK3	14
GO:0060045~positive regulation of cardiac muscle cell proliferation	0.003	TGFBR3, HEY2, GLI1, TBX5	14
GO:0016338~calcium-independent cell-cell adhesion via plasma membrane cell-adhesion molecules	0.019	CLDN11, CLDN10, CLDN3	14
GO:0014044~Schwann cell development	0.021	LAMB2, DAG1, PMP22	13
GO:0001964~startle response	0.023	GRIN2A, KCNA1, CSMD1	13
GO:0060038~cardiac muscle cell proliferation	0.004	TGFBR3, CXADR, HEY2, TBX5	12
GO:0006956~complement activation	0.030	C4B, COLEC11, CFH	11
GO:0043303~mast cell degranulation	0.006	MRGPRX2, MRGPRB1, LAT, MRGPRB2	11
GO:0007389~pattern specification process	0.000	PTCH1, HEY2, ALX3, MDGA2, TBX5, HOXA5	11
GO:0002009~morphogenesis of an epithelium	0.032	DAG1, TBX5, HOXA5	11
GO:0048286~lung alveolus development	0.000	SOX2, MMP12, BMP4, ACE, HOXA5, STRA6	10
GO:0050905~neuromuscular process	0.002	CFH, KCNA1, PMP22, MDGA2, STRA6	10
GO:0031214~biomineral tissue development	0.038	BGLAP, OTOP1, PHEX	10
GO:0050806~positive regulation of synaptic transmission	0.040	RIMS3, GRIK2, PRKCZ	9
GO:0006836~neurotransmitter transport	0.009	RIMS3, SLC29A4, SLC6A12, SLC6A4	9
GO:0001954~positive regulation of cell-matrix adhesion	0.043	DAG1, PRKCZ, CCL21A	9
GO:0031640~killing of cells of another organism	0.000	CCL19-PS3, CXCL9, FGL2, PRF1, GZMB, PGLYRP1, CCL21A	9
GO:0060412~ventricular septum morphogenesis	0.010	TGFBR3, WNT11, HEY2, SLIT3	9
GO:0051289~protein homotetramerization	0.003	GBP5, ALDH1A3, TDO2, UPB1, HCN1	9
GO:0090023~positive regulation of neutrophil chemotaxis	0.047	CCL19-PS3, DNM1L, CCL21A	9
GO:0003151~outflow tract morphogenesis	0.003	TGFBR3, BMP4, WNT11, HEY2, NPY1R	8
GO:0050807~regulation of synapse organization	0.049	GPM6A, RIMS3, DAG1	8
GO:0019228~neuronal action potential	0.013	KCNA1, PMP22, GRIK2, HCN1	8
GO:0048706~embryonic skeletal system development	0.014	BMP4, WNT11, DMRT2, HOXA5	8
GO:0050680~negative regulation of epithelial cell proliferation	0.001	SOX2, TGFBR3, BMP4, KRT4, PTCH1, GKN3	8
GO:0048167~regulation of synaptic plasticity	0.004	IGSF11, GRIN2A, RIMS3, ACE, DAG1	7
GO:0035249~synaptic transmission, glutamatergic	0.016	UNC13C, GRIN2A, PEG13, GRIK2	7
GO:0048704~embryonic skeletal system morphogenesis	0.019	BMP4, ALX3, HOXD4, HOXA5	7
GO:0030593~neutrophil chemotaxis	0.007	CCL24, CXCL9, CXADR, DPEP1, CCL21A	6
GO:0010951~negative regulation of endopeptidase activity	0.008	SERPIND1, SERPINB6C, SERPING1, TIMP3, SERPINB9B	6
GO:0030282~bone mineralization	0.025	WNT11, SBDS, PHEX, ASGR2	6
GO:0016485~protein processing	0.003	CMA1, PTCH1, CPZ, PCSK6, PHEX, PCSK4	6
GO:0070830~bicellular tight junction assembly	0.029	CLDN11, CLDN10, CLDN3, WNT11	6
GO:0042391~regulation of membrane potential	0.004	GABRB1, GRIN2A, RIMS3, KCNA1, GRIK2, HCN1	6
GO:0030336~negative regulation of cell migration	0.001	TGFBR3, GM266, CLDN3, WNT11, DAG1, DPEP1, KLF4, TBX5	6
GO:0001649~osteoblast differentiation	0.004	SOX2, TGFBR3, BMP4, WNT11, BGLAP, GLI1	6
GO:0001570~vasculogenesis	0.037	TGFBR3, HEY2, ITGB8, AMOT	5
GO:0030324~lung development	0.002	BMP4, FGF18, GLI1, TBX5, PHEX, HOXA5, STRA6	5
GO:0045165~cell fate commitment	0.045	SOX2, BMP4, WNT11, HEY2	5
GO:0001568~blood vessel development	0.045	TGFBR3, BMP4, HEY2, STRA6	5
GO:0006813~potassium ion transport	0.010	FXYD3, KCNC2, KCNA1, KCNJ16, KCNK3, HCN1	5
GO:0006935~chemotaxis	0.010	CCL24, CXCL9, RARRES2, EAR2, CCL21A, AMOT	5
GO:0002181~cytoplasmic translation	0.027	RPL34, RPS6, RPS21, RPS13, RPS12	4
GO:0001822~kidney development	0.008	BMP4, WNT11, ACE, FOXD1, CFH, AP1B1, STRA6	4
GO:0009887~animal organ morphogenesis	0.016	WNT11, LAMB2, PTCH1, FGF18, NTN4, SLIT3	4
GO:0006508~proteolysis	2.18E-07	CPA3, COLEC11, TPSB2, ACE, TPSG1, CFH, CMA1, MCPT4, HTRA3, GZMB, CPZ, PRSS12, TRHDE, PHEX, PCSK4, MMP12, ADAMTS5, FOLH1, MMP27, XPNPEP2, DPEP1, CLCA3A1, PAPPA2	4
GO:0070374~positive regulation of ERK1 and ERK2 cascade	0.008	CCL19-PS3, BMP4, CCL24, FGF18, NOD1, PRKCZ, MTURN,	4
GO:0030198~extracellular matrix organization	0.029	MMP12, ADAMTS5, MMP27, SPOCK2, COL4A4, KAZALD1	3
GO:0006954~inflammatory response	0.001	GBP5, CCL24, TPSB2, CXCL9, CFH, RARRES2, PRKCZ, C4B, IL2RA, DPEP1, CCL21A, IL18R1, LAT	3
GO:0009617~response to bacterium	0.006	GPM6A, GBP5, CXCL9, TGTP1, PMP22, GBP2, PGLYRP1, IKZF3,	3
GO:0006955~immune response	0.000	BCAP31, H2-T23, CCL24, CXCL9, TGTP1, CFH, H2-M2, TGFBR3, IL7, PMP22, ITGB8, SERPINB9B, MS4A2, CCL21A, LAT	3
GO:0034220~monoatomic ion transmembrane transport	0.005	GABRB1, GRIN2A, KCNC2, KCNA1, KCNJ16, OTOP1, GRIK2,	3
GO:0045087~innate immune response	0.000	GBP5, COLEC11, TGTP1, CFH, PELI3, RARRES2, UAP1, NOD1, IIGP1, ISG20, C4B, LCK, SERPING1, GBP2, PGLYRP1, KLRG1	3
GO:0030036~actin cytoskeleton organization	0.027	CLDN3, DMTN, CXADR, MOB2, SPECC1L, PMP22, AMOT	3
GO:0002376~immune system process	0.000	H2-T23, GBP5, COLEC11, CFH, PELI3, UAP1, NOD1, IIGP1, ISG20, MFSD6, IL2RA, SERPING1, GBP2, PGLYRP1, LAT, KLRG1	3
GO:0006811~monoatomic ion transport	0.000	GABRB1, STEAP4, SCARA5, KCNC2, KCNA1, KCNJ16, OTOP1, GRIK2, CP, CLDN10, GRIN2A, NIPAL1, FXYD3, CLCA3A1, ASIC3, KCNK3, HCN1	3
GO:0043065~positive regulation of apoptotic process	0.004	BMP4, ALDH1A3, GRIN2A, FOLH1, WNT11, ACE, RPS6, NOD1, DNM1L, HOXA5, NSMAF	3
GO:0007155~cell adhesion	0.001	CADM3, CXADR, LAMB2, HAPLN3, IGSF11, CLDN11, CLDN10, CLDN3, SPECC1L, PMP22, ITGB8, COL6A6, COL6A5, IGSF9B, CD34, CTNNAL1	3
GO:0007507~heart development	0.030	BMP4, NAT8F5, CXADR, HEY2, DAG1, AP1B1, TBX5, STRA6	3
GO:0010629~negative regulation of gene expression	0.014	TGFBR3, BMP4, CLDN3, ACE, HEY2, PMP22, ITGB8, SLIT3,	3
GO:0016477~cell migration	0.034	TGFBR3, LAMB2, SPECC1L, NTN4, ITGB8, IGFBP6, PRKCZ,	3
GO:0010467~gene expression	0.043	SOX2, BMP4, PEG13, ZIC2, CFH, MDGA2, KLF4, LAT	2
GO:0010628~positive regulation of gene expression	0.005	IRX1, FOXD1, KLF4, SLC6A4, MMP12, TGFBR3, BMP4, CLDN3, IL7, LCK, FGF18, PMP22, ITGB8, HOXA5	2
GO:0007275~multicellular organism development	0.034	COLEC11, FOXD1, RORB, GLI1, TBX5, KAZALD1, MTURN, SOX2, BMP4, WNT11, NAT8F5, ZIC2, HEY2, ALX3, DACT2, HOXD4, SLIT3, HOXA5	2

Table 4. 6: Overrepresented biological processes in brown module and their corresponding fold enrichment and p-value.

Brown Module			
Term	PValue	Genes	Fold Enrichment
GO:0008150~biological_process	1.2E-15	A930030B08RIK, 1110019D14RIK, 1700025N23RIK, GM11210, B230322F03RIK, C130083M11RIK, 1700028N14RIK, GM11211, 1700034P13RIK, PHXR4, 5730585A16RIK, A930027P06RIK, 1700024B18RIK, GM10729, 4930512B01RIK, GM13919, GM16191, HOXAAS3, GM11732, SNORA34, GM10209, 2700078F05RIK, 2810039B14RIK, GM12827, GM10371, 5430434F05RIK, GM9694, TEX50, GM13963, E230001N04RIK, 1700086P04RIK, A430035B10RIK, D630023O14RIK, GM16152, 9430065F17RIK, GM16150, 1600023N17RIK, GM13483, 6030443J06RIK, A230087F16RIK, GM2814, GM5447, A530041M06RIK, GM10657, GM10735, A430018G15RIK, E030026E10RIK, 0610043K17RIK, A630095N17RIK, 9330154J02RIK, 4930470G03RIK, MAN2C1OS, C130073E24RIK, GM11992, B130034C11RIK, D030055H07RIK, 4930445N18RIK, GM12522, 3110006O06RIK, 4933407E24RIK, 4921531C22RIK, 1110002L01RIK, PSORS1C2, 2310026L22RIK, A030005L19RIK, C230053D17RIK, A430090L17RIK, 1700113A16RIK, 1700016A09RIK, 4930578M07RIK, GM7932, 2900042K21RIK, GM13778, B930086L07RIK, GM4221, GM9750, 1010001B22RIK, C530005A16RIK, 1700027J07RIK, BC060293, GM15327, D830025C05RIK, GM11201, GM11444, BC049715, B230119M05RIK, GM10392, 1700112J16RIK, 2010109A12RIK, GM7967, GM12976, C230021G24RIK, GM4258, GM5148, B430010I23RIK, 9430060I03RIK	2
GO:1903902~positive regulation of viral life cycle	4.6E-02	CD209B, CLEC4G	42
GO:0044419~biological process involved in interspecies interaction between organisms	6.9E-02	CD209B, CLEC4G	28

Table 4. 7*:* Overrepresented biological processes in grey module and their corresponding fold enrichment and p-value.

Grey Module			
Term	PValue	Genes	Fold Enrichment
GO:0008150~biological_process	1.45E-04	ARL9, GM15894, GM10860, GM15535, F630206G17RIK, RAPGEF3OS2, 9930111H07RIK, GM10489, 2810030D12RIK, AW822252, A330032B11RIK, GM12472, GM12199, GM15008, GM14379, C130046K22RIK, GM13522, 2310002F09RIK, 6430573P05RIK, CCDC7B, B830042I05RIK, 0610038B21RIK, GM10874, GM10830, 2410080I02RIK	2
GO:0007612~learning	9.00E-02	ARC, AMPH	21
GO:0034097~response to cytokine	9.45E-02	SERPINA1B, CITED1	20

4.4 Discussion

Using our novel murine model of muscle loading, we were able to detect a number of interesting changes in gene expression over time and between treatment groups. Large numbers of DEG between the naïve and all other 1-week groups suggests a strong cellular response to the TGF-β1 injury model. Changes were gradual in the 50% BW loading group, with numbers of DEG spread across 1 and 2, and 2 and 4 week comparisons, whereas numbers of DEG were substantially higher, and focused, between 2 and 4 weeks for 100% BW loading. The highest numbers of DEG for the injured/untreated group were also observed between 2 and 4 weeks. However, the very high numbers of DEG between 100% BW loading and injured/untreated groups suggest differentially regulated gene patterns. These findings suggest that our exercise model does affect changes in gene expression compared to injured unloaded tendons and that the pattern of change is affected by the magnitude of load. The greatest magnitude of gene up- and down-regulation occurred between 2 and 4 weeks, regardless of treatment, and likely correlates with the transition from the inflammatory to repair stage of wound healing. Our patterns of DEG data correlate with the PCA analysis, which shows a divergence between exercised and unexercised groups at 4 weeks, supporting an effect of exercise on tendon healing.

All of the significant associations identified by WGCNA were at the 2-week timepoint, consistent with the transition from the inflammatory to repair stages of tendon healing. The yellow and red modules were significantly associated with the 100% BW loading group at 2 weeks and displayed the highest mean GeTMM expression level for all genes. The brown module, also associated with exercise, but at 50% BW loading, showed much lower mean expression levels than the red or yellow modules. Biological processes overrepresented in the red module are involved with response to prostaglandin F, cell to cell signaling, cytoskeleton organization, and cellular response to hypoxia. The yellow module identified key biological processes that regulate inflammation and extracellular matrix organization. These biological processes suggest that eccentric exercise increases expression crucial for wound healing and improving tendon function post-injury. The grey module, negatively associated with the unexercised group at 2 weeks, showed increasing expression over time, suggesting that these overrepresented biological processes did respond to injury but in a pattern different from how the response occurred in exercised tendons. The modules

associated with the exercise and unexercised groups match the patterns observed from DEG comparisons, suggesting the genes are correlated with individual loading magnitudes.

These data are consistent with our mechanical testing data, which showed a stronger association with treatment duration than individual BW loading. The 50% BW group showed a more gradual response, as observed by histologic observations and muscle strength assessments. The PCA demonstrated a tight clustering between the 50% BW and 100% BW groups at the 4-week treatment duration. Further analysis is needed to compare the transcriptomic data from this study to prior research using this injury model [50-53, 64, 65]. The PCA also showed the injured/untreated group converged toward the naïve group, suggesting that there is some degree of injury resolution with just cage activity. However, the exercised groups diverged away from the injured/untreated and naïve groups, suggesting that there is a temporal effect of exercise.

This study has identified key transcriptomic adaptations; however, there are some limitations that impact interpretation of our results. The small sample size likely limits the detection of some differences that may exist between treatments. This was designed as a short-term study to focus on the early transcriptional, biomechanical and histological changes in response to muscle loading. Increasing the treatment duration to 8 weeks and beyond will allow for a more comprehensive evaluation of the tendon healing cascade in response to exercise. Longer treatment periods will also make this data set more translatable to human and larger animal models that experience longer healing [66, 67].

These data showed similarities between the 50% BW and 100% BW loading groups, with a more gradual change in expression over time in the 50% BW group compared to the 100% BW group. The naïve and the injured/untreated groups at 4 weeks were clustered together, suggesting some degree of tendon healing with cage rest alone. Similar patterns of DEG were also observed when comparing within groups and between groups, further suggesting that there is an effect from exercise on tendon cells. Biological processes linked to regulating cell to cell signaling, extracellular matrix organization, and inflammatory response modulation were identified and significantly associated with exercised groups. Further analysis is needed to identify pathways and upstream regulators associated with these genes.

4.5 Conclusions

Our study using multidisciplinary RNA-sequencing techniques reveals key insights into the transcriptional adaptations of injured tendon and the healing response to eccentric-based loading. The large numbers of DEG between naïve and 1 week, regardless of treatment group, is likely a response to the TGF-β1 injury model. Magnitude of loading impacts the tendon healing process. This is shown by the different patterns of numbers of DEG at 50% BW (more consistent over time) and 100% BW loading (localized between 2 and 4 weeks). Differences in significantly associated eigengene modules between the two loading magnitudes further supports this conclusion. An overall effect of exercise compared to unexercised controls is supported by the large numbers of DEG between exercised and unexercised groups, especially at 4 weeks.

4.6 Acknowledgements

This work was supported by the Edward Via College of Osteopathic Medicine / Virginia-Maryland College of Veterinary Medicine Center for One Health Research Seed Grant, the VMCVM Internal Research Competition (IRC) and the Interdisciplinary Graduate Education Program in Regenerative Medicine (RM-IGEP) at Virginia Tech (DCE). The authors would like to extend a special thank you to Dr. Bruno Menarim for his guidance and assistance with the RNA sequencing analysis and interpretation and Dr. Shavahn Loux for her assistance with the GeTMM, PCA analysis, and groups comparison data sets.

References:

1. Chen, W., et al., Epidemiology of insertional and midportion Achilles tendinopathy in runners: A prospective cohort study. Journal of Sport and Health Science, 2024. **13**(2): p. 256-263.

2. Yasui, Y., et al., The Risk of Achilles Tendon Rupture in the Patients with Achilles Tendinopathy: Healthcare Database Analysis in the United States. BioMed Research International, 2017. **2017**(1): p. 7021862.

3. Maffulli, N., Current Concepts Review - Rupture of the Achilles Tendon*. JBJS, 1999. **81**(7).

4. Holmes, G.B. and J. Lin, Etiologic factors associated with symptomatic achilles tendinopathy. Foot & Ankle International, 2006. **27**(11): p. 952-959.

5. Martin, R.L., et al., Achilles Pain, Stiffness, and Muscle Power Deficits: Midportion Achilles Tendinopathy Revision 2018. Journal of Orthopaedic & Sports Physical Therapy, 2018. **48**(5): p. A1-A38.

6. Longo, U.G., M. Ronga, and N. Maffulli, Achilles Tendinopathy. Sports Medicine and Arthroscopy Review, 2009. **17**(2).

7. Nourissat, G., F. Berenbaum, and D. Duprez, Tendon injury: from biology to tendon repair. Nature Reviews Rheumatology, 2015. **11**(4): p. 223-233.

8. Paavola, M., et al., Chronic Achilles Tendon Overuse Injury: Complications after Surgical Treatment: An Analysis of 432 Consecutive Patients. The American Journal of Sports Medicine, 2000. **28**(1): p. 77-82.

9. Maffulli, N., U.G. Longo, and V. Denaro, Novel Approaches for the Management of Tendinopathy. JBJS, 2010. **92**(15).

10. Trofa, D.P., et al., Professional Athletes' Return to Play and Performance After Operative Repair of an Achilles Tendon Rupture. The American Journal of Sports Medicine, 2017. **45**(12): p. 2864-2871.

11. Kedia, M., et al., The effects of conventional physical therapy and eccentric strengthening for insertional achilles tendinopathy. International journal of sports physical therapy, 2014. **9**(4): p. 488.

12. Nilsson-Helander, K., et al., Acute Achilles Tendon Rupture:A Randomized, Controlled Study Comparing Surgical and Nonsurgical Treatments Using Validated Outcome Measures. The American Journal of Sports Medicine, 2010. **38**(11): p. 2186-2193.

13. Roos, E.M., et al., Clinical improvement after 6 weeks of eccentric exercise in patients with mid-portion Achilles tendinopathy – a randomized trial with 1-year follow-up. Scandinavian Journal of Medicine & Science in Sports, 2004. **14**(5): p. 286-295.

14. O'Neill, S., P.J. Watson, and S. Barry, WHY ARE ECCENTRIC EXERCISES EFFECTIVE FOR ACHILLES TENDINOPATHY? nternational journal of sports physical therapy, 2015. **10,4**(2159-2896 (Print)): p. 552-562.

15. Nichols, A.E.C., et al., Novel roles for scleraxis in regulating adult tenocyte function. BMC Cell Biology, 2018. **19**(1): p. 14.

16. Abate, M. and V. Salini, Mid-portion Achilles tendinopathy in runners with metabolic disorders. European Journal of Orthopaedic Surgery & Traumatology, 2019. **29**(3): p. 697-703.

17. Zhao, H., et al., Concurrent deficits of soleus and gastrocnemius muscle fascicles and Achilles tendon post stroke. Journal of Applied Physiology, 2015. **118**(7): p. 863-871.

18. Slane, L.C., et al., Non-uniformity in the healthy patellar tendon is greater in males and similar in different age groups. Journal of biomechanics, 2018. **80**: p. 16-22.

19. Moon, J.L., K.M. Moon, and D.M. Carlisle, Obesity-Related Foot Pain: Diagnosis and Surgical Planning. Clinics in Podiatric Medicine and Surgery, 2019. **36**(1): p. 141-151.

20. Godoy-Santos, A.L., et al., Fluoroquinolones and the risk of achilles tendon disorders: update on a neglected complication. Urology, 2018. **113**: p. 20-25.

21. Gao, S., et al., [Effect of different intensity treadmill training on repair of micro-injured Achilles tendon in rats]. Zhongguo xiu fu chong jian wai ke za zhi = Zhongguo xiufu chongjian waike zazhi = Chinese journal of reparative and reconstructive surgery, 2017. **31**(5): p. 574-581.

22. Tan, J., et al., Effect of treadmill training on fibrocartilage complex repair in tendon-bone insertion healing in the postinflammatory stage. Bone & Joint Research, 2023. **12**(5): p. 339-351.

23. Thampatty, B.P. and J.H.-C. Wang, Mechanobiology of young and aging tendons: In vivo studies with treadmill running. Journal of Orthopaedic Research, 2018. **36**(2): p. 557-565.

24. Thomopoulos, S., et al., The effect of muscle loading on flexor tendon-to-bone healing in a canine model. Journal of Orthopaedic Research, 2008. **26**(12): p. 1611-1617.

25. Eliasson, P., T. Andersson, and P. Aspenberg, Achilles tendon healing in rats is improved by intermittent mechanical loading during the inflammatory phase. Journal of Orthopaedic Research, 2012. **30**(2): p. 274-279.

26. Rezvani, S.N., Novel Preclinical Approaches to the Understanding and Treatment of Achilles Tendinopathy, in Biomedical Engineering. 2021, Virginia Tech.

27. Banes, A.J., et al., Mechanical load stimulates expression of novel genesin vivoandin vitroin avian flexor tendon cells. Osteoarthritis and Cartilage, 1999. **7**(1): p. 141-153.

28. Magnusson, S.P., et al., Human tendon behaviour and adaptation, in vivo. The Journal of physiology, 2008. **586**(1): p. 71-81.

29. Thomopoulos, S., et al., Fibrocartilage tissue engineering: the role of the stress environment on cell morphology and matrix expression. Tissue Engineering Part A, 2011. **17**(7-8): p. 1039-1053.

30. Lavagnino, M. and S.P. Arnoczky, In vitro alterations in cytoskeletal tensional homeostasis control gene expression in tendon cells. Journal of Orthopaedic Research, 2005. **23**(5): p. 1211-1218.

31. Lavagnino, M., et al., Effect of Amplitude and Frequency of Cyclic Tensile Strain on the Inhibition of MMP-1 mRNA Expression in Tendon Cells: An In Vitro Study. Connective Tissue Research, 2003. **44**(3-4): p. 181-187.

32. Galatz, L.M., et al., Complete removal of load is detrimental to rotator cuff healing. Journal of Shoulder and Elbow Surgery, 2009. **18**(5): p. 669-675.

33. Hillin, C.D., et al., Effects of immobilization angle on tendon healing after achilles rupture in a rat model. Journal of Orthopaedic Research, 2019. **37**(3): p. 562-573.

34. Murrell, G.A.C., et al., Effects of immobilization on achilles tendon healing in a rat model. Journal of Orthopaedic Research, 1994. **12**(4): p. 582-591.

35. Wang, J.H.C., et al., Cyclic Mechanical Stretching of Human Tendon Fibroblasts Increases the Production of Prostaglandin E 2 and Levels of Cyclooxygenase Expression: A Novel In Vitro Model Study. Connective Tissue Research, 2003. **44**(3-4): p. 128-133.

36. Arnoczky, S.P., et al., Activation of stress-activated protein kinases (SAPK) in tendon cells following cyclic strain: the effects of strain frequency, strain magnitude, and cytosolic calcium. Journal of Orthopaedic Research, 2002. **20**(5): p. 947-952.

37. Chen, Z., et al., Mechanical overload-induced release of extracellular mitochondrial particles from tendon cells leads to inflammation in tendinopathy. Experimental & Molecular Medicine, 2024. **56**(3): p. 583-599.

38. Millar, N.L., et al., Hypoxia: a critical regulator of early human tendinopathy. Annals of the Rheumatic Diseases, 2012. **71**(2): p. 302.

39. Benson, R., et al., Tendinopathy and tears of the rotator cuff are associated with hypoxia and apoptosis. The Journal of Bone & Joint Surgery British Volume, 2010. **92**(3): p. 448-453.

40. Millar, N.L., et al., Hypoxia: a critical regulator of early human tendinopathy. Annals of the rheumatic diseases, 2012. **71**(2): p. 302-310.

41. Rubenstein, A.B., et al., Skeletal muscle transcriptome response to a bout of endurance exercise in physically active and sedentary older adults. American Journal of Physiology-Endocrinology and Metabolism, 2022. **322**(3): p. E260-E277.

42. Fernandez-Gonzalo, R., et al. RNA-Sequencing Muscle Plasticity to Resistance Exercise Training and Disuse in Youth and Older Age. Physiologia, 2022. **2**, 164-179 DOI: 10.3390/physiologia2040014.

43. Willis, C.R.G., et al., Transcriptomic adaptation during skeletal muscle habituation to eccentric or concentric exercise training. Scientific Reports, 2021. **11**(1): p. 23930.

44. Pillon, N.J., et al., Transcriptomic profiling of skeletal muscle adaptations to exercise and inactivity. Nature Communications, 2020. **11**(1): p. 470.

45. Baumann, C.W., et al., Adaptability to eccentric exercise training is diminished with age in female mice. Journal of Applied Physiology, 2023. **135**(5): p. 1135-1145.

46. Ganji, E., et al., Optogenetic-induced muscle loading leads to mechanical adaptation of the Achilles tendon enthesis in mice. Science Advances. **9**(25): p. eadf4683.

47. Steffen, D., M.J. Mienaltowski, and K. Baar, Scleraxis and collagen I expression increase following pilot isometric loading experiments in a rodent model of patellar tendinopathy. Matrix Biology, 2022. **109**: p. 34-48.

48. Johnson, S.A., et al., Fast, non-eccentrically loaded exercise worsens tendinopathic healing responses in a murine model. American Journal of Veterinary Research, 2023. **84**(6): p. ajvr.23.01.0018.

49. Frizziero, A., et al., Efficacy of eccentric exercise in lower limb tendinopathies in athletes. JOURNAL OF SPORTS MEDICINE AND PHYSICAL FITNESS, 2016. **56**(11): p. 1352-1358.

50. Bell, R., et al., Controlled treadmill exercise eliminates chondroid deposits and restores tensile properties in a new murine tendinopathy model. Journal of biomechanics, 2013. **46**(3): p. 498-505.

51. Bell, R., et al., ADAMTS5 is required for biomechanically-stimulated healing of murine tendinopathy. Journal of Orthopaedic Research, 2013. **31**(10): p. 1540-1548.

52. Bittermann, A., et al., Oral Ibuprofen Interferes with Cellular Healing Responses in a Murine Model of Achilles Tendinopathy. LID - 049 [pii] LID - 10.23937/2572-3243.1510049 [doi]. Journal of Musculoskeletal Disorders and Treatment, 2018. **4**(2572-3243 (Electronic)): p. 49.

53. Sikes, K.J., et al., TGF-b1 or hypoxia enhance glucose metabolism and lactate production via HIF1A signaling in tendon cells. Connective Tissue Research, 2018. **59**(5): p. 458-471.

54. Capogrosso, R.F., et al., Contractile efficiency of dystrophic mdx mouse muscle: in vivo and ex vivo assessment of adaptation to exercise of functional end points. Journal of Applied Physiology, 2017. **122**(4): p. 828-843.

55. Ashton-Miller, J.A., et al., An apparatus to measure in vivo biomechanical behavior of dorsi- and plantarflexors of mouse ankle. Journal of Applied Physiology, 1992. **72**(3): p. 1205-1211.

56. Alfredson, H., et al., Heavy-Load Eccentric Calf Muscle Training For the Treatment of Chronic Achilles Tendinosis. The American Journal of Sports Medicine, 1998. **26**(3): p. 360-366.

57. Silbernagel, K.G., A. Brorsson, and M. Lundberg, The Majority of Patients With Achilles Tendinopathy Recover Fully When Treated With Exercise Alone: A 5-Year Follow-Up. The American Journal of Sports Medicine, 2010. **39**(3): p. 607-613.

58. Grinstein, M., et al., A robust method for RNA extraction and purification from a single adult mouse tendon. PeerJ, 2018.

59. Smid, M., Coebergh van den Braak RRJ, van de Werken HJG, et al. Gene length corrected trimmed mean of M-values (GeTMM) processing of RNA-seq data performs similarly in intersample analyses while improving intrasample comparisons. BMC Bioinf, 2018. **19**: p. 236.

60. Dobin, A., et al., STAR: ultrafast universal RNA-seq aligner. Bioinformatics, 2013. **29**(1): p. 15-21.

61. Menarim, B.C., et al., Transcriptional and Histochemical Signatures of Bone Marrow Mononuclear Cell-Mediated Resolution of Synovitis. Frontiers in Immunology, 2021. **12**.

62. Rezvani, S.N., et al., In-Vivo Efficacy of Recombinant Human Hyaluronidase (rHuPH20) Injection for Accelerated Healing of Murine Retrocalcaneal Bursitis and Tendinopathy. Journal of Orthopaedic Research, 2020. **38**(1): p. 59-69.

63. Huang, D.W., B.T. Sherman, and R.A. Lempicki, Systematic and integrative analysis of large gene lists using DAVID bioinformatics resources. Nature protocols, 2009. **4**(1): p. 44-57.

64. Freeberg, M.A.T., et al., Transcriptomic Analysis of Cellular Pathways in Healing Flexor Tendons of Plasminogen Activator Inhibitor 1 (PAI-1/Serpine1) Null Mice. Journal of Orthopaedic Research, 2020. **38**(1): p. 43-58.

65. Fu, W., R. Yang, and J. Li, Single-cell and spatial transcriptomics reveal changes in cell heterogeneity during progression of human tendinopathy. BMC biology, 2023. **21**(1): p. 132.

66. FACKELMAN, G.E., The Nature of Tendon Damage and its Repair. Equine Veterinary Journal, 1973. **5**(4): p. 141-149.

67. Sharma, P. and N. Maffulli, Biology of tendon injury: healing, modeling and remodeling. Journal of Musculoskeletal Neuronal Interactions, 2006. **6**(1108-7161 (Print)): p. 181-190.

Chapter 5- Conclusions and Future Directions

Physical therapy has been shown to provide symptomatic relief and improve limb functionality in patients with chronic Achilles tendinopathy. The healing mechanisms by which eccentric loading exercises initiate tissue repair remain poorly defined. Within this body of work, we have provided and investigated the effects from 3 distinct eccentric exercise magnitudes over 3 durations and characterized the resulting biomechanical properties, muscle strength adaptations, and histologic and transcriptomic alterations in an effort to improve AT healing.

The results from this work demonstrated that any eccentric loading improves the CSA, maximum stress, and elastic modulus of Achilles tendons after 2 and 4 weeks of treatment. While muscle strength was differentially affected, more intense muscle loading initially decreased muscle strength, then it improved to naïve levels. Conversely, the 50% muscle loading improves muscle strength at 2 weeks and it decreases strength after 4 weeks. The intermediate muscle loading initially does not decrease muscle strength but results in decreased strength as treatment durations continue. Histologic images highlighted the benefits from muscle loading, with exercise groups showing increased active fibroblasts and more linear fiber alignment compared to the IU group. Of particular note was the increased concentration of pericellular GAG in the IU group at 4 weeks, but GAG was absent in the exercised groups at the same time point. The 50% loading groups displayed gradual temporal improvements compared to the 100% loading group. Interestingly, similar trends were observed with our RNA-seq data. The 50% loading groups show gradual changes in the amount of DEG over time, whereas the 100% loading and IU group showed little change early in the treatment course (between 1 and 2 weeks), then a dramatic increase between 2 and 4 weeks. While the amount of DEG was similar, the genes expressed were different between those 2 groups.

One limitation to this study was sex as a biological factor was not considered. Clinical data has shown that women have worse outcomes after tendon injury. There may be key transcriptomic differences in response to injury that may impede the healing response. Another limitation was the relatively limited numbers of mice used in this study. Increasing sample number could expose some key differences in biomechanical properties that were not observed due to the small sample size. To better match clinical eccentric exercise, the treatment durations should be increased to

include 6, 8, and 12 week timepoints to characterize the adaptations from prolonged exposure to eccentric loading protocols.

To expand upon this body of work, immunohistochemistry staining should be performed to correlate a stronger relationship between the transcriptomic changes and the cellular response observed in Toluidine blue and Safranin-O staining. Furthermore, sequencing of the muscle tissue would provide a deeper insight into the differing muscle adaptations from eccentric muscle loading. This could provide valuable mechanistic insights that correlate with the changes seen in tendon tissue.

Appendix A

TGF-β1 Prep Protocol

**All steps for TGFb-1 prep should be done sterile. The separate solutions used should be sterile filtered before adding to the TGFb

1. TGFβ-1 is ordered from Peprotech Inc (Catalog No: 100-21-100ug). Contact Peprotech to receive quote before purchase through HokieMart. Current Peprotech eastern sales tech: Karen Park (kpark@peprotech.com)

2. Prepare citrate (pH 3.0) solution
    a. Prepare 800mL of DI water in a suitable container
    b. Add 24.087g of sodium citrate dihydrate to DI water
    c. Add 3.471g of citric acid to the solution
    d. Adjust solution to pH 3.0 using HCl or NaOH
    e. Add DI water to achieve a final volume of 1L
    f. Filter citrate solution through .45um filter and keep sterile

3. Prepare 0.1% BSA (in PBS) solution Appendices
    a. Prepare 1X PBS solution
    b. To prepare 10mL of 0.1% BSA add 10ug BSA to 9.9mL PBS and vortex vial
    c. Filter 0.1% BSA in PBS solution through 0.45um filter and keep sterile

4. Ensure all remaining steps (now that all components are sterile) are done in the hood

5. Add 150uL of the citrate solution to TGFb vial

    a. Flick bottom of the tube to help dissolve, DO NOT pipette up and down

6. Transfer contents of vial to a 5 or 15mL tube

7. Wash original TGFb vial with 500uL of 0.1%BSA solution. Add to the new tube from step 6

8. Add remaining 2350uL of 0.1%BSA to the tube (2850uL total BSA volume, 3mL total overall volume)

9. Vortex tube for up to 1 minute

10. Aliquot into 100uL aliquots (30 total) or 75uL aliquots (40 total vials) and store in -20C freezer. Aliquots will keep for up to 18 months at -20C

11. Note: When using aliquots, keep on ice, do not refreeze. Any remaining TGFb solution after injecting animals should be discarded

TGF-ß1 Injury Administration

TGFb Administration Protocol

1. TGFβ1 aliquots should be prepped prior to beginning.
2. Ensure work space is fully setup. Area for cage of animals next to the sink, receiving cage ready nearby to place in after ket/xyl injections, work area for TGFb injections, and heat lamp/pad area for animal recovery

3. Grab animal cages one at a time from vivarium room. Remove metal food tray from cage and place directly next to it

4. Place one animal at a time into the Isoflurane anesthesia chamber

5. Give the mouse 3 minutes to fully go under anesthesia in the receiving cage. During this time prep the TGFb syringes
    a. TGFb vial aliquot should be kept on ice the entire time
    b. Using a pipette, dispense 2-8uL dollops of TGFb solution onto the surface of a petri dish (16uL for each mouse being injected). Ensure this is done very carefully and the TGFb is in one "drop" on the surface of the petri dish. A bubble or two may form in the drop, that is fine
    c. Using a syringe (28G) aspirate up the TGFb drop. Note: Be very careful while doing this step, an extremely small amount of force is needed to be applied to the plunger to aspirate up such a small volume of solution. You want to make sure only the TGFb solution is being aspirate, no air in the syringe
    d. Prepare the second syringe in the same method as above

6. Weigh the mouse and record their mass and transfer them to the nose cone on the preheated Auora System testing platform. (A large fluctuation of mass could be the sign of issues with the animal)
7. Ensure that the mice are fully under anesthesia, not moving around, but torsos still moving up and down while breathing

8. Take one animal out from the receiving cage at a time to inject with TGFb. For the first injection day it is a good idea to do the ear notches right before the TGFb injection

9. Flip the mouse on its back and take the foot you plan on injecting between your thumb and index finger. Using a q-tip fully clean the entire posterior section of the lower hindlimb (knee down to heel) first with iodine, then 70% ethanol

10. With the foot still between your thumb and index finger, raise it up more (can put your pinkie underneath the body of the animal to support it further if necessary) to allow for ease of access to the gastrocnemius muscle complex

11. Insert the needle of the TGFb syringe just under the skin, entering about the midpoint of the gastrocnemius complex. Continue inserting the syringe distally down towards the Achilles tendon. When you reach the Achilles tendon, you should feel more resistance in the tissue as you move from the muscle to the tendon. Continue inserting the syringe until you are at the midpoint of the Achilles tendon and dispense of syringe contents

12. Repeat step 12 with a 2nd syringe of TGFb, however this time travel even further distally through the Achilles tendon and dispense contents of syringe at the calcaneal insertion region of the Achilles tendon

13. Carefully place mouse back into the receiving cage and position the cage underneath the heating lamp or top of heating pad

14. Repeat steps 12-14 for all mice you are injecting in the cage.

15. Repeat steps 5-14 for all the cages you are injecting that day

16. Continue to monitor animals while they are recovering, ensure you can see all animals breathing throughout

17. Most mice take around 3 to 5 minutes to wake up from isoflurane anesthesia. Mice should not be considered "recovered" and returned to their racks until they are all crawling around the cage. NOTE: all mice will react to anesthesia differently and the timeline for recovery can vary. Make sure to note down any odd behaviors on your testing sheets

18. 48 hours following the 1st TGFb injection repeat all steps in this protocol for the 2nd injection. NOTE: If doing the prolonged TGFb, both injections should be administered on both days

In Vivo Murine Muscle Loading

Shelby Hamm
5/15/17
*Adapted from Dr. Shelby Hamm and Dr. Robert Grange
*Methods modified from Jon Doering

Materials:
Need to bring into Vivarium in ILSB:

- DMC protocols/USB
- Experiment sheet(s)
- Isoflurane Anesthetic (there should be charcoal filter canisters to prevent the accumulation of anesthetic vapors).
- Scale (Room #1119)
- Pen
- Hokie Passport
- Povidone Iodine swab sticks (Antiseptic/germicide)– occasionally need to replenish 1119 stock from 1085 lab

Room 1119:

- Hair remover – (Nair)
- Povidone-Iodine swab sticks – (Antiseptic/germicide)
- Isoflurane Anesthetic (there should be charcoal filter canisters to prevent the accumulation of anesthetic vapors).
- Cotton-tipped applicator swab
- Isopropyl Alcohol – antiseptic
- Trimmer/shaver – electric + battery
- Gauze (2x2 and 4x4)
- First aid tape – clear
- Timer
- Sharpie
- Colored tape
- Kim wipes
- Ruler (cm & mm)
- Water bottle - diH_2O
- Eye-moistening lubricant (Puralube)
- Pipette tip box for nose cone support

Initial Prep:

1.) Set up scale on hood and plug into wall on the left of the hood.
2.) Turn the water bath on - 35°C.
3.) Weigh both charcoal canisters (individually) and write the weight of each on the outside of the can. *If the weight exceeds 50g over the original weight of the can, you must retrieve a new can and weigh again. New cans are in the big anesthesia room, in the cabinet on the right.
4.) Ensure there is adequate isoflurane in reservoir. See isoflurane refill SOP for instructions on how to add isoflurane.
5.) Set up nose code preparation area: tape down paper towel to the right of the experiment platform, tape nose cone securely on the right end portion of the paper towel prep area, place pipette tip box behind platform.
6.) Double check mouse number and experiment conditions (runner/non-runner, treatment type, diet, etc.)

Anesthesia:

7.) Turn on oxygen tank (NOT CO_2) and make sure there is adequate oxygen. Double check for spare tanks.
8.) Set oxygen to 1 on the green gage of the anesthetic cart by turning the sliver knob at the bottom.
9.) Make sure the nose cone hose is off and the anesthetic box hose is on. On = knob is parallel to hose, off = knob is perpendicular to hose.
10.) Pick up mouse by tail, place in box, close and lock box.
11.) Turn isoflurane on to 3 – press down white tab and turn to the correct tic mark. Start timer - this will run for the remainder of the experiment. Time for 3 minutes – monitor respiration ~1 minute in. Boot up computer and turn on DMC while waiting.
12.) Turn isoflurane off after 3 minutes and flush box with oxygen ~10 seconds. Immediately move mouse to nose cone preparation area, abdomen up.
13.) Quickly turn off box hose and turn on nose cone hose. Turn on isoflurane to 1.5. Wait for respiration to stabilize and perform foot pinch test.

14.) Place 1 small glob of Puralube on each eye. Check eyes periodically throughout experiment and apply again as needed.

*** **IMPORTANT: You will need to monitor respiration throughout the experiment. If the isoflurane is too low or too high, the mouse can die or wake up. Use your best judgment.**

Leg prep:

15.) Shave leg (from ankle to right above knee).
16.) Apply small drop of hair remover to swab, rub on shaved area, and let sit for 30 seconds.
17.) Wipe hair remover using a wet 2x2 gauze - make sure knee is exposed.
18.) Use povidone-iodine swab stick to coat the exposed knee.
19.) Move mouse to experiment platform. Pull mouse by tail and right leg to correct placement in the clamp. Tuck left leg to the inside of the clamp – you will most likely need to straighten this leg a little to get it through. Once the mouse is situated, tape the nose cone to the platform/pipette tip box.
20.) Place foot of shaved leg onto the motor foot-plate (make sure to get the heel in the cup) and tape foot to the pedal using clear tape.
21.) Clamp the knee in place so that the foot-plate is 90° to the tibia, and the tibia is 90° to the femur.
22.) Strap mouse gently to the table with clear tape if needed.
23.) Use ethanol to wipe off/ clean the electrodes.
24.) Insert electrodes according to below methods.

In vivo stimulation methods:

25.) Shelby method: insert electrodes ~1mm lateral to the tibia, ~1-2mm distal from the knee. They should be parallel to the tibia, not perpendicular. The blue side should be closer to the foot, red closer to the knee (alignment works better this way in my opinion). Jon method: Insert two electrodes 1-2mm on either side of the peroneal nerve, one distal to the fibular head, one distal (0.2mm) to the first.
26.) Start current at 30mA and adjust up to 50mA until maximal torque is achieved (Should be around 35-40mA). Once optimum voltage has been achieved, begin force frequency testing.

27.) Run protocols outlined on the experiment sheet.

Recovery and clean-up:

28.) Remove electrodes, place in a 2x2 gauze ethanol soak
29.) Measure foot length from heel to toe, and malleus to toe.
30.) Remove tape from foot – peel up.
31.) Swab knee with povidone iodine again.
32.) Flush nose cone for approx. 5 sec.
33.) Remove mouse and weigh.
34.) Place mouse into recover chamber, turn off isoflurane, turn up recovery chamber to 1 L/ min of Oxygen.
35.) Continuously monitor mouse being revived
36.) Clean box with water and towel
37.) Place electrodes inside a different 2x2 ethanol gauze and place into bag.
38.) Shut down computer.
39.) Clean all surfaces.

Refilling the isoflurane tank

1. Locate the purple connector tool – should be on the cart next to the pump.
2. Unscrew the cap to your isoflurane bottle.
3. Fit the round end of the purple connector tool onto the top of the isoflurane bottle – the two notches should line up and fit together – and screw it on tightly.
4. On the isoflurane pump, locate the rectangular metal piece with the red-colored notch. Pay attention to how this piece is oriented before you remove it – this will act as your guide for placement of the rectangular end of the purple connector. To remove it, unscrew the knob above it.
5. Remove the metal rectangle plug.
6. Uncap the plastic rectangle side of the purple connector and put it in the plug's place in the same orientation – knotch up. Be careful so that you don't spill isoflurane – try not to invert the bottle yet.

7. Screw the knob tightly so that isoflurane will not spill when you're filling the tank.
8. Invert the bottle and watch the gauge to see how much to add. Don't fill over the FULL line.
9. Take out the connector and recap it. Replace the metal rectangle, red up. Screw the knob back down.
10. Unscrew the connector and recap the bottle.
11. Wipe up any isoflurane that spilled.

Limb Fixation for Histology
One Health Project

Materials Needed:

1) **Tissue Cassettes**
2) **10% Buffered Formalin**
3) **Dissecting tools**

Procedure:

*****The following steps must be performed immediately following euthanasia*****

1) Carefully remove skin from limb, starting at the hip joint and ending at the ankle. Be careful to not pull skin roughly or it can damage underlying tissue.

2) Dissect out the limb at the hip joint.

3) Place the limb in the tissue cassette such that the top of the femur is positioned in the upper right corner of the cassette, limb flexed at the knee, paw placed on the bottom edge of the cassette, and the toes in the bottom left corner of the cassette as shown to the right:

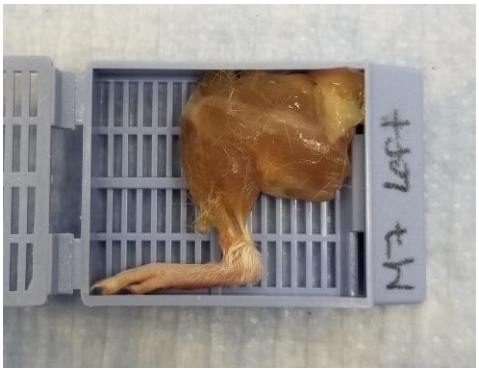

4) Label cassettes with pencil only (mouse ID and limb) and place in 10% Buffered Formalin. Ensure cassette is entirely submerged.

5) Leave cassettes in formalin for 24 to 48 hours.

6) Remove cassettes from formalin and proceed with decalcification protocol.

EDTA Decalcification Protocol
One Health Project

Materials Needed:

1) 5% EDTA in dH_2O
    a. 50g EDTA
    b. 1000mL dH_2O
    c. pH to 7.0 with 10N NaOH
2) Fixed tissues in histology cassettes
3) dPBS

Procedure:

1) Remove cassettes from formalin and wash 3x in dPBS with stirring.
    a. Should have been fixed in 10% buffered formalin for 3-5 days

2) Place cassettes into bottle containing 5% EDTA in dH_2O.
    a. Make sure solution volume is ~20x greater than the tissue volume to ensure proper decalcification.

3) Keep tissues in the EDTA solution for 4 to 5 weeks at room temperature, exchanging the solution every 3 days. Tissue is decalcified when bones are pliable.

4) Remove cassettes from EDTA solution and wash 3x in dPBS with stirring.

5) Tissues can be processed for embedding immediately or stored in 70% ethanol until ready.

Processing: Laudier Histology

1. Following Fixation and decalcification process, begin the dehydration process using 2-etoxyethanol and clear with benzyl benzoate.
2. Post dehydration, embed the samples in a custom hydrophobic resin.
3. Trim and carefully slice sample into 5-micron thick sections using a tungsten carbide blade.
4. Mount onto adhesive microscope slides.
5. Sections can then be plasticized using xylene and stained with Toluidine Blue or Safranin-O-Fast Green

Tendon Harvest Protocol for RNA Sequencing

Dylan Easley

Needed items:

- Scalpel and #10 and #11 blades
- Rat-toothed forceps and regular forceps
- RNAase away solution
- 70% EtOH
- Absorbate pads
- Tube rack
- RNase/DNase free Water
- Kimwipes
- **Prelabeled RNAse-free** microfuge or Bead beater tubes tubes filled with 600µL Trizol can do the day before (24-36 hours) just perform in sterile hood and keep in refrigerator overnight
- Liquid nitrogen, rack, and small/medium Styrofoam container
- **Keep all items in a large container that has been wiped with RNase away and wipe all equipment down with EtOH and RNase away prior to loading container**

Before starting:

- Be sure to have your hair contained and wear a clean lab coat and gloves. Wear gloves to handle EVERYTHING (tubes, utensils, etc) right from the start.
- Wipe down work bench with RNase Away!!!
- Remove clean absorbate pad and place on clean surface.
- Wipe utensils down with RNase Away

NOTE: It is best to euthanize the mice that are getting pooled together at the same time to ensure that you can work quickly and efficiently with minimal interruptions. If multiple groups are housed together separate the appropriate mice and euthanize them together. Avoid euthanizing multiple groups at the same time. <u>You want the samples to be harvested as close to the euthanasia time as possible.</u>

1. Collect the appropriate cage and euthanize mice using CO2 and cervical dislocation.
2. **CHANGE YOUR GLOVES**
3. Spray hind limb down with EtOH, then remove skin with rat toothed forceps to expose the Achilles tendon. BE Carful to not get hair on the tendon or utensils
4. Using the microscissors cut the Achilles just below the myotendinous junction while holding the tendon in place with the forceps. BE sure to only collect the tendon tissue NOT MUCSLE or accessory tendon
5. Then cut the AT close to the insertion site and place into corresponding labeled tube

6. Repeat steps 2-5 for all mice that are pooled together. Usually, 2-5 tendons are needed to make an adequate sample for RNA-sequencing
7. Immediately snap freeze tube in liquid nitrogen and place in a rack suspended in the mist of the liquid nitrogen in a Styrofoam container
8. Repeat for all samples that are to be collected that day.
9. Immediately transfer to -80ºC freezer near the shared lab space in vetmed (room 281). Ask Michelle Todd for the location of the freezer prior to starting experiments. Be sure you have building and room swipe access prior to performing and RNA harvests or isolations.

Direct-zol™ RNA Isolation Basic Protocol- Micro Kit

Dahlgren Lab

Needed items:

- Direct-zol RNA Microprep Kit (Zymo Research #R2062; Genesee # 11-330M)
- TRIzol Reagent (Life Technologies; Fisher #15596018 (200 mL) or 15596026 (100 mL))
- BeadBug 6 homogenizer
- Benchmark 1.5 mm zirconium bead kit (Genessee #D1032-15)
- Qiagen MaXtract High Density 1.5 mL tubes (Genessee #1038087)
- Filter tips
- Regular ice
- Rat tooth forceps, microfuge, table top centrifuge, RNase Away

Before starting:

- Be sure to have your hair contained and wear a clean lab coat and gloves. Wear gloves to handle EVERYTHING (tubes, kits, etc) right from the start.
- Create an uncluttered, clean workspace, including a fresh bench pad.
- Wipe down pipettes and any other tools with RNase-away before starting.
- Label Bead Beater tubes and organize in tube rack (1 per sample). Use RNase-free filter tips for all steps. Do not place hand in bag to retrieve tubes – shake the needed number out onto your clean bench pad.
- Place 1 column into 1 collection tube for each of your samples.
- Make sure ethanol has been added to the buffers.
    - *Make your own aliquot of each buffer by transferring to a 15mL conical tube. Do NOT pipet from stock buffers!!*
- Pre-warm Nuclease Free Water to 55C.
- Make sure there is DNAse I made up/Reconstitute DNAse I if not (add 275 µL DNase/RNase Free Water from kit, mix by inversion, do not vortex).
    - *Do NOT refreeze DNAse aliquots- once thawed, they cannot be reused*
    - Aliquot immediately after reconstituting
    - Store frozen aliquots in middle -20C freezer in 280C
    - Thaw required amount of DNAse (see step 14 below) on ice
- TRIzol contaminated plastic and waste must be disposed of separately (ie. not in regular trash and cannot be put down the drain).
- You will need 3, 1.5 microfuge tubes per sample
    - Label one tube for your final elution Sample ID, date, and initials

PREVIOUSLY PERFORMED: Harvest mouse Achilles tendons directly into 1.5 mL RNAse-free Bead beater tubes containing 600µL Trizol (1 tube per 1-3 tendons). Immediately snap freeze in liquid nitrogen and retain in liquid nitrogen until transfer to -80 freezer for storage (room 281).

1) **Thaw samples briefly on ice. Transfer tendon(s) into Bead Beater tube if not previously frozen in bead beater tubes.**

2) **Bead beat samples for 4 rounds of 45 sec at maximum speed (4350 rpm 50Hz). Briefly incubate samples on ice for 2 minutes to cool samples between each cycle. Repeat 1 cycle for 45 sec if further homogenization is needed, for a maximum of 5 cycles. Store samples on ice until full set of samples are homogenized.**

3) **Transfer liquid contents to new 1.5mL RNase/DNase free microfuge tube.**

4) **Incubate at room temperature for 5 minutes**

5) **Spin at 16,000xg (RCF) for 5 min at room temp.**

6) **Immediately prior to extracting supernatant, spin MaXtract tubes at 16,000 x g for 30 seconds after reaching 16,000 x g.**

7) **Transfer supernatant to new 1.5mL MaXtract High Density tube. Be careful not to disturb the pellet at the bottom (be conservative in this step).**

8) **Add 120 µL of chloroform to the MaXtract tube. Secure the cap and shake vigorously for 15 seconds mixing the organic and aqueous phase until they form a transiently homogenous suspension.**

9) **Incubate for 2-3 minutes at room temperature.**

10) **Centrifuge at 12,000 x g for 5 minutes at 4C to separate the phases.**

11) Transfer aqueous (upper) layer to a new 1.5ml RNase free centrifuge tube. You may have to remove the top layer of the gel to reach the aqueous phase approximately 250µl. Use a clean pipette tip and scrap gel to one side.

12) Add an equal volume of 100% EtOH (approximately 250µl). Mix by inversion or brief, mild vortex. Spin down briefly on small tabletop centrifuge.

13) Transfer 700 µL aqueous phase/EtOH mixture to Zymo spin column.

- Column max is 700µL. If needed, load 700µL first, spin, discard flow through, and then repeat for remainder of sample – see step 13.

14) Spin at 16,000xg (RCF) for 30 sec at room temp. Discard the flow through by pipetting and replace the column. <u>Be careful to not touch the bottom of the column to the tube.</u>

- Remove the flow through by pipetting (not pouring) and discard.
- Ethanol/TRIzol waste must be kept separate and disposed of through chemical waste.

15) Repeat steps 14 and 15 with the remainder of the ethanol/TRIzol solution. Discard the flow through and collection tube.

16) Transfer the column to a new collection tube.

17) Add 400µL Direct-Zol RNA Wash Buffer to the column. Spin at 16,000xg (RCF) for 30 sec at room temp. Discard the flow through (by pipetting).

18) Create master mix of DNase I in DNA Digestion Buffer (5µL DNase I + 35µL DNA Digestion Buffer per sample = 40µL per sample). Mix gently by inverting the tube and spin briefly in small table top centrifuge. <u>Do NOT vortex.</u>

- DNAse should only be freeze thawed once. If there is leftover, discard.

19) Add the DNAse I incubation mix (40µL) directly onto the column matrix. Be sure to place the small volume directly in the center of the column filter. Be careful not to touch the filter!

20) Incubate at room temp for 15 min.

21) Add 400µL Direct-zol RNA PreWash to the column. Spin at 16,000xg (RCF) for 30 sec at room temp. Discard the flow through (by pipetting).

22) Add another 400µL Direct-zol RNA PreWash Buffer to the column. Spin at 16,000xg (RCF) for 30 sec at room temp. Discard the flow through (by pipetting).

23) Add 700µL RNA Wash Buffer to the column and spin for *2 min* at 16,000xg (RCF) at room temp. Discard the flow through (by pipetting).

24) Spin dry column for 1 min at max speed (16,000xg) to remove any remaining buffer.

25) Transfer the column to a new RNase free 1.5mL microfuge tube.

- This is the tube into which you will elute and store your purified RNA. Label well BEFORE transferring the column.

26) Add 15µL of prewarmed DNase/RNase-free water directly to the center of the column matrix.

- Recommend eluting in at least 10µL in order to get sufficient quantities of concentrated RNA. You will not recover all 6-15 µL from the column and will use at least 1 µL to quantify. 15 uL will elute ~90% of RNA on column. Decreasing the volume will cause the elution profile to dip down.

27) Incubate for 1-2 minutes at room temperature to allow for adequate elution.

28) Spin at 13,000xg (RCF) for 30 sec to elute RNA. Place samples directly on ice immediately after spinning.

29) Repeat steps 26-28, eluting the RNA from the column with the original elution and transfer to a new tube.

30) Measure RNA concentration and purity using Nanodrop (Lab 203). Freeze at -80C until use.

- 260/280 ratio for pure RNA is 2.0. Anything >1.90 can be used for qPCR.
- 260/230 ratio for pure RNA is 2.0-2.2. Anything >1.70 can be used for qPCR. This is less important that 260/280.

More info on 260/280 and 260/230 significance here:

https://assets.fishersci.com/TFS-Assets/CAD/Product-Bulletins/TN52646-E-0215M-NucleicAcid.pdf

NanoDrop One/OneC for RNA Purity Protocol

Items needed:

- ddDH$_2$0
- Kim wipes
- 0.5-2.5µL pipet and filter tips (RNase/DNase free)
- Flash drive to copy data onto

Before starting:

- Transfer your samples to the room on ice.
- Raise the arm and clean the upper and lower pedestals of the NanoDrop with double DI water and dry with Kim wipes. Leave the arm raised and proceed to step 3.
- Select the RNA function on the touch screen
- Blank nanodrop with 1 µl of the solution in which samples eluted (DNAase/RNAase free water):

1. Pipette 1 µl of sample onto the lower pedestal
2. Lower the arm to begin measurement
3. When measurement is complete it will display on the screen
4. Lift arm and wipe upper and lower pedestals with dry Kim wipe to remove sample
5. Repeat with remaining samples
6. Clean pedestal after all the samples are measured with ddDH$_2$O on a Kim wipe, then dry with Kim wipe, and close the upper arm
7. Export the files to USB drive

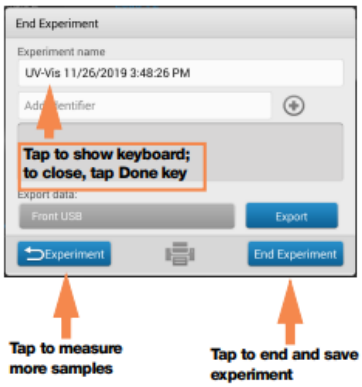

6. When you are finished measuring samples:
   - Tap End Experiment (see previous image)
   - Enter an experiment name (tap **Experiment Name** box to display keyboard), or leave the default experiment name
   - Tap End Experiment
   - Lift the arm and clean both pedestals with a new wipe

   If finished with the instrument for the day, clean the pedestals with DI H2O (see Clean pedestals between users)

Acquired data are automatically saved in an experiment with the entered name. In the default configuration, experiments are stored in a database on the local instrument according to acquisition date, experiment name, application used and any assigned labels (see Manage identifiers on the instrument).

User manual:
https://www.thermofisher.com/document-connect/document-connect.html?url=https%3A%2F%2Fassets.thermofisher.com%2FTFS-Assets%2FCAD%2Fmanuals%2Fts-nanodrop-nucleicacid-olv-r2.pdf

MTS Testing Achilles Tendon

Wang Lab

Tendon identification reference: https://www.biorxiv.org/node/120034.full#F1

1. Thaw out the mouse (keep in a little bag and put in a container of water for 25-45 minutes)
2. Put testing chamber on MTS and align the tank under the upper grip
3. Secure the testing chamber with two screws in opposite corners (back L and front R)
4. Plug in the laser and let it warm up while dissecting
5. Dissect out the Achilles and Refreeze the mouse
6. Use the labmat liner as a drop cloth during preparations
7. Gently scrape off muscles from the insertion up to 6 mm or so and trim the tibia
8. Measure the width and thickness at 3-5 points
9. Calculate both 5:1 and 6:1 ratio to ensure gauge length is in the ideal range for testing
10. Cut a 20 mm tube with the Dremel and file the ends
11. Get out a small bit of parafilm to cover one end of the tube
12. Wrap the tendon in a saline soaked gauze to keep moist
13. For 1 potting mix about a 0.5-0.75g of the cement powder and a ~.5mL of the solution together, keep mixing and adjusting ratios until you have a sticky gel like substance
14. Use a pipet to transfer the cement to the cylinder, fill it up almost to the top
15. Place the foot in the cylinder and make sure that it is centered and the majority of the foot is covered in cement – the heel should be about in line with the opening of the cylinder (ask Dr. Wang to show you if you have questions)
16. Wait 25-30 minutes for the cement to cure – make sure the gauze is still moist
17. Trim off the cement on the cylinder
18. Use the thin film grips to secure the origin portion of the tendon, check the chart for the gauge length. Make sure that the insertion site is facing you (the bottom of the foot)
19. Transfer the tendon to the vice and attach 3D printed clevis attachment to the loadcell, you will need to lower the cross head initially and then move it up and down to get the cylinder in the vice.
20. Tighten vice, nuts, cylinder screw, check alignment and make sure it has 0 load
21. Zero load

a. Fine tune the position of the tank
b. Move the crosshead so that it is between load and no load (~0.008 N) and zero crosshead

22. 2 minute preload (check the chart for the load value) and measure the preload gauge length, add this to the initial gauge length
23. Preconditioning – check the chart for details
24. 5 minute rest with no load
25. Preload as in step 27.
26. 2 minute preload (see step 27)
27. Failure Test- Rate of 0.05 mm/sec (3 mm/min)
28. Record peak load, elongation at peak load, stiffness, work, and failure location, export the data into a .csv file and rename for each sample according to the test (preconditioning or failure).

Testing Sheets

In Vivo Muscle Strength Experiment Sheet (IACUC Protocol #21-239)

Mouse Experiment:_____

Date: _____ Mouse:_____ D.O.B.:_____

Age Genotype:_____ Sex:_____

(wks):_____

Mass Int./Run?:_____ Cohort:_____

(g):_____

Data Files:

Leg R/L

Offset force at 25mN*m			
Manual twitch 1	_____.30mA	Start time:_____	Time revived:_____
Manual twitch 2	_____.35mA	Current: _____mA	Recovery time:_____
Manual twitch 3	_____.40mA	Time Down:_____	
Manual twitch 4	_____.45mA		
Manual twitch 5	_____.50mA		
Manual twitch 6	_____.55mA		
2’			
monitor respiration rate		Respiration	_____breathes/min
Force Freq. Twitch	_____.twi		
Force Freq. 10Hz	_____.010		
Force Freq. 30Hz	_____.030		
Force Freq. 50Hz	_____.050		
Force Freq. 65Hz	_____.065		
Force Freq. 80Hz	_____.080	Respiration	_____breathes/min
Force Freq. 100Hz	_____.100		
Force Freq. 120Hz	_____.120		
Force Freq. 150Hz	_____.150		
Force Freq. 180Hz	_____.180		
Force Freq. 200Hz	_____.200		

Date: _____ Tmt Code: _____

Sample #: _____ Data Label: _____

In Vivo Muscle Loading Experiment Sheet (IACUC Protocol #21-239)

Ear Punch __ Mouse: _____ Group: _____
Mass (g): __ Start Time: _____ Date: _____

Offset Force at 25mN-m HD Treatment #: _____

Manual Twitch 1	__	0.30mA	Manual Twitch 4	_____	0.45mA
Manual Twitch 2	__	0.35mA	Manual Twitch 5	_____	0.50mA
Manual Twitch 3	__	0.40mA	Manual Twitch 6	_____	0.55mA
Current:	__	Time: _____		Time: _____	
		Respiration: _____		Respiration: _____	

Total Time Down:
Notes:

Mass (g): __ Start Time: _____ Date: _____

Offset Force at 25mN-m HD Treatment #: _____

Manual Twitch 1	__	0.30mA	Manual Twitch 4	_____	0.45mA
Manual Twitch 2	__	0.35mA	Manual Twitch 5	_____	0.50mA
Manual Twitch 3	__	0.40mA	Manual Twitch 6	_____	0.55mA
Current:	__	Time: _____		Time: _____	
		Respiration: _____		Respiration: _____	

Total Time Down:
Notes:

Mass (g): __ Start Time: _____ Date: _____

Offset Force at 25mN-m HD Treatment #: _____

Manual Twitch 1	__	0.30mA	Manual Twitch 4	_____	0.45mA
Manual Twitch 2	__	0.35mA	Manual Twitch 5	_____	0.50mA
Manual Twitch 3	__	0.40mA	Manual Twitch 6	_____	0.55mA
Current:	__	Time: _____		Time: _____	
		Respiration: _____		Respiration: _____	

Total Time Down:
Notes:

Mass (g): __ Start Time: _____ Date: _____

Offset Force at 25mN-m HD Treatment #: _____

Manual Twitch 1	__	0.30mA	Manual Twitch 4	_____	0.45mA
Manual Twitch 2	__	0.35mA	Manual Twitch 5	_____	0.50mA
Manual Twitch 3	__	0.40mA	Manual Twitch 6	_____	0.55mA
Current:	__	Time: _____		Time: _____	
		Respiration: _____		Respiration: _____	

Total Time Down:
Notes:

Ex Vivo Mechanical Testing Sheet

Thaw Time:_____

Dissection Time: _____ **Testing Start: _____**

Potting Time: _____ **Testing End: _____**

Width:	**Thickness**:
_____	_____
_____	
_____	_____
AVG: _____	_____

Starting Gage Length: _____ mm

Gage Length for Preconditioning: _____

Gage Length for Load to Failure: _____

Notes:

DMA Software Muscle Stim Analysis Procedure

Kyle Cooper

1. Open DMA software
2. High Throughput à Force Frequency Analysis à Pick Folder
3. select desired folder
4. Set cutoff frequency to 30Hz
5. Do not change Falloff Order
6. Set cursor placement to “automatic”
7. Do not change automatic cursor settings
8. Press “Analyze”
9. Double click the first file
10. Unselect “Show Filtered”
11. Make sure the graph is not inverted
    a. If inverted, click the invert button so that the peak is up
12. Move the first cursor to the first dip of the top graph. Move the second cursor 1 or 2 small boxes past return to baseline.
13. Press “Update Cursors To Table”
14. Press “Next File”
15. Repeat steps 11-14 for the remaining files
16. Press “Export Data To Excel”
17. File à Save As à Browse à DMA Excel Files (on personal flashdrive)
18. Change Save as type to Excel Workbook
19. Name the file with mouse ID (ex: M## M1 or M## M2)

RNA Sequencing Data Organization and Processing

RNA Seq Data Formatting

Dylan Easley

1) Download the DEG file that has all genes listed (Not just the up or down regulated genes) for each comparison group
2) Make sure the numbers are associated with the GeTMM output not RAW Read counts (NOVOGene uses raw read counts and this is incorrect)
3) Match the associated genes to the Module using vlookup/xlookup in excel
    a. Make sure that the Module Membership value and adjusted p-values are included before proceeding
4) Vlookup process
    a. Create range of the ENSEMBL Gene ID Usually A2:AXX
    b. AXX= number of total genes associated with the comparison (It will vary from comparison to comparison
    c. Link the Modules (clusters of associated genes by color) to the ENSEMBLE ID by creating a new sheet that has the entire list of genes and model they are associated with. I named my sheets 'Modules'
    d. Select the entire range A1:B22904
    e. Select 2 to pull from the second column then FALSE to have it an exact match
    f. Formula =vlookup(A2:AXX, 'Sheet with Link IDs'!A1:B22904,2,FALSE)

DAVID Annotation

Dylan Easley

1) Load DAVID website
2) Under Upload tab: Paste the list of genes into box from entire list of genes from module/cluster of interest (the color modules ie brown, yellow, red, grey, blue)
    a. (this list is generated from the list of genes from NOVOgene outputs from the modules/clusters derived from WGCNA)
    b. (double check that the number of genes matches your input, copy the list and repaste it into excel)
3) Select the appropriate identifier
    a. i.e. ENSEMBL_GENE_ID or Official_Gene_Symbol (this one more beneficial later)
4) Select list type: Gene list and species then click “Submit List”
5) Move to list tab: select species Mus Musculus and list Click “Use”
6) Expand Gene_Ontology
7) click “Chart” next to GOTERM_BP_Direct
8) This will open a new window of the functional chart as a .txt file
9) Right click and save this window as a .txt file
10) Open this .txt file using excel (DO NOT COPY AND PASTE from the .txt to excel
11) Sort this data using the custom sort function (in excel)
    a. 1st p-value low to high
    b. 2nd using fold enrichment (FE) high to low
    c. Copy p-values to new sheet <0.05
    d. Filter again with p-value <0.01 (if your list of sig findings is too large can go more restrictive of <0.001
    e. Can also sort using False Discovery Rate (FDR) in same way This can be used to further sort and filter relevant genes if working with LARGE data sets. Helpful to do both FE and FDR
12) Blast against IPA to compare and compliment DAVID information/ outputs

Protocol for 3D Graphs in Origin

Sam Hubert

Note **3D plots do not appear in thesis**

Origin software has the capability to put error bars on 3D graphs unlike Excel, MATLAB, or JMP. This can be useful for visualizing and publishing data generated from experiments with multiple factors. Origin can support multiple different file upload types including ASCII, but this tutorial will be specifically for data in Excel. This software is a free download for students with any university email address.

1. After opening Origin, an Excel file can be imported using the "Import Excel" button on the second toolbar at the top of the screen. Origin can only import one Excel sheet per Project, so any data categories across multiple sheets that need to be plotted together should be appended to one sheet.

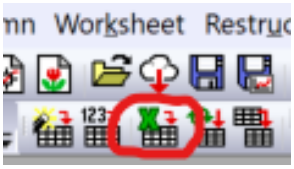

2. Although it is sometimes prompted to the user, to unlock the worksheet for editing within the Origin environment, click on the green folder with a blue electrical plug in the upper left hand corner of the sheet and select "Unlock Imported Data." This step is required to delete rows and edit cells.

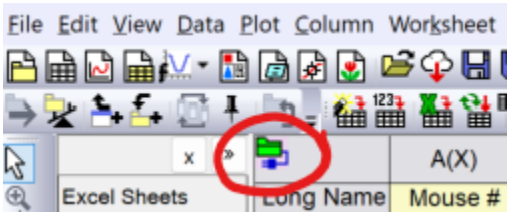

3. Each column in an Origin worksheet identifies the plot position on either the X, Y, or Z axes. This can be checked in the top row of the worksheet by identifying the letter in parentheses. The selected plot axis can be changed by highlighting the column and clicking on the respective variable button on the right end of the first toolbar.

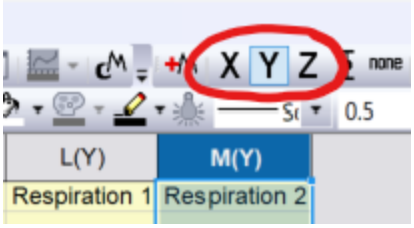

4. To plot a 3D graph, select columns for at least 3 variables (one each in X, Y, and Z). Selecting an additional column in Z defines the size of the error in that dimension. Then, click on the Plot dropdown menu and click on "3D" and then on "3D Scatter + Z Error Bar".

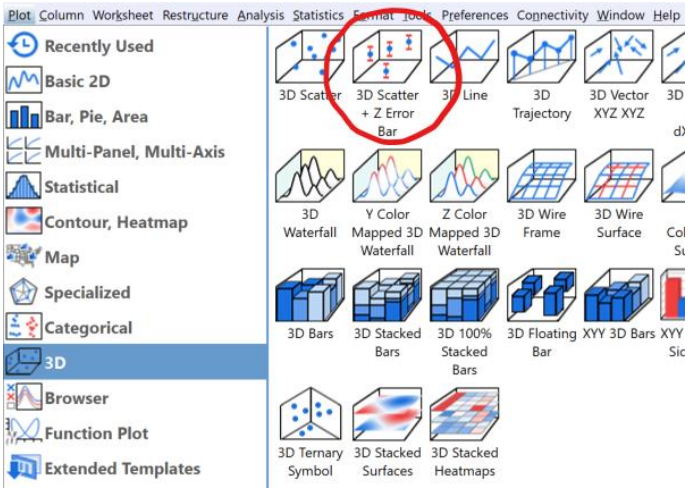

5. Since separate data categories have been appended into one file, it can be useful to plot them as independent sets because otherwise Origin will plot lines between them when connecting the plotted symbols later. This can be done by holding down the Ctrl key on the keyboard and selecting the additional data categories and then plotting.
6. The data set(s) will be plotted as a red 3D sphere by default, to change this on any particular data category, right click any individual data point to open a dropdown menu and select "Plot Details…"
7. To replicate the preferred formatting, in the Plot Details menu:
    a. Under the Symbol tab, change the symbol type to "2D", select a shape with an outline and specify a black Edge Color.
    b. Under the Error Bar tab, verify the correct column name is selected for the Error Data, then change Cap to "Y Line".
    c. Under the Line tab, check the box next to "Connect Symbols", which will add a line between associated data points. If points are still unintentionally connected, refer back to **Step 5**.
8. To format the rest of the graph, left click inside of the graph area and hover the mouse slightly up and to the right. Graph gridlines can be toggled off for all 3 planes in the Grid Lines tab (circled in red). To remove the cube wireframe connected to the front right

edge, select “Front Corner” from the Cube dropdown (circled in yellow) and toggle off the “ZX Plane” in the Plane dropdown (circled in green).

9. To format axes, right click anywhere on the graph and select “Axis…” from the dropdown menu.
    a. Under the Scale tab for each respective axis, set the lower axis limit of numerical variables to 0 by entering it into the box next to “From”
    b. Under the Line and Ticks tab for each respective axis, remove intermediate ticks for categorical variables by setting the box next to “Style” under Minor Ticks to “None”
10. Axis labels can be manually edited by double clicking on the label on the graph, otherwise it will default to the entry in “Long Name” for the column in the worksheet.
11. Graph perspective can be modified by the various buttons on the toolbar at the bottom of the screen displaying orange boxes with blue arrows. More minute adjustments can be accomplished by decreasing the value in the associated dropdown menu.

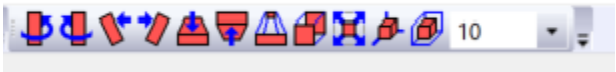

12. All of the graph preferences specified above can be copied across multiple graphs for uniformity by right clicking anywhere within the graph and selecting “Copy Format > All”. After plotting a set of data, instead of proceeding with **Step 6**, simply right click and select “Paste Format”. The same can be done for data point formatting by right clicking on any data point and selecting “Copy Format”.
13. Once all graphs have been generated and formatted, export them to a Powerpoint file using the “Send Graphs to Powerpoint” button in the Apps menu on the right.

Appendix B

SAS Analysis Outputs-

Cross Sectional Area:

Simple Effect Comparisons of Group*Time Least Squares Means By Group
Adjustment for Multiple Comparisons: Tukey

Simple Effect Level	Time	_Time	Estimate	Standard Error	DF	t Value	Pr > |t|	Adj P	Alpha	Lower	Upper	Adj Lower	Adj Upper
Group IU	1	2	−0.04192	0.01741	105	−2.41	0.0178	0.0464	0.05	−0.07644	−0.00741	−0.08331	−0.00054
Group IU	1	4	−0.06709	0.01741	105	−3.85	0.0002	0.0006	0.05	−0.1016	−0.03258	−0.1085	−0.02571
Group IU	2	4	−0.02517	0.01741	105	−1.45	0.1512	0.3214	0.05	−0.05969	0.009348	−0.06656	0.01622
Group Na久e	1	2	0.04282	0.01741	105	2.46	0.0155	0.0408	0.05	0.008301	0.07734	0.001432	0.08421
Group Na久e	1	4	0.06799	0.01741	105	3.91	0.0002	0.0005	0.05	0.03347	0.1025	0.02660	0.1094
Group Na久e	2	4	0.02517	0.01741	105	1.45	0.1512	0.3213	0.05	−0.00935	0.05969	−0.01622	0.06656
Group T0.5	1	2	0.05818	0.01741	105	3.34	0.0012	0.0033	0.05	0.02366	0.09270	0.01680	0.09957
Group T0.5	1	4	0.07135	0.01741	105	4.10	<.0001	0.0002	0.05	0.03683	0.1059	0.02996	0.1127
Group T0.5	2	4	0.01316	0.01741	105	0.76	0.4512	0.7305	0.05	−0.02135	0.04768	−0.02822	0.05455
Group T0.75	1	2	0.05311	0.01741	105	3.05	0.0029	0.0081	0.05	0.01859	0.08762	0.01172	0.09449
Group T0.75	1	4	0.03685	0.01741	105	2.12	0.0366	0.0913	0.05	0.002331	0.07137	−0.00454	0.07824
Group T0.75	2	4	−0.01626	0.01741	105	−0.93	0.3525	0.6201	0.05	−0.05078	0.01826	−0.05765	0.02513
Group T1	1	2	0.01436	0.01741	105	0.82	0.4113	0.6885	0.05	−0.02016	0.04888	−0.02703	0.05575
Group T1	1	4	0.01062	0.01741	105	0.61	0.5433	0.8151	0.05	−0.02390	0.04513	−0.03077	0.05200
Group T1	2	4	−0.00374	0.01741	105	−0.21	0.8302	0.9749	0.05	−0.03826	0.03078	−0.04513	0.03764

Simple Effect Comparisons of Group*Time Least Squares Means By Time Adjustment for Multiple Comparisons: Tukey													
Simple Effect Level	Group	_Group	Estimate	Standard Error	DF	t Value	Pr > |t|	Adj P	Alpha	Lower	Upper	Adj Lower	Adj Upper
Time 1	IU	Na欠e	0.03530	0.01741	105	2.03	0.0451	0.2601	0.05	0.000782	0.06982	-0.01302	0.08362
Time 1	IU	T0.5	0.01701	0.01741	105	0.98	0.3309	0.8651	0.05	-0.01751	0.05152	-0.03132	0.06533
Time 1	IU	T0.75	0.04268	0.01741	105	2.45	0.0159	0.1099	0.05	0.008167	0.07720	-0.00564	0.09101
Time 1	IU	T1	0.03866	0.01741	105	2.22	0.0285	0.1803	0.05	0.004139	0.07317	-0.00967	0.08698
Time 1	Na欠e	T0.5	-0.01829	0.01741	105	-1.05	0.2957	0.8309	0.05	-0.05281	0.01622	-0.06662	0.03003
Time 1	Na欠e	T0.75	0.007386	0.01741	105	0.42	0.6722	0.9931	0.05	-0.02713	0.04190	-0.04094	0.05571
Time 1	Na欠e	T1	0.003357	0.01741	105	0.19	0.8475	0.9997	0.05	-0.03116	0.03787	-0.04496	0.05168
Time 1	T0.5	T0.75	0.02568	0.01741	105	1.48	0.1432	0.5808	0.05	-0.00884	0.06020	-0.02264	0.07400
Time 1	T0.5	T1	0.02165	0.01741	105	1.24	0.2164	0.7258	0.05	-0.01287	0.05617	-0.02667	0.06997
Time 1	T0.75	T1	-0.00403	0.01741	105	-0.23	0.8174	0.9994	0.05	-0.03855	0.03049	-0.05235	0.04429
Time 2	IU	Na欠e	0.1200	0.01741	105	6.90	<.0001	<.0001	0.05	0.08552	0.1546	0.07172	0.1684
Time 2	IU	T0.5	0.1171	0.01741	105	6.73	<.0001	<.0001	0.05	0.08259	0.1516	0.06879	0.1654
Time 2	IU	T0.75	0.1377	0.01741	105	7.91	<.0001	<.0001	0.05	0.1032	0.1722	0.08939	0.1860
Time 2	IU	T1	0.09494	0.01741	105	5.45	<.0001	<.0001	0.05	0.06042	0.1295	0.04662	0.1433
Time 2	Na欠e	T0.5	-0.00293	0.01741	105	-0.17	0.8666	0.9998	0.05	-0.03745	0.03159	-0.05125	0.04539
Time 2	Na欠e	T0.75	0.01767	0.01741	105	1.02	0.3123	0.8478	0.05	-0.01684	0.05219	-0.03065	0.06599
Time 2	Na欠e	T1	-0.02510	0.01741	105	-1.44	0.1523	0.6021	0.05	-0.05962	0.009415	-0.07342	0.02322
Time 2	T0.5	T0.75	0.02060	0.01741	105	1.18	0.2393	0.7607	0.05	-0.01391	0.05512	-0.02772	0.06893
Time 2	T0.5	T1	-0.02217	0.01741	105	-1.27	0.2056	0.7079	0.05	-0.05669	0.01235	-0.07049	0.02615
Time 2	T0.75	T1	-0.04278	0.01741	105	-2.46	0.0156	0.1086	0.05	-0.07729	-0.00826	-0.09110	0.005545
Time 4	IU	Na欠e	0.1704	0.01741	105	9.79	<.0001	<.0001	0.05	0.1359	0.2049	0.1221	0.2187
Time 4	IU	T0.5	0.1554	0.01741	105	8.93	<.0001	<.0001	0.05	0.1209	0.1900	0.1071	0.2038
Time 4	IU	T0.75	0.1466	0.01741	105	8.42	<.0001	<.0001	0.05	0.1121	0.1811	0.09830	0.1949
Time 4	IU	T1	0.1164	0.01741	105	6.68	<.0001	<.0001	0.05	0.08185	0.1509	0.06804	0.1647
Time 4	Na欠e	T0.5	-0.01494	0.01741	105	-0.86	0.3928	0.9114	0.05	-0.04945	0.01958	-0.06326	0.03338
Time 4	Na欠e	T0.75	-0.02376	0.01741	105	-1.36	0.1753	0.6515	0.05	-0.05827	0.01076	-0.07208	0.02457
Time 4	Na欠e	T1	-0.05402	0.01741	105	-3.10	0.0025	0.0204	0.05	-0.08853	-0.01950	-0.1023	-0.00569
Time 4	T0.5	T0.75	-0.00882	0.01741	105	-0.51	0.6135	0.9866	0.05	-0.04334	0.02570	-0.05714	0.03950
Time 4	T0.5	T1	-0.03908	0.01741	105	-2.24	0.0269	0.1716	0.05	-0.07360	-0.00456	-0.08740	0.009242
Time 4	T0.75	T1	-0.03026	0.01741	105	-1.74	0.0851	0.4153	0.05	-0.06478	0.004257	-0.07858	0.01806

Maximum Load:

Simple Effect Comparisons of Group*Time Least Squares Means By Group Adjustment for Multiple Comparisons: Tukey													
Simple Effect Level	Time	_Time	Estimate	Standard Error	DF	t Value	Pr > |t|	Adj P	Alpha	Lower	Upper	Adj Lower	Adj Upper
Group IU	1	2	-3.4494	1.2629	105	-2.73	0.0074	0.0201	0.05	-5.9535	-0.9452	-6.4518	-0.4469
Group IU	1	4	-4.0948	1.2629	105	-3.24	0.0016	0.0045	0.05	-6.5989	-1.5907	-7.0972	-1.0923
Group IU	2	4	-0.6454	1.2629	105	-0.51	0.6104	0.8661	0.05	-3.1495	1.8587	-3.6479	2.3570
Group Na久e	1	2	0.7575	1.2629	105	0.60	0.5499	0.8205	0.05	-1.7466	3.2616	-2.2450	3.7599
Group Na久e	1	4	1.2102	1.2629	105	0.96	0.3401	0.6048	0.05	-1.2939	3.7143	-1.7922	4.2126
Group Na久e	2	4	0.4527	1.2629	105	0.36	0.7207	0.9317	0.05	-2.0514	2.9568	-2.5497	3.4552
Group T0.5	1	2	-2.3482	1.2629	105	-1.86	0.0658	0.1557	0.05	-4.8524	0.1559	-5.3507	0.6542
Group T0.5	1	4	-2.4716	1.2629	105	-1.96	0.0530	0.1281	0.05	-4.9757	0.03249	-5.4741	0.5308
Group T0.5	2	4	-0.1234	1.2629	105	-0.10	0.9224	0.9948	0.05	-2.6275	2.3807	-3.1258	2.8791
Group T0.75	1	2	-0.8127	1.2629	105	-0.64	0.5213	0.7964	0.05	-3.3168	1.6915	-3.8151	2.1898
Group T0.75	1	4	-2.8689	1.2629	105	-2.27	0.0251	0.0643	0.05	-5.3730	-0.3648	-5.8713	0.1336
Group T0.75	2	4	-2.0562	1.2629	105	-1.63	0.1065	0.2384	0.05	-4.5603	0.4479	-5.0587	0.9462
Group T1	1	2	0.1118	1.2629	105	0.09	0.9296	0.9957	0.05	-2.3923	2.6159	-2.8906	3.1143
Group T1	1	4	-1.6517	1.2629	105	-1.31	0.1938	0.3940	0.05	-4.1558	0.8524	-4.6541	1.3507
Group T1	2	4	-1.7635	1.2629	105	-1.40	0.1655	0.3465	0.05	-4.2676	0.7406	-4.7660	1.2389

Simple Effect Comparisons of Group*Time Least Squares Means By Time Adjustment for Multiple Comparisons: Tukey													
Simple Effect Level	Group	_Group	Estimate	Standard Error	DF	t Value	Pr > |t|	Adj P	Alpha	Lower	Upper	Adj Lower	Adj Upper
Time 1	IU	Na久e	-5.2851	1.2629	105	-4.18	<.0001	0.0006	0.05	-7.7893	-2.7810	-8.7907	-1.7796
Time 1	IU	T0.5	-2.6457	1.2629	105	-2.09	0.0386	0.2300	0.05	-5.1498	-0.1416	-6.1512	0.8598
Time 1	IU	T0.75	-2.8921	1.2629	105	-2.29	0.0240	0.1563	0.05	-5.3962	-0.3880	-6.3976	0.6134
Time 1	IU	T1	-4.3050	1.2629	105	-3.41	0.0009	0.0081	0.05	-6.8091	-1.8008	-7.8105	-0.7994
Time 1	Na久e	T0.5	2.6395	1.2629	105	2.09	0.0390	0.2322	0.05	0.1354	5.1436	-0.8661	6.1450
Time 1	Na久e	T0.75	2.3931	1.2629	105	1.89	0.0609	0.3265	0.05	-0.1110	4.8972	-1.1124	5.8986
Time 1	Na久e	T1	0.9802	1.2629	105	0.78	0.4394	0.9370	0.05	-1.5239	3.4843	-2.5253	4.4857
Time 1	T0.5	T0.75	-0.2464	1.2629	105	-0.20	0.8457	0.9997	0.05	-2.7505	2.2577	-3.7519	3.2591
Time 1	T0.5	T1	-1.6593	1.2629	105	-1.31	0.1918	0.6833	0.05	-4.1634	0.8448	-5.1648	1.8462
Time 1	T0.75	T1	-1.4129	1.2629	105	-1.12	0.2658	0.7963	0.05	-3.9170	1.0912	-4.9184	2.0926
Time 2	IU	Na久e	-1.0783	1.2629	105	-0.85	0.3951	0.9128	0.05	-3.5824	1.4258	-4.5838	2.4272
Time 2	IU	T0.5	-1.5446	1.2629	105	-1.22	0.2241	0.7380	0.05	-4.0487	0.9595	-5.0501	1.9609
Time 2	IU	T0.75	-0.2554	1.2629	105	-0.20	0.8401	0.9996	0.05	-2.7595	2.2487	-3.7609	3.2501
Time 2	IU	T1	-0.7438	1.2629	105	-0.59	0.5572	0.9765	0.05	-3.2479	1.7603	-4.2493	2.7617
Time 2	Na久e	T0.5	-0.4663	1.2629	105	-0.37	0.7127	0.9960	0.05	-2.9704	2.0379	-3.9718	3.0393
Time 2	Na久e	T0.75	0.8229	1.2629	105	0.65	0.5161	0.9660	0.05	-1.6812	3.3270	-2.6826	4.3284
Time 2	Na久e	T1	0.3345	1.2629	105	0.26	0.7916	0.9989	0.05	-2.1696	2.8386	-3.1710	3.8400
Time 2	T0.5	T0.75	1.2892	1.2629	105	1.02	0.3097	0.8452	0.05	-1.2149	3.7933	-2.2163	4.7947
Time 2	T0.5	T1	0.8008	1.2629	105	0.63	0.5274	0.9692	0.05	-1.7033	3.3049	-2.7047	4.3063
Time 2	T0.75	T1	-0.4884	1.2629	105	-0.39	0.6997	0.9952	0.05	-2.9925	2.0157	-3.9939	3.0171
Time 4	IU	Na久e	0.01983	1.2629	105	0.02	0.9875	1.0000	0.05	-2.4843	2.5239	-3.4857	3.5253
Time 4	IU	T0.5	-1.0225	1.2629	105	-0.81	0.4200	0.9271	0.05	-3.5266	1.4816	-4.5280	2.4830
Time 4	IU	T0.75	-1.6662	1.2629	105	-1.32	0.1899	0.6799	0.05	-4.1703	0.8379	-5.1717	1.8393
Time 4	IU	T1	-1.8619	1.2629	105	-1.47	0.1434	0.5814	0.05	-4.3660	0.6422	-5.3674	1.6436
Time 4	Na久e	T0.5	-1.0424	1.2629	105	-0.83	0.4110	0.9222	0.05	-3.5465	1.4618	-4.5479	2.4632
Time 4	Na久e	T0.75	-1.6860	1.2629	105	-1.34	0.1848	0.6701	0.05	-4.1901	0.8181	-5.1915	1.8195
Time 4	Na久e	T1	-1.8817	1.2629	105	-1.49	0.1392	0.5713	0.05	-4.3858	0.6224	-5.3872	1.6238
Time 4	T0.5	T0.75	-0.6436	1.2629	105	-0.51	0.6114	0.9862	0.05	-3.1478	1.8605	-4.1492	2.8619
Time 4	T0.5	T1	-0.8394	1.2629	105	-0.66	0.5077	0.9635	0.05	-3.3435	1.6648	-4.3449	2.6662
Time 4	T0.75	T1	-0.1957	1.2629	105	-0.15	0.8771	0.9999	0.05	-2.6998	2.3084	-3.7012	3.3098

Stiffness (Linear Regression):

Simple Effect Comparisons of Group*Time Least Squares Means By Group Adjustment for Multiple Comparisons: Tukey													
Simple Effect Level	Time	_Time	Estimate	Standard Error	DF	t Value	Pr > |t|	Adj P	Alpha	Lower	Upper	Adj Lower	Adj Upper
Group IU	1	2	-2.0342	1.0594	105	-1.92	0.0576	0.1381	0.05	-4.1348	0.06643	-4.5529	0.4845
Group IU	1	4	-3.2329	1.0594	105	-3.05	0.0029	0.0080	0.05	-5.3335	-1.1322	-5.7515	-0.7142
Group IU	2	4	-1.1987	1.0594	105	-1.13	0.2604	0.4970	0.05	-3.2993	0.9020	-3.7173	1.3200
Group Na久e	1	2	0.9729	1.0594	105	0.92	0.3606	0.6300	0.05	-1.1277	3.0735	-1.5458	3.4916
Group Na久e	1	4	0.8370	1.0594	105	0.79	0.4313	0.7099	0.05	-1.2636	2.9377	-1.6816	3.3557
Group Na久e	2	4	-0.1359	1.0594	105	-0.13	0.8982	0.9910	0.05	-2.2365	1.9648	-2.6545	2.3828
Group T0.5	1	2	-1.2328	1.0594	105	-1.16	0.2472	0.4775	0.05	-3.3334	0.8679	-3.7514	1.2859
Group T0.5	1	4	-1.1272	1.0594	105	-1.06	0.2898	0.5385	0.05	-3.2278	0.9735	-3.6458	1.3915
Group T0.5	2	4	0.1056	1.0594	105	0.10	0.9208	0.9945	0.05	-1.9950	2.2062	-2.4131	2.6243
Group T0.75	1	2	-1.0188	1.0594	105	-0.96	0.3384	0.6026	0.05	-3.1195	1.0818	-3.5375	1.4998
Group T0.75	1	4	-1.8372	1.0594	105	-1.73	0.0858	0.1974	0.05	-3.9378	0.2635	-4.3558	0.6815
Group T0.75	2	4	-0.8183	1.0594	105	-0.77	0.4416	0.7207	0.05	-2.9189	1.2823	-3.3370	1.7003
Group T1	1	2	-0.3405	1.0594	105	-0.32	0.7486	0.9447	0.05	-2.4411	1.7602	-2.8591	2.1782
Group T1	1	4	-1.8792	1.0594	105	-1.77	0.0790	0.1834	0.05	-3.9799	0.2214	-4.3979	0.6394
Group T1	2	4	-1.5388	1.0594	105	-1.45	0.1494	0.3181	0.05	-3.6394	0.5619	-4.0574	0.9799

Simple Effect Comparisons of Group*Time Least Squares Means By Time Adjustment for Multiple Comparisons: Tukey													
Simple Effect Level	Group	_Group	Estimate	Standard Error	DF	t Value	Pr > |t|	Adj P	Alpha	Lower	Upper	Adj Lower	Adj Upper
Time 1	IU	Na久e	-3.8363	1.0594	105	-3.62	0.0005	0.0041	0.05	-5.9370	-1.7357	-6.7770	-0.8957
Time 1	IU	T0.5	-1.8356	1.0594	105	-1.73	0.0861	0.4187	0.05	-3.9362	0.2650	-4.7763	1.1051
Time 1	IU	T0.75	-1.7371	1.0594	105	-1.64	0.1041	0.4758	0.05	-3.8377	0.3635	-4.6778	1.2036
Time 1	IU	T1	-2.0196	1.0594	105	-1.91	0.0593	0.3204	0.05	-4.1202	0.08102	-4.9603	0.9211
Time 1	Na久e	T0.5	2.0007	1.0594	105	1.89	0.0617	0.3299	0.05	-0.09990	4.1014	-0.9399	4.9414
Time 1	Na久e	T0.75	2.0993	1.0594	105	1.98	0.0501	0.2822	0.05	-0.00137	4.1999	-0.8414	5.0399
Time 1	Na久e	T1	1.8167	1.0594	105	1.71	0.0893	0.4294	0.05	-0.2839	3.9174	-1.1239	4.7574
Time 1	T0.5	T0.75	0.09853	1.0594	105	0.09	0.9261	1.0000	0.05	-2.0021	2.1992	-2.8421	3.0392
Time 1	T0.5	T1	-0.1840	1.0594	105	-0.17	0.8625	0.9998	0.05	-2.2846	1.9166	-3.1247	2.7567
Time 1	T0.75	T1	-0.2825	1.0594	105	-0.27	0.7902	0.9989	0.05	-2.3832	1.8181	-3.2232	2.6581
Time 2	IU	Na久e	-0.8293	1.0594	105	-0.78	0.4355	0.9351	0.05	-2.9299	1.2714	-3.7699	2.1114
Time 2	IU	T0.5	-1.0342	1.0594	105	-0.98	0.3312	0.8654	0.05	-3.1348	1.0664	-3.9749	1.9065
Time 2	IU	T0.75	-0.7217	1.0594	105	-0.68	0.4972	0.9601	0.05	-2.8224	1.3789	-3.6624	2.2189
Time 2	IU	T1	-0.3259	1.0594	105	-0.31	0.7590	0.9980	0.05	-2.4265	1.7747	-3.2666	2.6148
Time 2	Na久e	T0.5	-0.2049	1.0594	105	-0.19	0.8470	0.9997	0.05	-2.3056	1.8957	-3.1456	2.7357
Time 2	Na久e	T0.75	0.1075	1.0594	105	0.10	0.9194	1.0000	0.05	-1.9931	2.2081	-2.8332	3.0482
Time 2	Na久e	T1	0.5034	1.0594	105	0.48	0.6357	0.9894	0.05	-1.5972	2.6040	-2.4373	3.4441
Time 2	T0.5	T0.75	0.3125	1.0594	105	0.29	0.7686	0.9983	0.05	-1.7882	2.4131	-2.6282	3.2531
Time 2	T0.5	T1	0.7083	1.0594	105	0.67	0.5052	0.9627	0.05	-1.3923	2.8089	-2.2324	3.6490
Time 2	T0.75	T1	0.3959	1.0594	105	0.37	0.7094	0.9958	0.05	-1.7048	2.4965	-2.5448	3.3365
Time 4	IU	Na久e	0.2335	1.0594	105	0.22	0.8260	0.9995	0.05	-1.8671	2.3342	-2.7071	3.1742
Time 4	IU	T0.5	0.2701	1.0594	105	0.25	0.7993	0.9991	0.05	-1.8305	2.3707	-2.6706	3.2108
Time 4	IU	T0.75	-0.3414	1.0594	105	-0.32	0.7479	0.9976	0.05	-2.4420	1.7592	-3.2821	2.5993
Time 4	IU	T1	-0.6660	1.0594	105	-0.63	0.5310	0.9701	0.05	-2.7666	1.4346	-3.6067	2.2747
Time 4	Na久e	T0.5	0.03653	1.0594	105	0.03	0.9726	1.0000	0.05	-2.0641	2.1372	-2.9041	2.9772
Time 4	Na久e	T0.75	-0.5749	1.0594	105	-0.54	0.5885	0.9826	0.05	-2.6756	1.5257	-3.5156	2.3657
Time 4	Na久e	T1	-0.8995	1.0594	105	-0.85	0.3978	0.9145	0.05	-3.0001	1.2011	-3.8402	2.0412
Time 4	T0.5	T0.75	-0.6115	1.0594	105	-0.58	0.5651	0.9781	0.05	-2.7121	1.4892	-3.5521	2.3292
Time 4	T0.5	T1	-0.9361	1.0594	105	-0.88	0.3790	0.9024	0.05	-3.0367	1.1646	-3.8767	2.0046
Time 4	T0.75	T1	-0.3246	1.0594	105	-0.31	0.7599	0.9981	0.05	-2.4252	1.7760	-3.2653	2.6161

Maximum Stress:

Simple Effect Comparisons of Group*Time Least Squares Means By Group Adjustment for Multiple Comparisons: Tukey												
Simple Effect Level	Time	_Time	Estimate	Standard Error	DF	t Value	Pr > |t|	Adj P	Alpha	Lower	Upper	Adj Lower	Adj Upper
Group IU	1	2	-7.5654	4.2682	105	-1.77	0.0792	0.1838	0.05	-16.0284	0.8975	-17.7125	2.5817
Group IU	1	4	-6.9029	4.2682	105	-1.62	0.1088	0.2429	0.05	-15.3659	1.5601	-17.0500	3.2442
Group IU	2	4	0.6625	4.2682	105	0.16	0.8769	0.9868	0.05	-7.8004	9.1255	-9.4846	10.8097
Group Na久e	1	2	-1.6066	4.2682	105	-0.38	0.7074	0.9249	0.05	-10.0696	6.8563	-11.7538	8.5405
Group Na久e	1	4	-3.0242	4.2682	105	-0.71	0.4802	0.7590	0.05	-11.4871	5.4388	-13.1713	7.1230
Group Na久e	2	4	-1.4175	4.2682	105	-0.33	0.7405	0.9410	0.05	-9.8805	7.0454	-11.5647	8.7296
Group T0.5	1	2	-11.2707	4.2682	105	-2.64	0.0095	0.0256	0.05	-19.7336	-2.8077	-21.4178	-1.1235
Group T0.5	1	4	-13.3219	4.2682	105	-3.12	0.0023	0.0065	0.05	-21.7848	-4.8589	-23.4690	-3.1748
Group T0.5	2	4	-2.0512	4.2682	105	-0.48	0.6318	0.8806	0.05	-10.5142	6.4117	-12.1984	8.0959
Group T0.75	1	2	-7.1778	4.2682	105	-1.68	0.0956	0.2170	0.05	-15.6407	1.2852	-17.3249	2.9693
Group T0.75	1	4	-11.9343	4.2682	105	-2.80	0.0062	0.0168	0.05	-20.3973	-3.4714	-22.0815	-1.7872
Group T0.75	2	4	-4.7565	4.2682	105	-1.11	0.2676	0.5074	0.05	-13.2195	3.7064	-14.9037	5.3906
Group T1	1	2	-0.5691	4.2682	105	-0.13	0.8942	0.9902	0.05	-9.0321	7.8938	-10.7163	9.5780
Group T1	1	4	-5.7119	4.2682	105	-1.34	0.1837	0.3773	0.05	-14.1749	2.7511	-15.8590	4.4352
Group T1	2	4	-5.1428	4.2682	105	-1.20	0.2309	0.4529	0.05	-13.6057	3.3202	-15.2899	5.0044

Simple Effect Comparisons of Group*Time Least Squares Means By Time Adjustment for Multiple Comparisons: Tukey													
Simple Effect Level	Group	_Group	Estimate	Standard Error	DF	t Value	Pr > |t|	Adj P	Alpha	Lower	Upper	Adj Lower	Adj Upper
Time 1	IU	Na久e	-16.7886	4.2682	105	-3.93	0.0002	0.0014	0.05	-25.2516	-8.3257	-28.6360	-4.9413
Time 1	IU	T0.5	-8.5720	4.2682	105	-2.01	0.0472	0.2692	0.05	-17.0349	-0.1090	-20.4193	3.2753
Time 1	IU	T0.75	-10.4910	4.2682	105	-2.46	0.0156	0.1084	0.05	-18.9540	-2.0280	-22.3383	1.3563
Time 1	IU	T1	-14.4494	4.2682	105	-3.39	0.0010	0.0087	0.05	-22.9124	-5.9865	-26.2968	-2.6021
Time 1	Na久e	T0.5	8.2166	4.2682	105	1.93	0.0569	0.3106	0.05	-0.2463	16.6796	-3.6307	20.0640
Time 1	Na久e	T0.75	6.2976	4.2682	105	1.48	0.1431	0.5806	0.05	-2.1653	14.7606	-5.5497	18.1450
Time 1	Na久e	T1	2.3392	4.2682	105	0.55	0.5848	0.9820	0.05	-6.1238	10.8022	-9.5081	14.1865
Time 1	T0.5	T0.75	-1.9190	4.2682	105	-0.45	0.6539	0.9914	0.05	-10.3820	6.5440	-13.7663	9.9283
Time 1	T0.5	T1	-5.8775	4.2682	105	-1.38	0.1714	0.6436	0.05	-14.3404	2.5855	-17.7248	5.9699
Time 1	T0.75	T1	-3.9584	4.2682	105	-0.93	0.3558	0.8857	0.05	-12.4214	4.5045	-15.8058	7.8889
Time 2	IU	Na久e	-10.8299	4.2682	105	-2.54	0.0126	0.0902	0.05	-19.2928	-2.3669	-22.6772	1.0175
Time 2	IU	T0.5	-12.2772	4.2682	105	-2.88	0.0049	0.0383	0.05	-20.7402	-3.8143	-24.1246	-0.4299
Time 2	IU	T0.75	-10.1034	4.2682	105	-2.37	0.0198	0.1326	0.05	-18.5663	-1.6404	-21.9507	1.7440
Time 2	IU	T1	-7.4532	4.2682	105	-1.75	0.0837	0.4106	0.05	-15.9161	1.0098	-19.3005	4.3942
Time 2	Na久e	T0.5	-1.4474	4.2682	105	-0.34	0.7352	0.9971	0.05	-9.9103	7.0156	-13.2947	10.4000
Time 2	Na久e	T0.75	0.7265	4.2682	105	0.17	0.8652	0.9998	0.05	-7.7365	9.1895	-11.1208	12.5738
Time 2	Na久e	T1	3.3767	4.2682	105	0.79	0.4306	0.9327	0.05	-5.0863	11.8397	-8.4706	15.2240
Time 2	T0.5	T0.75	2.1739	4.2682	105	0.51	0.6116	0.9863	0.05	-6.2891	10.6368	-9.6735	14.0212
Time 2	T0.5	T1	4.8241	4.2682	105	1.13	0.2609	0.7902	0.05	-3.6389	13.2870	-7.0233	16.6714
Time 2	T0.75	T1	2.6502	4.2682	105	0.62	0.5360	0.9714	0.05	-5.8128	11.1132	-9.1971	14.4975
Time 4	IU	Na久e	-12.9099	4.2682	105	-3.02	0.0031	0.0255	0.05	-21.3729	-4.4470	-24.7573	-1.0626
Time 4	IU	T0.5	-14.9910	4.2682	105	-3.51	0.0007	0.0058	0.05	-23.4539	-6.5280	-26.8383	-3.1437
Time 4	IU	T0.75	-15.5224	4.2682	105	-3.64	0.0004	0.0039	0.05	-23.9854	-7.0595	-27.3698	-3.6751
Time 4	IU	T1	-13.2585	4.2682	105	-3.11	0.0024	0.0202	0.05	-21.7214	-4.7955	-25.1058	-1.4111
Time 4	Na久e	T0.5	-2.0811	4.2682	105	-0.49	0.6269	0.9884	0.05	-10.5440	6.3819	-13.9284	9.7663
Time 4	Na久e	T0.75	-2.6125	4.2682	105	-0.61	0.5418	0.9729	0.05	-11.0755	5.8504	-14.4598	9.2348
Time 4	Na久e	T1	-0.3485	4.2682	105	-0.08	0.9351	1.0000	0.05	-8.8115	8.1144	-12.1959	11.4988
Time 4	T0.5	T0.75	-0.5314	4.2682	105	-0.12	0.9011	0.9999	0.05	-8.9944	7.9315	-12.3788	11.3159
Time 4	T0.5	T1	1.7325	4.2682	105	0.41	0.6856	0.9942	0.05	-6.7304	10.1955	-10.1148	13.5799
Time 4	T0.75	T1	2.2640	4.2682	105	0.53	0.5969	0.9840	0.05	-6.1990	10.7269	-9.5833	14.1113

Elastic Modulus (Linear Regression):

Simple Effect Comparisons of Group*Time Least Squares Means By Group Adjustment for Multiple Comparisons: Tukey													
Simple Effect Level	Time	_Time	Estimate	Standard Error	DF	t Value	Pr > |t|	Adj P	Alpha	Lower	Upper	Adj Lower	Adj Upper
Group IU	1	2	-206.92	176.09	105	-1.18	0.2426	0.4707	0.05	-556.08	142.24	-625.56	211.72
Group IU	1	4	-248.96	176.09	105	-1.41	0.1604	0.3375	0.05	-598.12	100.20	-667.60	169.68
Group IU	2	4	-42.0404	176.09	105	-0.24	0.8118	0.9691	0.05	-391.20	307.12	-460.68	376.60
Group Na久e	1	2	-18.8108	176.09	105	-0.11	0.9151	0.9937	0.05	-367.97	330.35	-437.45	399.83
Group Na久e	1	4	-171.65	176.09	105	-0.97	0.3319	0.5944	0.05	-520.80	177.51	-590.29	246.99
Group Na久e	2	4	-152.84	176.09	105	-0.87	0.3874	0.6616	0.05	-501.99	196.32	-571.48	265.81
Group T0.5	1	2	-364.77	176.09	105	-2.07	0.0408	0.1008	0.05	-713.93	-15.6132	-783.41	53.8709
Group T0.5	1	4	-416.79	176.09	105	-2.37	0.0198	0.0513	0.05	-765.95	-67.6341	-835.43	1.8500
Group T0.5	2	4	-52.0209	176.09	105	-0.30	0.7683	0.9531	0.05	-401.18	297.14	-470.66	366.62
Group T0.75	1	2	-366.93	176.09	105	-2.08	0.0396	0.0981	0.05	-716.09	-17.7759	-785.58	51.7082
Group T0.75	1	4	-422.79	176.09	105	-2.40	0.0181	0.0472	0.05	-771.95	-73.6326	-841.43	-4.1484
Group T0.75	2	4	-55.8567	176.09	105	-0.32	0.7517	0.9461	0.05	-405.01	293.30	-474.50	362.79
Group T1	1	2	-108.54	176.09	105	-0.62	0.5390	0.8115	0.05	-457.70	240.62	-527.18	310.10
Group T1	1	4	-327.49	176.09	105	-1.86	0.0657	0.1556	0.05	-676.65	21.6697	-746.13	91.1538
Group T1	2	4	-218.95	176.09	105	-1.24	0.2165	0.4305	0.05	-568.10	130.21	-637.59	199.70

Simple Effect Comparisons of Group*Time Least Squares Means By Time
Adjustment for Multiple Comparisons: Tukey

Simple Effect Level	Group	_Group	Estimate	Standard Error	DF	t Value	Pr > |t|	Adj P	Alpha	Lower	Upper	Adj Lower	Adj Upper
Time 1	IU	Na欠e	-635.52	176.09	105	-3.61	0.0005	0.0042	0.05	-984.68	-286.36	-1124.31	-146.74
Time 1	IU	T0.5	-306.75	176.09	105	-1.74	0.0844	0.4131	0.05	-655.91	42.4074	-795.54	182.04
Time 1	IU	T0.75	-357.38	176.09	105	-2.03	0.0449	0.2593	0.05	-706.54	-8.2205	-846.17	131.41
Time 1	IU	T1	-374.37	176.09	105	-2.13	0.0358	0.2169	0.05	-723.53	-25.2105	-863.16	114.42
Time 1	Na欠e	T0.5	328.77	176.09	105	1.87	0.0647	0.3415	0.05	-20.3855	677.93	-160.02	817.56
Time 1	Na欠e	T0.75	278.14	176.09	105	1.58	0.1172	0.5138	0.05	-71.0135	627.30	-210.64	766.93
Time 1	Na欠e	T1	261.15	176.09	105	1.48	0.1411	0.5757	0.05	-88.0034	610.31	-227.63	749.94
Time 1	T0.5	T0.75	-50.6280	176.09	105	-0.29	0.7743	0.9985	0.05	-399.79	298.53	-539.42	438.16
Time 1	T0.5	T1	-67.6179	176.09	105	-0.38	0.7018	0.9953	0.05	-416.78	281.54	-556.40	421.17
Time 1	T0.75	T1	-16.9899	176.09	105	-0.10	0.9233	1.0000	0.05	-366.15	332.17	-505.78	471.80
Time 2	IU	Na欠e	-447.41	176.09	105	-2.54	0.0125	0.0895	0.05	-796.57	-98.2564	-936.20	41.3731
Time 2	IU	T0.5	-464.60	176.09	105	-2.64	0.0096	0.0707	0.05	-813.76	-115.44	-953.39	24.1851
Time 2	IU	T0.75	-517.39	176.09	105	-2.94	0.0041	0.0324	0.05	-866.55	-168.23	-1006.18	-28.6055
Time 2	IU	T1	-275.99	176.09	105	-1.57	0.1201	0.5216	0.05	-625.15	73.1669	-764.78	212.80
Time 2	Na欠e	T0.5	-17.1879	176.09	105	-0.10	0.9224	1.0000	0.05	-366.35	331.97	-505.97	471.60
Time 2	Na欠e	T0.75	-69.9785	176.09	105	-0.40	0.6919	0.9947	0.05	-419.14	279.18	-558.77	418.81
Time 2	Na欠e	T1	171.42	176.09	105	0.97	0.3325	0.8665	0.05	-177.73	520.58	-317.36	660.21
Time 2	T0.5	T0.75	-52.7906	176.09	105	-0.30	0.7649	0.9982	0.05	-401.95	296.37	-541.58	436.00
Time 2	T0.5	T1	188.61	176.09	105	1.07	0.2866	0.8209	0.05	-160.55	537.77	-300.18	677.40
Time 2	T0.75	T1	241.40	176.09	105	1.37	0.1733	0.6475	0.05	-107.76	590.56	-247.39	730.19
Time 4	IU	Na欠e	-558.21	176.09	105	-3.17	0.0020	0.0167	0.05	-907.37	-209.05	-1047.00	-69.4230
Time 4	IU	T0.5	-474.58	176.09	105	-2.70	0.0082	0.0614	0.05	-823.74	-125.42	-963.37	14.2047
Time 4	IU	T0.75	-531.21	176.09	105	-3.02	0.0032	0.0261	0.05	-880.37	-182.05	-1020.00	-42.4217
Time 4	IU	T1	-452.90	176.09	105	-2.57	0.0115	0.0831	0.05	-802.05	-103.74	-941.68	35.8906
Time 4	Na欠e	T0.5	83.6277	176.09	105	0.47	0.6358	0.9895	0.05	-265.53	432.79	-405.16	572.41
Time 4	Na欠e	T0.75	27.0013	176.09	105	0.15	0.8784	0.9999	0.05	-322.16	376.16	-461.79	515.79
Time 4	Na欠e	T1	105.31	176.09	105	0.60	0.5511	0.9751	0.05	-243.84	454.47	-383.47	594.10
Time 4	T0.5	T0.75	-56.6264	176.09	105	-0.32	0.7484	0.9977	0.05	-405.78	292.53	-545.41	432.16
Time 4	T0.5	T1	21.6859	176.09	105	0.12	0.9022	0.9999	0.05	-327.47	370.84	-467.10	510.47
Time 4	T0.75	T1	78.3123	176.09	105	0.44	0.6574	0.9918	0.05	-270.85	427.47	-410.47	567.10

Interobserver Kappa Statistical Measures

Collagen Orientation

Kappa Statistics				
Statistic	Estimate	Standard Error	95% Confidence Limits	
Simple Kappa	0.7811	0.0909	0.6030	0.9592
Weighted Kappa	0.8194	0.0786	0.6653	0.9735

Cellular Density

Kappa Statistics				
Statistic	Estimate	Standard Error	95% Confidence Limits	
Simple Kappa	0.8273	0.0830	0.6646	0.9899
Weighted Kappa	0.8628	0.0683	0.7289	0.9967

Cellular Appearance

Kappa Statistics				
Statistic	Estimate	Standard Error	95% Confidence Limits	
Simple Kappa	0.7058	0.1016	0.5067	0.9048
Weighted Kappa	0.7608	0.0864	0.5915	0.9301

Safranin-O Staining Intensity

Kappa Statistics				
Statistic	Estimate	Standard Error	95% Confidence Limits	
Simple Kappa	0.7985	0.0829	0.6360	0.9611
Weighted Kappa	0.8190	0.0794	0.6633	0.9747

Appendix C

Yield Analysis Code- Slope Analysis

7/22/24 - Sam Hubert

- Added sampleNumber to facilitate extraction from compiled Excel sheets
- Changed stretch_peak and stress_peak to stretch2peak and stress2peak
- Added workRatio and energyRatio to predict ductility

7/24/24 - Sam Hubert

- Matched data inputs for DCE data
- Added manual CSA, stress, and strain calculations
- Added automatic plot export

7/25/24 - Sam Hubert

- Added comments

```
% Hannah Schwenker

% Import Data
% Import CSV or Excel file
clc; clearvars; close all;
[mtsfile, mtspath] = uigetfile({
   '*.csv;*.CSV', 'CSV tables (*.csv)';
   '*.xls;*.xlsx', 'Excel workbooks (*.xls, *.xlsx)';
}, "Select MTS failure data");
data = readmatrix(strcat(mtspath, mtsfile));

% Prompt for and save mouse index
promptmnumber = "What mouse number? ";
mnumber = input(promptmnumber);
sample = ['M', num2str(mnumber)];
sample = string(sample);

startIndex = 1; % where the data starts in the mts export file

% Assign variables from CSV import
mtsdata.load =          data(startIndex:end, 1);
mtsdata.time =          data(startIndex:end, 2);
mtsdata.ext =          data(startIndex:end, 3); % value unused, equivalent to mtsdata.crosshead
mtsdata.stress =        data(startIndex:end, 4)*1000; % replaced in Stress Correction step
```

```
mtsdata.strain =        data(startIndex:end, 5); % replaced in Strain Correction step
mtsdata.crosshead =     data(startIndex:end, 6);
```

CSA Calculation

```
% Prompts to manually input physical sample measurements made before PTF Test
promptw = "Width? ";
width = input(promptw);
promptt = "Thickness? ";
thickness = input(promptt);
promptGL = "PTF Gage Length? ";
initial_GL = input(promptGL);

csa = (pi*thickness*width)/4; % [mm^2], elliptical cross sectional area approximation
```

Stress Correction

```
stress = mtsdata.load./csa; % [MPa]
maxStress = max(stress);
```

Strain Correction

```
% Manually calculate strain based on GL
strain = (mtsdata.crosshead(1:end) - mtsdata.crosshead(1))/initial_GL;
```

Stretch Ratio Calculation

```
% Find stretch ratio
stretch_ratio = (initial_GL+mtsdata.crosshead)/initial_GL;
```

Finding Derivative of Smooth Stress v. Strain Curve

```
maxStressIndex = find(stress == max(stress));
strainAtMaxStress = strain(maxStressIndex); % {SLH - changed "MaxStrain" to "strainAtMaxStress"}

toeregion = find(stress > 0.35*maxStress); % Yield point must be greater than 30% of max load to put us out of toe region
toeregionInd = toeregion(1,1); % Mark the end of the toe region
stretch2peak = stretch_ratio(toeregionInd:maxStressIndex,1); % subset of stretch ratio between the end of the toe region and max load
stress2peak = stress(toeregionInd:maxStressIndex,1); % subset of stress between the end of the toe region and max stress
```

```
% fit a smooth spline to data between the toe region and max stress
spline1= fit(stretch2peak, stress2peak, 'smoothingspline', 'SmoothingParam', 0.9999); % can change final value to make the curve smoother/rougher

% find first derivative of smooth spline
[r1,r2] = differentiate(spline1, stretch2peak); % dload/dstretch
[yieldy, yieldindex] = max(r1); % yield occurs at the maximum stiffness in the linear region
yieldx= stretch2peak(yieldindex); % yield stretch ratio
yieldy_stress= stress2peak(yieldindex); % yield stress [MPa]

yieldInd= yieldindex+toeregionInd; % add toe region indexes back to total yield index
[maxLoad, maxLoadInd] = max(mtsdata.load);
yieldStrain= strain(yieldInd);
```

Elastic Modulus

```
p = .3; % linear regression must include > 30% of data
[MaxLoad, maxLoadIndex] = max(mtsdata.load);
ExtAtMaxLoad = mtsdata.crosshead(maxLoadIndex);
index = maxLoadIndex; % index to stop at (usually max load or yield load)
start = max(round(0*index), 1); % ignore first x% (pre-processing)
load = mtsdata.load(start:index); % load from start to max load
ext = mtsdata.crosshead(start:index); % crosshead from start to max load
l = length(ext); % # of timesteps to maximum
w = round(p*l); % 30% of l, give or take

% Stiffness from Load vs. Extension (crosshead)
s_guess = (load(w+1:end) - load(1:l-w))./(ext(w+1:end) - ext(1:l-w)); % the slope of all possible lines w wide from start to max load
[s, t] = max(s_guess); % max slope region, w wide, may not include max load since LvE graph begins to flatten near maximum load
b_s = load(t) - s*ext(t); % y-intercept of selected maximum slope line
Stiffness = s; % interpretation, [N/mm]

% Modulus from Stress vs. Strain
m_guess = (stress(w+1:l) - stress(1:l-w))./(strain(w+1:l) - strain(1:l-w)); % the slope of all possible lines w wide from start to max stress
[m, n] = max(m_guess);
b_m = stress(n) - m*strain(n);
Modulus = m; % interpretation, [MPa]

% create regression lines
regy_s = s.*ext + b_s;
regy_m = m.*strain + b_m;
```

```
% determine stiffness R^2
yresid = load(t:t+w) - regy_s(t:t+w);
SSresid = sum(yresid.^2);
SStotal = (l - 1)*var(load);
rsq = 1 - SSresid/SStotal;
StiffnessRSQ = rsq;

% determine modulus R^2
yresid_m = stress(t:t+w) - regy_m(t:t+w);
SSresid_m = sum(yresid_m.^2);
SStotal_m = (l - 1)*var(stress);
rsq_m = 1 - SSresid_m/SStotal_m;
ModulusRSQ = rsq_m;
```

Graphs

```
figure(1)
plot(mtsdata.crosshead, mtsdata.load)
hold on
plot(ext(t:t+w), regy_s(t:t+w)) % {SLH - changed "index" to "n+w"}
plot(mtsdata.crosshead(index), mtsdata.load(index), "xr") % plot max load point
hold off
title("Load vs Extension");
xlabel("Extension (mm)"); ylabel("Load (N)");
filename = append(sample, '_LvE_regline_maxpoint.png');
exportgraphics(figure(1),filename);
```

```
figure(2)
plot(mtsdata.crosshead, mtsdata.load)
hold on
plot(mtsdata.crosshead(yieldInd, 1), mtsdata.load(yieldInd, 1), '*')
hold off
xlabel("Extension (mm)")
ylabel("Load (N)")
filename = append(sample, '_LvE_yieldpoint.png');
fig = gcf;
exportgraphics(fig,filename);
```

```
figure(3)
plot(stretch_ratio, stress)
hold on
plot(yieldx, yieldy_stress, '*')
hold off
xlabel("Stretch Ratio (\lambda)")
ylabel("Stress (\sigma, kPa)")
%title("Stress vs. Stretch Ratio")
filename = append(sample, '_StressvStretchRatio_yieldpoint.png');
fig = gcf;
exportgraphics(fig,filename);
```

```
figure(4)
plot(stretch2peak, stress2peak, 'k')
hold on
plot(spline1, stretch2peak, stress2peak, 'b')
plot(yieldx, yieldy_stress, '*')
hold off
xlabel("Stretch Ratio")
ylabel("Stress (MPa)")
legend('data','regression line','yield point','Location','southeast')
filename = append(sample, '_StressvStretchRatio_regline.png');
fig = gcf;
exportgraphics(fig,filename);
```

```
figure(5)
plot(stretch2peak, r1)
hold on
plot(yieldx, yieldy, '*')
hold off
xlabel("Stretch Ratio (\lambda)")
ylabel("d\sigma/d\lambda")
filename = append(sample, '_DStressDStretchRatio.png');
fig = gcf;
exportgraphics(fig,filename);
```

```
figure(6)
plot(strain,stress)
hold on
plot(strain(n:n+w), regy_m(n:n+w))
plot(strain(index), stress(index), "xr") % plot max load point
hold off
title("Stress vs. Strain");
xlabel("Strain (mm/mm)"); ylabel("Stress (MPa)");
filename = append(sample, '_StressvStrain_regline_maxpoint.png');
fig = gcf;
exportgraphics(fig,filename);
```

Output Table- Elastic Modulus, Yield Point, Energy to Yield, etc.

```
% Gather Outputs
YieldStress = yieldy_stress;
yieldLoad= mtsdata.load(yieldInd);
ExtAtYield = mtsdata.crosshead(yieldInd);
PostYieldExt = mtsdata.crosshead(maxLoadInd) - mtsdata.crosshead(yieldInd);
NormalizedYieldLoad = yieldLoad/maxLoad;
ExtAtMax = mtsdata.crosshead(yieldInd);
NormExtAtYield = ExtAtYield/ExtAtMax;
NormPYE = PostYieldExt/ExtAtMax;

% Trapezoidal integration for work and energy
WorkToYieldLoad = trapz(mtsdata.crosshead(1:yieldInd), mtsdata.load(1:yieldInd));
WorkToMaxLoad = trapz(mtsdata.crosshead(1:maxLoadIndex), mtsdata.load(1:maxLoadIndex));
EnergytoYield = trapz(strain(1:yieldInd), stress(1:yieldInd));
EnergytoMax = trapz(strain(1:maxLoadIndex),stress(1:maxLoadIndex));
WorkRatio = WorkToYieldLoad/WorkToMaxLoad;
EnergyRatio = EnergytoYield/EnergytoMax;

% Output to Excel table
output= table(sample, width, thickness, csa, initial_GL, maxStress, strainAtMaxStress, yieldStrain,
yieldLoad, YieldStress, maxLoad, Stiffness, StiffnessRSQ, Modulus, ModulusRSQ, WorkToYieldLoad,
WorkToMaxLoad, EnergytoYield, EnergytoMax, WorkRatio, EnergyRatio)
```

output = 1×21 table

	sample	width	thickness	csa	initial_GL	maxStress	…
1	"M139"	0.5550	0.5550	0.2419	4.2000	55.8631	

```
  filenameexp = 'MechDataforSAS_NEW.xlsx';
  writetable(output,filenameexp,'Sheet',1,'WriteVariableNames',false,'WriteMode','append'); %
WriteVariableNames is only "true" the first run
```